Studies on Propagation and Interaction of Multi-solitons in Inhomogeneous Optical Systems

Thesis submitted to the University of Calicut

in partial fulfillment of the requirements

for the award of the degree of

Doctor of Philosophy

in

Physics

MUSAMMIL. N. M

Department of Physics

University of Calicut

Malappuram, Kerala-673 635, India.

October 2018

CERTIFICATE

Certified that the work presented in this thesis entitled 'Studies on Propagation and Interaction of Multi-solitons in Inhomogeneous Optical Systems' is a bona fide work done by Mr. N. M. Musammil under my guidance in the Department of Physics, University of Calicut and that this work has not been included in any other thesis submitted previously for the award of any degree.

Farook College
October 2018

Dr. P. A. Subha
(Supervising Guide)

CERTIFICATE

This is to certify that the thesis entitled 'Studies on Propagation and Interaction of Multi-solitons in Inhomogeneous Optical Systems' has been checked for plagiarism using the URKUND software, at the CHMK library, University of Calicut. Also, the thesis has undergone all corrections suggested by the adjudicators and there are no further errors. The contents in the hard copy and soft copy of the thesis are same.

Farook College — Dr. P. A. Subha

Date: — (Supervising Guide)

DECLARATION

I hereby declare that the work presented in this thesis entitled 'Studies on Propagation and Interaction of Multi-solitons in Inhomogeneous Optical Systems' is based on the original work done by me under the guidance of Dr. P. A. Subha, Department of Physics, Farook College, University of Calicut, and has not been included in any other thesis submitted previously for the award of any degree.

University of Calicut

October 2018 N. M. Musammil

Dedicated to

My Beloved

Parents and Family

Acknowledgements

Your depression is connected to your insolence and refusal to praise (Rumi)

I would like to take this opportunity to express my heartfelt gratitude to all those who helped me to fulfill my dream, this thesis.

I express my sincere and whole hearted thanks to my esteemed research supervisor **Dr. P. A. Subha**, Head of the Department of Physics, Farook College, Kerala, for giving me an opportunity to work under her guidance. Her understanding, guidance, encouragement, patience and personal involvement have helped me a lot to overcome all the uncertainty arises during this period. I am highly indebted to her untiring perseverance, which helped me to present this work in the right perspective.

I would like to express my deep sense of gratitude to **Prof. K. Porsezian**, Department of Physics, Pondicherry University, who, although no longer with us, continues to inspire by his example and dedication to the research activities over his entire career.

I express my heart full thanks, to my friend and esteemed mentor **Dr. K. Nithyanandan**, CNRS Post-Doctoral fellow, Laboratoire Interdisciplinaire de Physique, UMR 5588 CNRS, Université Grenoble Alpes, Saint Martin de Heres, France, for his grateful supports, motivations, valuable suggestions and fruitful discussions. I feel honored to have worked with him, who cares to keep enthusi-

asm in research programmes.

I was introduced to the interesting world of solitons by none other than **Dr. R. Radhakrishnan**, Department of Physics, Jamal mohammed college, Trichy, whose extensive knowledge and expertise in the subject guided me to choose this research area.

I express my sincere gratitude to **Prof. P. P. Pradyumnan**, Head of the Department of Physics and **Prof. M. M. Musthafa** and **Prof. Antony Joseph**, former Heads of the Department of Physics, University of Calicut for providing me all the support and essential facilities to carry out the research. I am deeply indebted to **Dr. T. Mohamed Shahin,** who is my co-guide for his kindness and encouragements. I also thank all the faculty members, library and office staff of the department for the help they rendered during the entire course of my research study.

Its my pleasure to acknowledge **Dr. E. P. Imbichikoya**, the former principal and **Dr. K. M. Naseer**, the Principal, Farook college for their support to complete my research work. **Prof. K. K. Abdullah**, the former HOD, Physics department deserves special mentioning for his interests in my research study and suggestions to improve the thesis. I am indebted to all the faculties of Department of Physics, Farook college for their encouragement. I owe greatly to **Amith**, IISc, Bengaluru, for his great support through providing necessary books.

I am deeply indebted to my **Mom**, who supported and encouraged me at every moment of my personal and academic life. There are no words to express my gratitude and thanks to My Beloved **Father**, **Wife**, **Sisters**, **All Family members**, **Teachers**, and **Friends**. Their love has been the major spiritual support in my life.

I would like to express my special thanks to the **UGC**, Government of India,

for the financial support through **MANF** without which this work would have been impossible.

I am really thankful to all my friends I really enjoyed the company of my research teams; K. Usha, T. P. Suneera, Sreepriya M.K, K. Aysha Muhsina, Remi, Jubeer, and Dr. Sudha Shankar and I express my gratitude for their encouragement and the fruitful discussions. I fondly remember the moments spent with all other research scholars especially Sulaiman, Ahammed Raseen, Prashanth, Shabeer, Shan, Jamshihas, Sebastian, Irshad, Nighilnadh, Najumunneesa, Sahra, Vidya Rajan, Divya, Deepthy Maria, Nithu, Ramsiya, Jisha, Hajara, Salma, Shabeeba, Safna hussain, Sitha Jagan, Vishnu, Anju, Sravan, Bintu, Bineesh, Sanila.

Research life in the University campus would have been miserable without the company of my co-researchers. We talked and argued over many topics at the evening unofficial tea breaks. I am really grateful to them for the delightful moments. The solitary life through the sound of forest, sound of birds and formidable silence of nights of the University campus was really enjoyable and unforgettable. Many time I have interrupted the deep sleep of my family, they deserve special thanks, I also express my gratitude towards them.

Above all, I thank **Almighty** who made me what I am and for providing all suitable circumstances for this achievement. As a final word, I would like to thank each and every individual who have been a source of support and encouragement and helped me to achieve my goal and complete my Thesis work successfully.

N. M. Musammil

List of Figures

List of Tables

Contents

Preface

Soliton is a localized wave which can propagate through nonlinear media without any considerable change of its form and preserve its identity even after collisions with each other. The solitons exhibit particle like properties due to its energy confinement to a limited region of space. The most significant technical application of the soliton is as a carrier of digital information along an optical fibre. The optical soliton formation is the outcome of exact balance between the group velocity dispersion (GVD) and the self-phase modulation (SPM).

The nonlinear Schrödinger equation (NLSE) is the governing model of soliton dynamics in single mode optical fibre. Based on the different signs of dispersion parameter, the NLSE admits temporal bright and dark optical solitons in fiber. Nevertheless, in many real situations, there exist two different polarizations in single-mode fibers, which split the injected soliton into two separate beams. The coupling of these bimodal propagation of pulses result in many fascinating phenomena, one such is the vector soliton. The coupled NLS equation (CNLSE) provides a quantitative description of such co-propagating solitons via the cross-phase modulation (XPM) mechanism. Several experiments on optical soliton propagation in fibres have shown that the output pulse has been found to be asymmetric due to the self-steepening(SS) effect. The modified nonlinear Schrödinger equation (MNLSE) is the governing model of the soliton propagation with SS effect. The SS results from the intensity dependence of the group velocity. This leads to an asymmetry in the SPM-broadened spectra of ultrashort pulses.

Recently, the NLSE with variable coefficients has been widely used for the

investigations of soliton propagation in real optical system. As a result of non-uniformities, influenced by the spatial variations of the fiber parameters, the realistic optical fiber medium exhibits inhomogeneous behavior. The conventional form of NLSE equations are inadequate in describing the various inhomogeneous behavior of fiber such as pulse amplification/absorption, periodic varying dispersion and nonlinearity, nonlinear tunneling, etc,. Thus to model a realistic fiber system, we have considered the variable coefficient NLSE (Vc-NLSE) governing the propagation of optical beam in an inhomogeneous fiber.

In this thesis, we have comprehensively studied the propagation and interaction of multi-solitons in inhomogeneous optical fiber system. We have studied the dark multi-solitons dynamics and corresponding phase evolution in Vc-NLSE model. The bright soliton intensity and the spatial dependent phase profiles in Vc-NLSE models has been investigated. The studies have been extended to Vc-CNLSE model which enable the vector dark soliton propagation in birefringent fiber systems. The bright and dark vector soliton propagation and phase dynamics of multi-solitons interactions in inhomogeneous Manakov model has been studied. Finally, the ultrashort dark soliton propagation with SS effect are deliberately studied by means of Vc-MNLSE model. The exact soliton solutions for these inhomogeneous models have been derived by Hirota bilinear method. The soliton phase dynamics has been investigated by an ansatz method. Numerically, the stability of the obtained solutions have been discussed. The obtained results are presented in appropriate chapters. The structure of the thesis is organized as follows:

In chapter 1, we describe a basic introduction to solitons, optical solitons, GVD, SPM, NLS equation, bright and dark temporal solitons in NLSE. Birefringent fiber, XPM, SS and soliton propagation in inhomogeneous fiber system. Moreover, a detailed explanations for analytical tools have been described in section methodology and the structure of dissertation is also presented with a brief highlight of each chapter. **Chapter 2** deals with the dark soliton dynamics in the Vc-NLSE with distributed dispersion, SPM and linear gain/loss. The one and

two dark soliton solutions have been derived by using Hirota's bilinear method. Numerically, we have studied the dark soliton propagation in the continuous wave background, and the simulations confirm that the soliton solution is stable and robust against perturbations. We have derived exact solution for the phase of dark solitons and studied the effect of blackness parameter and gain/loss coefficient on soliton phase profiles. Black and gray soliton interactions and elastic collision between dark solitons are exclusively studied via the asymptotic analysis. The studies on nonlinear tunneling of dark soliton through barrier/well, has been verified that the intensity of the tunneling soliton either forms a peak or valley and retains its shape after tunneling through barrier/well. **In chapter 3**, we investigate bright solitons dynamics in the Vc-NLSE model. Many fascinating results underlying spatial dependent bright soliton phase, which gives more insight for well-known inhomogeneous phenomena, such as dispersion managed system, pulse compression and especially nonlinear tunneling effect, have been studied. By connecting an ansatz method with Hirota bilinear technique, we have introduced an explicit form of bright soliton phase. **In chapter 4**, we extend the studies to the dynamics of vector soliton propagation in inhomogeneous fibres which has been modeled by Vc-CNLSE (inhomogeneous Manakov system). The dark soliton solutions in Vc-CNLSE have been derived by Hirota's bilinear method. **Chapter 5** deals with the phase dynamics of Manakov bright and dark vector soliton in inhomogeneous fibers by employing two component Vc-CNLS model. We have applied a general ansatz method to study the phase dynamics of the system, which enabled explicit analytical expressions for intensity as well as phase of the soliton. **In chapter 6**, we study the dynamics of ultrashort pulse propagation in the inhomogeneous fibre systems by means of Vc-MNLS model with distributed dispersion, SPM, SS and linear gain/loss. The effect of self-steepening such as shock wave formation during the propagation, has been confirmed through direct numerical simulation. **Chapter 7** summarizes the findings of the thesis and describes future prospects of this work.

List of Acronyms:

NLD	Nonlinear Dynamics
NLPDE	Nonlinear Partial Differential Equation
NLO	Nonlinear Optics
GVD	Group Velocity Dispersion
AGVD	Anomalous Group Velocity Dispersion
SPM	Self-Phase Modulation
EM	Electro Magnetic
NLSE	Nonlinear Schrodinger Equation
ZDW	Zero Dispersion Wavelength
DGD	Differential Group Delay
PMD	Polarization-Mode Dispersion
CNLSE	Coupled Nonlinear Schrodinger Equation
XPM	Cross-phase modulation
MNLSE	Modified Nonlinear Schrodinger Equation
SS	Self-Steepening
EDFA	Erbium Doped Fiber Amplifier
DM	Dispersion-management
Vc-NLSE	Variable coefficient Nonlinear Schrodinger Equation
HB	Hirota's bilinear

List of Publications

1. N.M. Musammil, P.A. Subha and K. Nithyanandan, Phase dynamics of inhomogeneous Manakov vector solitons, PHYSICAL REVIEW E 100, (2019)012213 (I. F:2.35, American Physical Society, ISSN 2470-0053).

2. N.M. Musammil, P.A. Subha and K. Nithyanandan, Black and gray soliton interactions and cascade compression in the variable coefficient nonlinear Schrödinger(NLS)equation. Optik 159 (2018) 176188 (I. F: 1.2, ELSEVIER, ISSN: 0030-4026).

3. N.M. Musammil, K. Porsezian , K. Nithyanandan, P.A. Subha, P. Tchofo Dinda, Ultrashort dark solitons interactions and nonlinear tunneling in the modified nonlinear Schrödinger(NLS)equation with variable coefficient. Optical Fiber Technology 37 (2017) 1120 (I. F: 1.64, ELSEVIER, ISSN:1068-5200) .

4. N. M. Musammil, K. Porsezian, P. A. Subha, and K. Nithyanandan, Dynamics of vector dark solitons propagation and tunneling effect in the variable coefficient coupled nonlinear Schrödinger(NLS)equation. Chaos 27 (2017), 023113 (I. F: 2.41, American Institute of Physics, ISSN 1089-7682)

5. N.M. Musammil and P.A. Subha, Bright solitons dynamics in the variable coefficient nonlinear Schrödinger equation, (Communicated).

List of International / National conference presentations:

1. Black and gray soliton propagation in the nonlinear Schrödinger(NLS)equation, International Conference on Nonlinear Physics: Theory and Experiment (NPTE-2016), Farook College, Kozhikode, Kerala.

2. Nonlinear tunneling effect of the antidark soliton, 28th Kerala Science Congress, 2016, University of Calicut, Kerala.

3. Pulse compression of antidark soliton in the vc-mnls equation, 27th Kerala Science Congress, 2015, Alappuzha, Kerala.(Best poster award)

4. Nonlinear tunneling effect of the dark soliton, National Conference on Modern Optics and Material Science (NCMOMS-2015), Farook College, Kozhikode, Kerala

5. Bright and dark optical solitons in the variable coefficient modified nonlinear schrodinger model with gain/ loss, 26th Kerala Science Congress, 2014, KVASU Wayanad.

6. Antidark soliton solutions in vc-mnlse, DAE-National Laser Symposium (NLS-23), 2014, Sri Venkateswara University, Andhra Pradesh.

7. Pulse compression of optical solitons in the variable coefficient modified nonlinear schrodinger model, DAE-National Laser Symposium (NLS-22), 2014, Manipal University, Karnataka.

8. The self-steepening effect on ultrashort bright and dark solitons in the vc-mnlse, Interational Conference on Nonlinear System and Dynamics (CNSD-2013), IIT Indore.

List of Seminars/ Workshops/ Schools attended:

1. National seminar on theoretical physics. March 2017, University of Calicut, Kerala.

2. National workshop on fourier transform and digital signal processing. Jan 2017, S. A. R. B. T. M GOVT. College, Koyilandi, Kerala.

3. National workshop on foundations of statistical and quantum mechanics. Jan 2017, S. A. R. B. T. M GOVT. College, Koyilandi, Kerala.

4. DAE-SERC School. March 2016, Pondicherry University, Puducherry.

5. National seminar on ibnul-haytham and his world of science. November 2015, University of Calicut, Kerala.

6. National conference on enchanting developments in advanced materials. July 2015, University of Calicut, Kerala.

7. National workshop on applications of matlab in basic sciences. July 2015, Farook College, Kozhikode, Kerala.

8. National seminar on light energy and enviorment. March 2015, Farook College, Kozhikode, Kerala.

9. National seminar on human rights education, July 2014, University of Calicut, Kerala

Chapter 1

Basic Concepts and Thesis Outline

1.1 Introduction

Nonlinearity is an ubiquitous behavior of nature in our day to day life. Nonlinear dynamics (NLD) provides mathematical implications of such mysterious, drastic and unpredictable phenomena of the real physical world. The terms chaos and solitons are the most commonly referred nomenclature in NLD, but their fundamental characteristics in nonlinear systems are completely different. Chaotic systems are unpredictable owing to great sensitivity to initial inputs, while soliton systems exhibit highly predictable behavior during the evolutions. In fact, most of the nonlinear systems are non-integrable but admit self-trapped solutions known as solitary waves.

A physical system which is driven by a nonlinear force and whose dynamics is described by nonlinear differential equation is referred to as a nonlinear dynamical system. In view of their important technological applications, soliton driven nonlinear systems have been focused throughout this thesis. Nowadays, solitons are observed in a large number of physical systems, but here we limit our focus to nonlinear optical systems especially to optical fibers. This introductory chapter

is intended to provide an overview of common behavior of solitons and their formation in optical systems. The review given here will play an indispensable role to understand the soliton dynamics discussed in later chapters. The objectives and the methodology of this thesis have been addressed. The structure of thesis is also presented with a brief highlight of each chapter.

1.2 Soliton

In the past few decades or so, the concept of soliton has created an enchanting areas of research across different fields of science and technology. Different types of solitons with approximately one hundred different mathematical models of nonlinear partial differential equations(NLPDE)have been reported in almost all diverse fields of science. Based on its behavior and the mathematical formulation of integrability, the commonly accepted description of the soliton can be defined as the 'solitons are localized waves which can propagate through nonlinear media without any considerable change of its form and preserve its identity even after collisions with each other' [1–5]. The solitons exhibit particle like properties due to its instantaneous energy confinement to a limited region of space.

Historically, the first documented observation of a solitary wave was made by a Scottish engineer, John Scott Russell in 1834. He observed a solitary wave evolution as, a rounded, smooth and well-defined heap of water propagating along the canal apparently without any change of its speed and shape over long distance[3]. He named it as the 'wave of Translation'. Later, Kortweg and de Vries considered the wave phenomenon underlying the observations of J S Russel and introduced the well-known KdV equation for the fluid dynamics. In this model, velocity is a function of wave amplitude, hence the higher amplitude wave travel faster than lower amplitude one. The word 'soliton' was first used by Zabusky and Kruskal in 1964. The shape preserving collision between solitary waves have been reported in their studies[3]. In recent trend, soliton-bearing systems get much attention from researchers, because of its presence are confirmed in various models such as nonlinear optics [1], Bose-Einstein Condensates

[6], hydrodynamics [3, 7], plasma [8] and waveguide arrays [9]. In this thesis, we have studied optical soliton propagation in the laser induced fiber systems.

1.2.1 Optical solitons

Nonlinear optics (NLO) describes the features of light-matter interaction in nonlinear media. Courtesy to the invention of lasers, by taking advantage of the high optical power to change the optical properties of materials, the nonlinear fiber optics finds important role in data transmission systems such as optical communication, switching, pulse reshaping, amplifiers, pulse compression, etc. The most significant technical application of the soliton is as a carrier of digital information along an optical fibre. In 1973, Akira Hasegawa was the first to suggest that solitons could exist in fibers and he also suggested the idea of a soliton-based transmission system to increases the bit rate of optical telecommunications [10]. The balancing between dispersion and nonlinearity is the reason to the formation of optical soliton in fiber [1, 10, 11]. That is, when high intense pulse propagate though a medium which usually gets broadening due to chromatic dispersion or diffraction. However the nonlinearity of the medium acts against this chirp and produce self-trapped light beams. These localized beams are called optical solitons. Based on its nature of confinement in time or in space, optical solitons are mainly classified into two types such as temporal and spatial optical solitons. In this thesis, we have focused on the temporal soliton dynamics in optical fiber media. The symbolic representation of temporal soliton is depicted in figure(1.1).

1.3 Group Velocity dispersion

When an optical pulse is propagated through dielectric waveguide, it suffers pulse broadening due to dispersion. An envelop of electromagnetic waves has many Fourier components which travel with different velocities in dispersive media. The measure of frequency dependent group velocity is referred to as Group Velocity dispersion(GVD) or chromatic dispersion [1, 4]. GVD is the

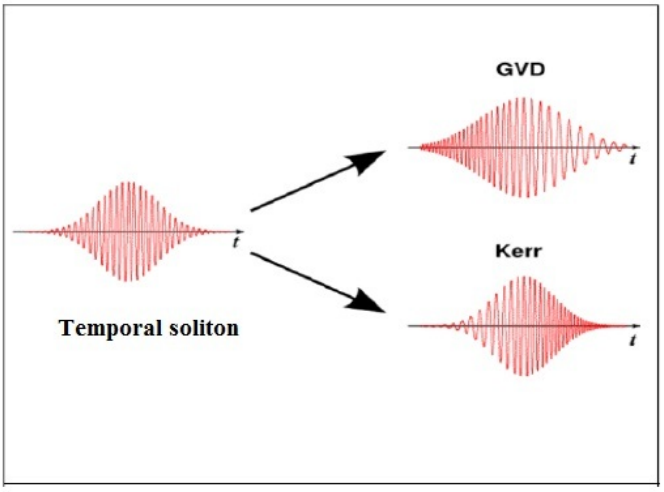

Figure 1.1: Temporal soliton formation (https://en.wikipedia.org/wiki/Soliton-(optics))

derivative of the inverse group velocity with respect to the angular frequency ($GVD = \frac{\partial}{\partial\omega}\frac{1}{v_g}$). As we know, the refractive index of optical system is a function of frequency ($n(\omega)$), the various Fourier components of the pulse will experience different indices of refraction in a dielectric medium. Change in refractive index with frequency may be increase or decrease, correspondingly two different kinds of pulse broadening occurs. The positive and the negative sign of the GVD is generally referred to as anomalous dispersion and normal dispersion regimes respectively. In the anomalous(normal) dispersion regime, the high frequency components travel faster(slower) than the low frequency components. In order to account the dispersion-induced broadening of a Gaussian pulse or hyperbolic secant pulse inside a fiber a parameter is important called dispersion length. It is defined as $L_D = \frac{T_0^2}{|\beta_2|}$. Where T_0 is the pulse width and β_2 is the GVD parameter [1].

1.4 Nonlinear phenomena in optical fiber

When an intense optical beam propagate through a dielectric medium, the bound electrons undergo anharmonic oscillation which produce nonlinear response in medium. As a result, higher order susceptibilities are inevitable and the total

induced polarization $\mathbf{P}$ by applied electric field satisfy the relation as

$$\mathbf{P} = \epsilon_{\mathbf{0}}(\chi^{(\mathbf{1})}.\mathbf{E} + \chi^{(\mathbf{2})}.\mathbf{EE} + \chi^{(\mathbf{3})}.\mathbf{EEE} + ...] \tag{1.1}$$

where ϵ_0 is the permittivity of vacuum, $\chi^{(j)}(j = 1, 2, ...)$ is the j^{th} order susceptibility. The $\chi^{(1)}$ represents linear effect and $\chi^{(2)}$, $\chi^{(3)}, ...$ are the nonlinear parts of higher order susceptibilities. In centrosymmetric materials, like silica the $\chi^{(2)}$ effect become zero due to the inversion symmetry of crystal. In silica fibers, the cubic nonlinearity ($\chi^{(3)}$) is responsible for various phenomena such as Kerr-effect, four-wave mixing, third harmonic generation, etc [1, 2, 5].

1.4.1 Self-phase modulation.

The Kerr effect is the phenomenon in which the refractive index of a material changes proportional to the square of the applied electric field. As a result, a intensity dependent nonlinear phase shift is happen along the fiber length. That is, the refractive index obeys the relation[1, 2, 4, 5]:

$$n = n_0 + n_2 I,$$

where $I = |E|^2$ is the intensity of laser beam, n_0 is the linear index of refraction and n_2 represent the Kerr nonlinearity. This implies that the phase velocity also becomes intensity dependent leading to broadening of the optical spectrum. This phenomenon is referred to as Self-phase modulation (SPM). That is, the self-induced phase shift due to its own intensity is called SPM [1].

The optical soliton formation is the outcome of exact balance between the group velocity dispersion (GVD) and the self-phase modulation (SPM). It was proposed by Hasegawa and Tappert [10] and experimentally reported later by Mollenauer *et al.*[11].

1.5 Nonlinear Schrödinger Equation

Nonlinear Schrödinger equation(NLSE) is an elegant basic model equation describing envelope wave propagation in optical media. In addition to that the NLSE is an example of a universal nonlinear model that describes many physical nonlinear systems such as hydrodynamics, nonlinear optics, nonlinear acoustics, quantum condensates, heat pulses in solids and various other nonlinear instability phenomena. The derivation of NLSE is described as follows;

The propagation of electromagnetic(EM) wave through a dielectric waveguide can be described by using Maxwells equations. The Maxwell's equation governing the propagation of EM wave through a dielectric medium is given by [1, 2, 4]:

$$\nabla^2 E - \frac{1}{c^2}\frac{\partial^2 E(r,t)}{\partial t^2} = \frac{1}{\epsilon_0 c^2}\frac{\partial^2 P(r,t)}{\partial t^2}, \tag{1.2}$$

where E is the electric field, c is the speed of light in free space, and ϵ_0 is the dielectric permittivity of the free space. The induced polarization P includes linear and nonlinear contributions:

$$\begin{aligned} &P(r,t) = P_L(r,t) + P_{NL}(r,t), \qquad (1.3)\\ &P_L(r,t) = \epsilon_0 \int \chi^{(1)}(t-t^{'})E(r,t^{'})dt^{'},\\ &P_{NL}(r,t) = \epsilon_0 \int\int\int \chi^{(3)}(t-t_1)(t-t_2)(t-t_3)E(r,t_1)E(r,t_2)E(r,t_3)dt_1dt_2dt_3. \end{aligned}$$

Here $\chi^{(j)}$ are the susceptibility tensors of corresponding orders. The time-dependent nature of the envelop of the pulse is written as:

$$E(r,t) = A(Z,t)F(x,y)e^{i\beta_0 Z}, \tag{1.4}$$

in which β_0 is the propagation constant and $F(x,y)$ is the transverse field distribution of the fundamental mode in a single-mode fiber. $A(Z,t)$ is the time-dependent amplitude which implies that each spectral component of the pulse moves with different speed inside the fiber owing to the chromatic dispersion.

Hence the refractive index varies with the frequency ω which is expressed as:

$$\tilde{n} = n(\omega) + n_2|E|^2. \tag{1.5}$$

The analysis is carried out in Fourier domain to incorporate the chromatic dispersion. The nonlinearity is treated as a perturbation. The Fourier transform of $A(Z,t)$ is represented by $\tilde{A}(Z,t)$ which obeys the equation:

$$\frac{\partial \tilde{A}(Z,t)}{\partial Z} = i[\beta(\omega) + \Delta\beta - \beta_0]\tilde{A}(Z,t). \tag{1.6}$$

Here $\beta(\omega) = k_0 n(\omega)$. The nonlinear part $\Delta\beta$ satisfies the relation:

$$\Delta\beta = k_0 n_2 |A|^2 \frac{\int_{-\infty}^{\infty}\int_{-\infty}^{\infty} |F(x,y)|^4 dxdy}{\int_{-\infty}^{\infty}\int_{-\infty}^{\infty} |F(x,y)|^2 dxdy}. \tag{1.7}$$

The Taylor expansion of $\beta(\omega)$ around ω_0 is written as:

$$\beta(\omega) = \beta_0 + (\omega - \omega_0)\beta_1 + (\omega - \omega_0)^2\beta_2 + ..., \tag{1.8}$$

where $\beta_j = \frac{d^j\beta}{d\omega^j}$. Taking inverse Fourier transform of equation 1.6 after substituting for $\beta(\omega)$, $A(Z,t)$ is obtained as:

$$\frac{\partial A}{\partial Z} + \beta_1\frac{\partial A}{\partial t} + i\beta_2\frac{\partial^2 A}{\partial t^2} = i\gamma|A|^2 A, \tag{1.9}$$

where $(\omega - \omega_0) \simeq \frac{\partial}{\partial t}$ in inverse Fourier transform, β_1 and β_2 are the first order dispersion effect $\frac{1}{v_g}$ and the group velocity dispersion parameter $\frac{d^2\beta}{d\omega^2}$ respectively. The nonlinear parameter γ is given by $\frac{n_2\omega}{cA_{eff}}$, n_2 being the intensity dependent refractive index with the effective mode area $A_{eff} = \frac{k_0 n_2 |A|^2}{\Delta\beta}$.

Transforming equation 1.9 by introducing new coordinates to a reference frame moving with the pulse such that $\tau = \frac{(t - \frac{z}{v_g})}{T_0}$, $z = \frac{Z}{L_D}$, and $u = \sqrt{\gamma L_D A}$, the NLSE for the optical field is obtained as:

$$i\frac{\partial u}{\partial z} + \frac{\beta_2}{2}\frac{\partial^2 u}{\partial t^2} + \beta|u|^2 u = 0. \tag{1.10}$$

where β_2 represents GVD and the third term β represent the SPM.

1.5.1 Bright and dark Solitons

As in any medium, the dispersion varies with wavelength and the optical fiber is no way exceptional. One of the characteristic features of silica glass fiber is the so-called zero dispersion wavelength (ZDW). It is the wavelength at which the GVD becomes zero, and with reference to the ZDW, there exist two regimes of dispersion based on the sign of the dispersion coefficient. Based on the different signs of dispersion parameter, the NLSE admits temporal bright and dark solitons. The temporal bright soliton exist in the case of anomalous dispersion while normal dispersion leads to dark soliton. In similar way, the spatial bright (dark) optical solitons are observed due to the balancing between diffraction and self-focusing (self-defocusing) nonlinearity of medium. The simple form of well-known bright and dark solitons in NLSE model are obtained as follows [1, 2]

$$u(z,t) = sech(t)\ exp(i\frac{z}{2}) \tag{1.11}$$

$$u(z,t) = tanh(t)\ exp(iz) \tag{1.12}$$

Here, the Eq. (1.11) and (1.12)respectively represent the bright and dark temporal solitons and its intensity profile is depicted in figure (1.2)

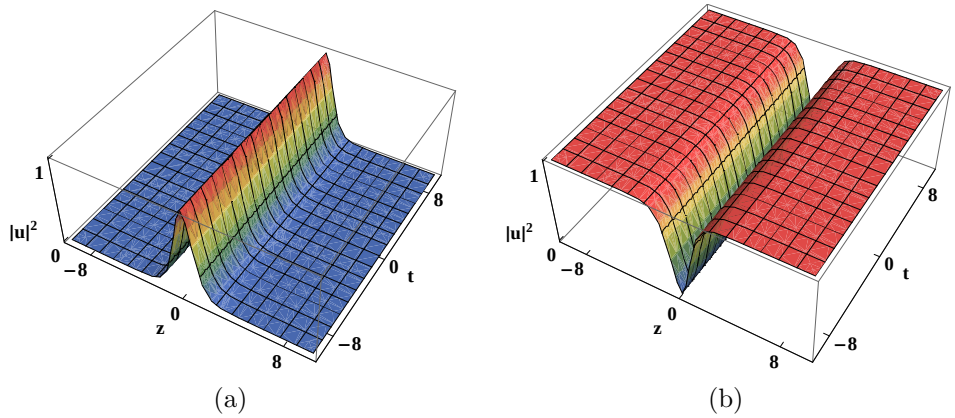

Figure 1.2: (a) bright soliton (b)dark soliton.

1.6 Birefringent fiber and soliton models

In real single-mode fibers, perfectly cylindrical core of uniform diameter is impossible due to anisotropic stress which produce considerable variation in the shape of their core along the fiber length [2]. This asymmetry of the core accounts for the emergence of birefringence in fiber. The effect of birefringence in single-mode optical fibers is an important consideration for soliton propagation because of a single injected soliton being split into two solitons of different polarizations [1]. These two modes may have different group velocities. That is, birefringence causes one polarization mode to travel faster than the other, resulting in a difference in the propagation time called the differential group delay(DGD), which results pulse broadening along the fiber. This phenomenon is called polarization-mode dispersion (PMD)[2]. A PMD is depicted in figure (1.3). The governing equations for bimodal propagation in a birefringent optical fiber are[1]

$$iq_{1z} + i\delta q_{1t} + \frac{1}{2}q_{1tt} + \mu(|q_1|^2 + B|q_2|^2)q_1 = 0 \tag{1.13}$$

$$iq_{2z} + i\delta q_{2t} + \frac{1}{2}q_{2tt} + \mu(|q_2|^2 + B|q_1|^2)q_2 = 0 \tag{1.14}$$

where B is the cross-phase modulation coupling parameter and δ governs the group-velocity mismatch between the two polarization components (walk-off effect).

In high birefringence fibers, the group-velocity mismatch between the fast and slow components of the input pulse cannot be neglected($\delta \neq 0$). But, in the case of low birefringence fibers, the difference between group velocities can typically be ignored ($\delta \approx 0$). The group-velocity mismatch can be neglected, if wave guide exhibit nearly constant birefringence along their entire length. This kind of birefringence is called linear birefringence. In practice, optical fibers exhibit randomly varying birefringence, over a length scale $10m$ unless special precautions are taken [1]. Generally, the walk-off term cannot be neglected in random birefringence model. It means that co-propagation of pulse (vector soli-

ton) can observe in fiber under the consideration of small length where the fiber is assumed to have linear birefringence. In polarization-maintaining fibers, the built-in birefringence is made much larger than random changes occurring due to stress and core-shape variations. As a result, polarization-maintaining fibers exhibit nearly constant birefringence along their entire length [1].

The walk-off effect plays an important role in the description of the nonlinear phenomena involving two or more closely spaced optical pulses. It arises due to the group-velocity mismatch of pulses. But, under certain conditions the two orthogonally polarized solitons move with a common group velocity in spite of their different modal indices or PMD. This phenomenon is called soliton trapping [1] . The phenomenon of soliton trapping suggests that the coupled NLS equations (CNLSE) may possess exact solitary-wave solutions with the property that the orthogonally polarized components propagate in a birefringent fiber without change in shape. Such solitary waves are referred to as vector solitons [1]. In this thesis, we have focused such kind of vector soliton propagation in the two component CNLSE with the specific value of parameter $B = 1$ (so-called Manakov model) in fiber system. It does not contain walk off term under certain mathematical and physical assumptions. The existence of these solitons model can be employed under specific conditions that involves severe constraints on the nonlinearity coefficient. From a physical view point, these constraints impose the condition that the ratio between the SPM and XPM in the coupling constants must be equal to unity and the SPM coefficients need to be equal for the two polarizations. Thus, the Manakov model can be written as [12–18];

$$iq_{1z} + \frac{1}{2}q_{1tt} + \mu(|q_1|^2 + |q_2|^2)q_1 = 0 \tag{1.15}$$

$$iq_{2z} + \frac{1}{2}q_{2tt} + \mu(|q_2|^2 + |q_1|^2)q_2 = 0 \tag{1.16}$$

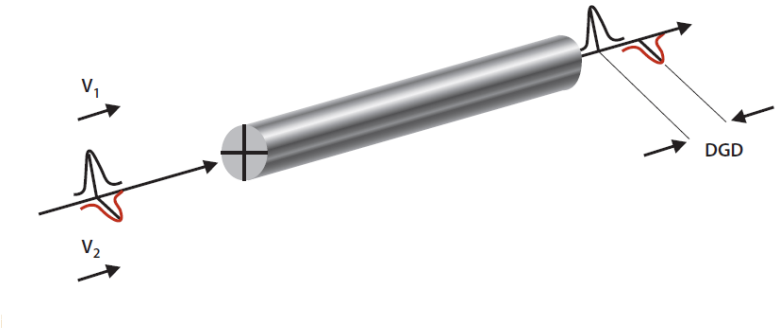

Figure 1.3: Polarization mode dispersion (http://fobasics.blogspot.com /2012/07/ polarization-mode-dispersion.html)

1.6.1 Cross-phase modulation

Cross-phase modulation refers to the the nonlinear phase shift of an optical field induced by another field having a different mode of polarization, different wavelength or direction usually referred to as Cross-phase modulation (XPM) [1]. When considering multiple signals in same fiber with different wavelengths, one wavelength of light can affect the phase of another wavelength through the XPM mechanism. It acts between multiple signals rather than within a single signal. It also deals the coupling phenomenon between the two orthogonally polarized components in birefringent fibers [1, 2].

1.7 Self-steepening effect

Self-steepening (SS) results from the intensity dependence of the group velocity. This leads to an asymmetry in the SPM-broadened spectra of ultrashort pulses. In several experiments on optical soliton propagation in fibers, the output pulse has been found to be asymmetric due to the SS effect[1]. This is found to be crucial in optical communication system, especially in the ultrashort pulse propagation in long distance optical fibers system. Self-steepening creates an optical shock on the trailing edge of the pulse in the absence of the GVD effects. This phenomenon is due to the intensity dependence of the group velocity that results in the peak of the pulse moving slower than the wings[1]. The modified nonlin-

ear Schrödinger equation (MNLSE) is governing model of the soliton propagation with SS effect [19–24]

$$iq_z + \frac{1}{2}q_{tt} + \mu(q|q|^2) + is(q|q|^2)_t = 0 \tag{1.17}$$

where the coefficient s represent the SS effect.

1.8 Soliton propagation in inhomogeneous fiber

Signal degradation in optical fibers mainly occurs due to attenuation and dispersion. The attenuation is a measure of power loss of beams that occurs as signal propagates through the length of fiber. The optical signal will be weaker as it propagates down the fiber because impurities in the glass can absorb light. As a result its power gradually decreases with distance. By considering the mode of fiber, the signal distortion mechanism due to dispersion effect can be classified into two types such as modal dispersion and chromatic dispersion. In multi-mode fibers, velocity of the optical signal is not the same for all modes which usually referred to as modal dispersion. Here, we have restricted our discussion to single-mode fibers, which are the commonly used fibers for long distance communication systems. In single-mode fibers, chromatic dispersion is inevitable which occurs by the different spectral components of a pulse that travel at different velocities.

In fact, in order to transmit signals over long distances it is necessary to regenerate optical pulses which have been distorted by dispersion and attenuation within the fiber. To compensate the power loss by amplification, one way is to use Raman gain of the fiber itself. The inventions of Erbium Doped Fiber Amplifier (EDFA) have augmented the concept of all-optical transmission systems to more realistic levels. It helps to overcome fiber loss. However, due to considerable chromatic dispersion it does not retain the amplified signal to its original state. Dispersion-management(DM) schemes attempt to compensate this dispersion problem so that the input signal can be restored back to its original shape.

Recently, DM fiber is realized for high-speed long-distance optical communication. In this thesis, we have also explained gain/loss and DM soliton in optical fiber systems by means of inhomogeneous NLS equations.

In all the earlier investigations, the NLSE considered was for the ideal optical fiber with constant coefficients. However, as a result of non-uniformities, influenced by the spatial variations of the fiber parameters, the realistic optical fiber medium exhibits inhomogeneous behavior. The variable coefficient NLS (Vc-NLSE) model may serve as a practical model for describing the soliton dynamics in inhomogeneous systems [25–31].

$$iq_z + \frac{1}{2}D(z)q_{tt} + R(z)(q|q|^2) + ip(z)q = 0 \tag{1.18}$$

where, the dispersion, Kerr nonlinearity and amplification/absorption effects are related to the respective coefficient functions $D(z)$, $R(z)$ and $p(z)$.

1.9 Methods of Analysis

Nowadays, different analytical methods are available to find out explicit form of soliton solutions for NLPDE model such as Bcklund transformation, Inverse scattering transform (IST) method, Lax pair, Hirota's bilinearization method, etc. Out of which we particularly focused on Hirota's approach which is a versatile analytical method capable of rendering exact soliton solution for many nonlinear evolution equations, including NLS, K-dV and sine-Gordon equation.

1.9.1 Hirota's bilinearization method

Ryogo Hirota invented this method in 1971 which was one of the milestones in the history of solitons solution. He published an article giving a new method called the Hirota direct method to find the exact solution of the KdV equation for multiple collisions of solitons [8]. In his successive articles, he dealt also with many other nonlinear evolution equations such as the modified Korteweg-de Vries (mKdV) , sine-Gordon (sG) , nonlinear Schrödinger(NLS) and Toda lattice (TL) equations. Hirota bilinear method is the one of the most famous

method to construct multi-soliton solutions. Single soliton solutions can be found easily by using the travelling wave ansatz f = f(x - vt), but explicit N-soliton solutions can only be found for integrable equations. Although several analytical techniques continue to evolve over the years, arguably the Hirota bilinear method remain as the most reliable method for N-soliton solutions. It is important to realize that PDE's appearing in a given physical problem is not usually in the best form for the subsequent mathematical analysis. Hirota noticed that the best dependent variables for constructing soliton solutions are those in which the solution appears as a finite sum of exponentials [32].

The first step of this method is to make suitable transformations for NLPDE which provide a set of equations in quadratic form. This new form is called 'bilinear form'. To find such a transformation is not easy for some equations and sometimes it requires the introduction of new dependent and sometimes even independent variables. As a second step we introduce a special differential operator called Hirota D-operator which is used to write the bilinear form of the equation as a polynomial of D-operator which we call the Hirota bilinear form. The last step of the Hirota method is using the perturbation expansion, which becomes finite as we will see, in the Hirota bilinear form and analyzing the coefficients of the perturbation parameter and its powers separately. At that point the information we gained makes us to reach to multi-soliton solutions if the equation is integrable. The Hirota direct method has taken an important role in the study of integrable systems. Hirotas method requires: a clever change of dependent variable, the introduction of a novel differential operator and a perturbation expansion to solve the resulting bilinear equation.

Properties of Hirotas Bilinear Operators

Here, we give some insights of properties of the Hirota derivative operators, D_z, D_t that defined by [32]

$$D_z^m D_t^n (g.f) = (\frac{\partial}{\partial z} - \frac{\partial}{\partial z'})^m (\frac{\partial}{\partial t} - \frac{\partial}{\partial t'})^n \times g(z,t) f(z,t)|_{z'=z, t'=t}$$

There are some first few derivatives of above equation are given explicitly as follows:

$$D_z(g.f) = g'f - gf'$$

$$D_z^2(g.f) = g''f - 2f'g' + gf''$$

and so on..

From this definitions, one can find the relations between D-operators and partial differential operators as follows;

$$\begin{aligned}
D_z^m(f.1) &= (\frac{\partial}{\partial z})^m\ f \\
D_z^m(f.g) &= (-1)^m D_z^m(f.g) \\
D_z^m(f.f) &= 0 \quad (for\ odd\ m) \\
D_z D_t(f.f) &= 2D_z(f_t.f) \\
D_z(fg.h) &= (\frac{\partial f}{\partial z})gh + f(D_z(f.g)) \\
\frac{\partial}{\partial z}(\frac{f}{g}) &= \frac{D_z(f.g)}{g^2} \\
\frac{\partial^2}{\partial z^2}(\frac{f}{g}) &= \frac{D_z^2(f.g)}{g^2} - \frac{f}{g}\frac{D_z^2(f.g)}{g^2}
\end{aligned}$$

and so on...

The Hirotas perturbation method and the multi-soliton solutions.

In fact, Hirota introduced this new technique to find exact soliton solution of NLPDE. As in the standard perturbation method, we can expand g and f as a power series in a small parameter ε. Substituting the expansion series into bilinear equation and collecting terms of each order of ε we obtain some relations. This procedure may look as a common practice of perturbation method, but the effect of D-operator will be quite different from normal derivative in the collected terms of each order. If the series is truncated at particular level (say N) then we can choose the next term of perturbation expansion (N+1) equal to zero. It would not be possible in normal derivative. This shows that the expansion of g and f may be truncated as the finite sum. When substituting all the terms

back into the expansion of the original fields, the perturbation parameter ε can be absorbed into the phase constant of exponential function. *i.e.* its effect will not be presented in final solution. In this context, the phenomenon of re-enforcing of small parameter will not happen in full solution. It is the procedure of Hirota bilinearization method. Thus, the final form gives an exact solution of the bilinear equation. Here, the perturbation method is used for finding exact solution [32–38].

Consider the nonlinear partial differential equation $F[u] = 0$ whose Hirota bilinear form is in the form $P(D)g.f = 0$ and we give some steps to finding exact solutions of $F[u] = 0$ by using its Hirota bilinear form. We can use the perturbation series, For this purpose, let us write $f = 1+\varepsilon^1 f_1+\varepsilon^2 f_2+\varepsilon^3 f_3+....$ and $g = 1+\varepsilon^1 g_1+\varepsilon^2 g_2+\varepsilon^3 g_3+....$ where f_j and g_j $(j = 1, 2, ..)$ are functions of $z, t, .$ and so on. ε is called the perturbation parameter. Then,

$$P(D)(g.f) = P(D)(1.1) + \varepsilon\ P(D)(g_1.1 + 1.f_1)+ \\ \varepsilon^2\ P(D)(g_2.1 + g_1.f_1 + 1.f_2) + ... = \ 0$$

Let $u = T[f(x, t)]$ be a bilinearizing transformation of a given equation $F[u] = 0$, which can be written in the Hirota bilinear form $P(D)(g.f) = 0$. To satisfy this equation we make the coefficients ε^j trivially zero. By equating the the coefficient of small parameter ε^j given us,

$$\varepsilon^0 = P(D)(1.1)$$
$$\varepsilon^1 = P(D)(g_1.1 + 1.f_1)$$
$$\varepsilon^2 = P(D)(g_2.1 + g_1.f_1 + 1.f_2)$$

One-Soliton solution

To construct one-soliton solution $F[u] = 0$ we can take lowest order of expansion series as $f = 1 + \varepsilon^1 f_1$ and $g = 1 + \varepsilon^1 g_1$. Where $f_1 = g_1 = e^{\theta_1}$ with $\theta_1 = k_1 x + \omega_1 t + \theta_0$. Then the coefficients of ε^0 is, $P(D)(1.1) = 0$. Similarly the

coefficients of ε^1 obtained as

$$P(D)(g_1.1 + 1.f_1) = 2P(\partial)e^{\theta_1} = 0$$

Here we obtain a dispersion relation $P(k_1, \omega_1) = 0$. Then, take the coefficients of ε^2;

$$P(D)(g_2.1 + g_1.f_1 + 1.f_2) = 0$$

this satisfy the condition that

$$P(D)(g_2.1 + 1.f_2) = -P(D)(g_1.f_1)$$

$$P(D)(e^{\theta_1}.e^{\theta_1}) = P(p_1 - p_1)e^{2\theta_1} = 0$$

we get $f_2 = g_2 = 0$. This is an important difference between bilinear and normal differential equations. That is, we can choose the second term of perturbation expansion f_2 equal to zero. After absorbing ε (we may set $\varepsilon = 1$), the exact one-soliton solution of $F[u] = 0$ can be written as

$$u = T[f(x,t)] = T[1 + e^{\theta_1}]$$

Two-Soliton solution

To construct two-soliton solution $F[u] = 0$ we can take the expansion series as $f = 1 + \varepsilon^1 f_1 + \varepsilon^2 f_2$ and $g = 1 + \varepsilon^1 g_1 + \varepsilon^2 g_2$, where $f_1 = g_1 = e^{\theta_1} + e^{\theta_2}$, $\theta_1 = k_1 x + \omega_1 t + \theta_{01}$ and $\theta_2 = k_2 x + \omega_2 t + \theta_{02}$. Similar to the one-soliton case, the coefficients of ε^0 is, $P(D)(1.1) = 0$. The coefficients of ε^1 turns out to be

$$P(D)(g_1.1 + 1.f_1) = 2P(\partial)(e^{\theta_1} + e^{\theta_2}) = 0$$

by taking the coefficients of ε^2, we have

$$P(D)(g_2.1 + g_1.f_1 + 1.f_2) = 2P(\partial)f_2 + 2P(D)[(e^{\theta_1}.e^{\theta_2}).(e^{\theta_1}.e^{\theta_2})]$$
$$= 2P(\partial)f_2 + 2P(p_1 - p_2)(e^{\theta_1+\theta_2}) = 0$$

Thus, f_2 should be in this form $f_2 = A_{12}\ e^{\theta_1+\theta_2}$. From the above equation, we get

$$A_{12} = -\frac{P(p_1 - p_2)}{P(p_1 + p_2)}$$

The coefficient of ε^3 becomes,

$$P(D)(g_3.1 + g_2.f_1 + g_1.f_2 + 1.f_3) = 0$$

Here, we can choose the third term of perturbation expansion $f_3 = g_3$ equal to zero. Then,

$$P(D)(g_2.f_1 + g_1.f_2) = A_{12}[P(D)((e^{\theta_1} + e^{\theta_2}).e^{\theta_1+\theta_2}) + P(D)(e^{\theta_1+\theta_2}.(e^{\theta_1} + e^{\theta_2}).e^{\theta_1+\theta_2})]$$
$$= A_{12}[P(D)((e^{\theta_1}).(e^{\theta_1+\theta_2})) + P(D)((e^{\theta_2}).(e^{\theta_1} + e^{\theta_2}))]$$
$$= A_{12}[P(p_2)e^{2\theta_1+\theta_2} + P(p_2)e^{2\theta_1+2\theta_2}]$$

Thus, the two-soliton solution of $F[u] = 0$ can be written as

$$u = T[f(x,t)] = T[1 + e^{\theta_1} + e^{\theta_2} + A_{12}\ e^{\theta_1+\theta_2}]$$

By the same procedures of Hirotas biliniarization method one can find out the exact solution for N-solitons level. These are the fundamental steps of HB method.

1.9.2 Ansatz method for Soliton solution

A basic form of NLS equation for the anomalous regime can be written as [1];

$$iq_z + \frac{1}{2}q_{tt} + q|q|^2 = 0 \tag{1.19}$$

The corresponding fundamental bright soliton can be obtained by solving Eq. (1.19) directly, with assuming a solution of the form[4]

$$q(z,t) = \sqrt{\rho(z,t)}e^{i\phi(z,t)} \tag{1.20}$$

Substituting this expression into Eq. (1.19) and separating the real and imaginary parts, we obtain[4]

$$\rho_z + \frac{\partial}{\partial t}(\rho\phi_t) = 0 \tag{1.21}$$

$$\rho + \frac{1}{8\rho^2}\rho_t^2 - \frac{1}{4\rho}\rho_{tt} - \frac{1}{2}\phi_t^2 - \phi_z = 0 \tag{1.22}$$

The stationary condition for $|q|^2$ gives $\rho_z = 0$. By using Eq. (1.21), we obtain $\phi = \int \frac{c_1}{\rho}dt + \Omega z$, where $\Omega = \frac{dA}{dz}$, c_1 and $A(z)$ are integration constants. Hence, the expression for phase can be written as

$$\phi = \int \frac{c_1}{\rho_0}dt + \Omega z \tag{1.23}$$

by using this expression in (1.22), we obtain the following ordinary differential equation for $\rho(t)$

$$(\frac{d\rho}{dt})^2 = -4\rho^3 + 8\Omega\rho^2 - c_2\rho - 4c_1^2 \tag{1.24}$$

In the case of bright envelop, we can take $c_1 = c_2 = 0$ [4]. Then Eq.(1.24)can be reduce as

$$(\frac{d\rho}{dt})^2 = -4\rho^2(\rho - \rho_s) \tag{1.25}$$

where $\rho_s = 2\Omega$. By integrating Eq.(1.25), we obtain the bright soliton solution

as follows

$$q(z,t) = \sqrt{\rho_s} Sech[\sqrt{\rho_s} t] \;\; e^{i\phi(z,t)} \tag{1.26}$$

Similarly, NLS equation for the normal dispersion regime can be written as;

$$iq_z - \frac{1}{2} q_{tt} + q|q|^2 = 0 \tag{1.27}$$

by assuming a solution of the form as given in Eq. (1.20), we get

$$(\frac{d\rho}{dt})^2 = 4\rho^3 + 8\Omega\rho^2 + c_2\rho - 4c_1^2 \tag{1.28}$$

for the dark soliton, Eq.(1.28)can be cast into the following form

$$(\frac{d\rho}{dt})^2 = 4(\rho - \rho_0)^2(\rho - \rho_s) \tag{1.29}$$

By integrating Eq.(1.29), we obtain the dark soliton solution as follows[4]

$$q(z,t) = \sqrt{\rho_0[1 - a^2 Sech^2[\sqrt{\rho_0} t]} \;\; e^{i\phi(z,t)} \tag{1.30}$$

These are the basic form of bright and dark soliton.

1.10 Outline of the thesis

This thesis presents a comprehensive theoretical study on the propagation and interaction of multi-solitons in inhomogeneous optical systems. The exact one and multi soliton solutions of the NLS model is derived by Hirota bilinear method. Solitons phase are studied by using direct ansatz method. Soliton interactions are investigated by the asymptotic analysis.

In Chapter 2, we present the theoretical study of dark soliton dynamics in inhomogeneous fiber system by means of a variable coefficient nonlinear Schrödinger equation (Vc-NLSE). The dark soliton interaction in the dispersion-managed system with gain/loss and cascaded compression of solitons by the

nonlinear tunneling phenomena are studied in detail. Numerically, we study the dark soliton propagation in the continuous wave background, and the soliton solution is found to be robust against perturbations. The elastic collision behavior of the dark solitons are observed by means of asymptotic analysis. For better insight, we study the impact of the blackness factor in the phase profile and also on the interaction dynamics of the different dark soliton settings, such as black and gray soliton. Additionally, we extend the study to the investigation of tunneling of the dark soliton across the barrier/well with a particular emphasize on the role of blackness parameter in the nonlinear tunneling phenomena, and demonstrated a cascaded compression of soliton in the inhomogeneous system.

In Chapter 3, we have investigated the bright solitons dynamics in the Vc-NLS equation. Many fascinating results underlying spatial dependent bright soliton phase, which gives more insights for wellknown inhomogeneous phenomenons, such as dispersion managed system, pulse compression and especially nonlinear tunneling effect, have been reported. By connecting an ansatz method with Hirota bilinear technique, we have introduced an explicit form of bright soliton phase. Exact bright two-soliton solution has also been derived by using the Hirota bilinear method. The elastic collision behavior of the bright solitons are observed by means of asymptotic analysis. Two-soliton phase are studied by the asymptotic expression which gives the description of individual solitons that existing before and after collision. Moreover, with a particular interest, we have been investigated the tunneling effect through the dispersion barrier or well. Soliton intensity either forms a peak or valley and regain its shape after the tunneling through the barrier/well. For the case of exponential background, the soliton tends to compress after tunneling. Corresponding phase evolutions are illustrated in detail. For better insight, we have studied the cascade compression of solitons with multiple successive dispersion barriers.

In Chapter 4, we have extended the studies to the dynamics of vector soliton propagation in inhomogeneous fibres which have been modeled by Vc-CNLSE (inhomogeneous Manakov system). The dark soliton solutions in Vc-CNLSE

have been derived by Hirota's bilinear method. Through the analytical soliton solutions and detailed graphical illustration, the propagation dynamics and collision behaviors of the dark soliton pulses in inhomogeneous fibers have been discussed. Especially, we have studied the almost all dynamical related physical quantities up to the level of three-dark solitons interactions. The inhomogeneous effects on the evolution and interaction between dark solitons have also been considered. The shapes and velocities of the dark solitons can be controlled by modulating dispersion and gain/loss terms. The gain or loss term affects the amplitude and energy. The results obtained in this paper will be of good scientific value to the studies related to the propagation of dark solitons in the dispersion and nonlinear managed fiber systems. Finally, we have investigated the nonlinear tunneling effect of optical dark solitons with and without exponential background. It has been reported that tunneling of the soliton depends on a condition related to the height of the barrier and the soliton amplitude. The intensity of the tunneling soliton either forms a peak or valley and retains its shape after tunneling through barrier/well. We also identified the tunneling of dark soliton with exponential background tends to compress the pulse.

In Chapter 5, we report the exact phase of Manakov bright and dark vector solitons in inhomogeneous optical systems by means of Vc-CNLS equation. To investigate the phase dynamics, we have modified Manakov system with a relation between two modes of propagation, that obtained by the Hirota bilinear method. The importance of phase study in soliton interactions are revealed by asymptotic analysis of two-soliton solutions. In contrast with Manakov bright soliton, the time dependent dark vector soliton exhibit a gradual phase shift due to the blackness factor. The various inhomogeneous effects on the soliton phase are investigated, with a particular emphasize on nonlinear tunneling. The intensity and corresponding phase of the tunneling soliton either forms a peak or valley and retains its shape after the tunneling. Unlike the bright counterpart, the gain or loss term significantly affects on the phase of dark soliton. Apart from the study of soliton intensity, the phase profile of bright and dark vector

solitons and its dynamical importance are explored.

In Chapter 6, we present the study of the dark soliton dynamics in an inhomogeneous fiber by means of a variable coefficient modified nonlinear Schrdinger equation (Vc-MNLSE) with distributed dispersion, self-phase modulation, self-steepening and linear gain/loss. The ultrashort dark soliton pulse evolution and interaction is studied by using the Hirota bilinear (HB) method. In particular, we give much insight into the effect of self-steepening (SS) on the dark soliton dynamics. The study reveals a shock wave formation, as a major effect of SS. Numerically, we study the dark soliton propagation in the continuous wave background, and the stability of the soliton solution has been analysed in the presence of photon noise. The elastic collision behaviors of the dark solitons are discussed by the asymptotic analysis. On the other hand, considering the nonlinear tunneling of dark soliton through barrier/well, we find that the tunneling of the dark soliton depends on the height of the barrier and the amplitude of the soliton. The intensity of the tunneling soliton either forms a peak or valley and retains its shape after the tunneling. For the case of exponential background, the soliton tends to compress after tunneling through the barrier/well.

Chapter 7 summarizes the findings of the thesis and describes future prospects of this work.

Bibliography

[1] G.P. Agrawal, Nonlinear Fiber Optics, Academic, New York, 2013.

[2] G.P. Agrawal , Fiber-Optic Communication Systems, John Wiley and Sons,2002

[3] M.Lakshmanan and S.Rajashekar, Nonlinear dynamics Integrability chaos and patterns (Springer 2002)

[4] A.Hasegawa and M.Matsumoto, Optical Solitons in Fibers,Springer-Verlag Berlin Heidelberg, 2003

[5] N. N. Akhmediev and A. A. Ankiewicz. Solitons Nonlinear Pulses and Beams. Chapman and Hall, London, 1997.

[6] T. Tsurumi and M. Wadati,Soliton Propagation in a Bose-Einstein Condensate, J.Phys. Soc. Jpn. 67 (1998)2294-2299 .

[7] A. Chabchoub, O. Kimmoun, H. Branger, N. Hoffmann, D. Proment, M. Onorato, and N. Akhmediev, Phys. Rev. Lett. 110 124101(2013)1-4

[8] Tao Xu, Bo Tian, Li-Li Li, Xing L, and Cheng Zhang, Phys. Plasmas 15 102307(2008)1-6

[9] D. Mandelik, R. Morandotti, J. S. Aitchison, and Y. Silberberg Phys. Rev. Lett. 92 093904(2004)1-4

[10] A. Hasegawa and F.D. Tappert, Appl. Phys. Lett. 23 (1973) 142144.

[11] L.F. Mollenauer, R.H. Stolen, and J.P. Gordon, Phys. Rev. Lett. 45 (1980) 10951098.

[12] S.V. Manakov, Sov. Phys. JETP **38**,248 (1974).

[13] G. Agrawal, Phys. Rev. Lett. **59**, 880 (1987).

[14] C. R. Menyuk, IEEE J. Quantum Electron, **QE-25**, 2674(1989).

[15] J. U. Kang, G. I. Stegeman, J. S. Aitchison, and N. Akhmediev, Phys. Rev. Lett. **76**, 3699 (1996).

[16] B. Frisquet, B. Kibler, J. Fatome, P. Morin, F. Baronio, M. Conforti, G. Millot and S. Wabnitz , Phys. Rev. A **92**,053854(2015).

[17] B. Crosignani and P. Di Porto, Opt. Lett. **6**, 329 (1981).

[18] D. J. Kaup and B.A. Malomed, Phys. Rev. A **48**,599 (1993).

[19] F. De Martini, C. H. Townes, T. K. Gustafsson, and P. L. Kelley, Self-Steepening of Light Pulses,Phys. Rev. 164(1967)312-323 .

[20] D. Anderson and M. Lisak, Phys. Rev. A 27(1983)1393-1398 .

[21] J. R. de Oliveira and M. A. Moura, Phys. Rev. E 57(1998) 4751-4756 .

[22] Jeffrey Moses, Boris A. Malomed and Frank W. Wise1, Phys. Rev. A 76 021802(R)(2007)1-4 .

[23] Seung-Ho Han and Q-Han Park, Phys. Rev. E 83 066601(2011)1-6 .

[24] Yu Yu , Jia Wei-Guo, Yan Qing,Menke Neimule and Zhang Jun-Ping, Chin. Phys. 24(8) 084210(2015) 1-7.

[25] V.N. Serkin, A. Hasegawa, Phys. Rev. Lett. 85 (2000) 45024505.

[26] I. Gabitov, E.G. Shapiro, S.K. Turitsyn, Phys. Rev. E 55 (1997) 3624

[27] Lakoba T I and Kaup D J, Phys. Rev. E 58 (1998)6728

[28] V.I. Kruglov, A.C. Peacock, J.D. Harvey, Phys. Rev. Lett. 90 (2003) 113902.

[29] S.H. Chen, L. Yi, Phys. Rev. E 71(2005)016606

[30] W.J. Liu, B. Tian, H.Q. Zhang, Phys. Rev. E 78(2008) 066613 .

[31] Rongcao Yang, Lu. Ruiyu Hao, Xiaojuan Shi Li, Zhonghao Li, Guosheng Zhou, Opt. Commun. 253 (2005) 177185.

[32] R. Hirota, The Direct Method in Soliton Theory Cambridge University Press, Cambridge, 2004.

[33] T. Kanna, M. Lakshmanan, Phys. Rev. Lett. 86(2001)5043-5046

[34] W.J. Liu, B. Tian, H.Q. Zhang, L.L. Li, Y.S. Xue, Phys.Rev. E 77 (2008)066605

[35] R.Radhakrishnan and M.Lakshmanan, J.Phys.A:Math.Gen.28 (1995)2683-2692.

[36] K. Porsezian, K. Nakkeeran, Phys. Rev. Lett. 76 (1996)3955 .

[37] Liu W J, B Tian, H Q Zhang, T Xu and H Li, Phys. Rev. A 79(2009) 063810

[38] N. M. Musammil, K. Porsezian, P. A. Subha3, and K. Nithyanandan, Chaos 27, 023113 (2017)1-12

Chapter 2

Black and gray soliton interactions and cascade compression in the Vc-NLS equation

2.1 Introduction

The stable propagation of localized bright and dark optical pulse were verified in many different theoretical and experimental settings. Unlike the bright soliton on a zero-intensity background, the dark soliton appears as rapid intensity dips on a continuous wave background. Compared to the bright, the dark solitons are said to exhibit better stability and robustness against the various fiber noises and perturbation effects. Although there are certain similarities between the two soliton types, conceptually they are different and therefore, naturally both exhibit distinct properties and applications [1–9].

Recently, the NLSE with variable coefficients has been widely used for the investigations of soliton propagation in real optical system. The conventional form of NLSE equations are inadequate in describing the various inhomogeneous

behavior of fiber such as pulse amplification/absorption, periodically varying dispersion and nonlinearity etc., and therefore, realizing complex phenomena like nonlinear tunneling remain far-fetched. Thus to model a realistic fiber system, we consider the following variable coefficient NLSE(Vc-NLSE) governing the propagation of optical beam in an inhomogeneous fiber [10–17]:

$$iq_z - \frac{1}{2}D(z)q_{tt} + R(z)(q|q|^2) + ip(z)q = 0 \tag{2.1}$$

where $q(z,t)$ is the complex amplitude of the pulse envelope, the variables z and t represent the normalized spatial and temporal coordinates. The dispersion, Kerr nonlinearity and amplification/absorption effects are related to the respective coefficient functions $D(z)$, $R(z)$ and $p(z)$. To construct the dark soliton solutions for the model (2.1), we use Hirota's bilinear method, which can provide an explicit analytical expressions for the soliton pulses [18–26]. Through this approach, we report a more general form of dark soliton solutions for the Vc-NLSE.

Of late, the dark solitons have been investigated in different physical systems such as optical fiber, fiber lasers, plasmas, Bose-Einstein condensates, etc. As reported in many theoretical and experimental works, the dark solitons have further been classified into black and gray soliton based on its intensity profiles [27–32]. Very recently, the black and gray solitons in water tank and surface gravity waves have been observed by Chochab et al. [32]. All these leading works have shown that the study of temporal/spatial black and gray mode propagation of dark solitons are very important due to its existing background media. In this work, the possibilities of the black and gray mode of dark soliton and their dependence on other dynamical variables, especially the energy variations due to the blackness factor of solitons are revealed.

The Vc-NLSE for the bright solitons propagation with various inhomogeneous effects have been studied comprehensively in many literature [10–15]. However, there have not been enough attention towards the investigation of dark soliton

dynamics in the view of exploring the elastic collision nature and NL tunneling effect. In this chapter, we will study the dark multi-soliton propagation and its elastic collision behavior in the context of Vc-NLSE. As in many interesting research works for the bright solitons [33–39], we investigated the cascade compression of dark solitons induced by the multiple NL barriers, for the first time to the best of our knowledge. Unlike the bright soliton, we observed that the height of the barrier/well in NL tunneling is related to the blackness factor of dark soliton solution. The NL tunneling phenomena of soliton is one of the fascinating area of research, particularly in the context of optical switching and logic circuits.

After the detailed explanation of one soliton dynamics, we have extended our analytical approach to the study the multi-soliton propagation, where the elastic collision behavior of dark solitons are discussed in detail. The possibilities of black and gray mode interactions of dark solitons in the NLSE are numerically studied in [27]. The first experimental study of the interaction between black and gray solitons in an optical fiber were reported in [28]. Here, via the two-soliton solutions of Vc-NLSE, we analytically demonstrate the elastic collision between the two-dark solitons with its possible pair of black and gray mode. The interaction of dark solitons and its relevant physical quantities are reported by the asymptotic analysis.

The organization of the chapter is as follows. Following a detailed introduction, Sec. 2 presents the exact dark soliton solutions by Hirota's method. Sec 3 and 4 describes the dynamics of one and two soliton solutions respectively. Asymptotic analysis to study the collision behavior is also presented in Sec. 4. A brief discussion about the cascaded compression of dark soliton features Sec. 5, and the chapter concludes with a summary of results in Sec. 6.

2.2 Dark soliton solutions by Hirota method

In this section, we use Hirota's bilinear (HB) method to investigate the analytical dark soliton solution for Eq. (2.1). To derive the dark soliton solutions, we apply

the following bilinear transformation [23–26];

$$q(z,t) = g(z)\frac{G}{F} \tag{2.2}$$

where G is a complex function and F is a real function. By substituting Eq. (2.2) into Eq. (2.1), we get the following bilinear equations

$$[iD_z - \frac{1}{2}D(z)D_t^2 + \lambda(z)](G.F) = 0 \tag{2.3}$$

$$\delta|G|^2 + D_t^2(F.F) = \frac{2\lambda(z)}{D(z)}F^2 \tag{2.4}$$

with the condition $g_z(z) + g(z)p(z) = 0$. Here, the D_m^n represents the Hirota bilinear operator, $\lambda(z)$ is an analytic function to be determined. To solve the above set of equations (2.3)-(2.4), we introduce the power series expansion with ε as the formal expansion parameter of G and F as,

$$G = g_0[1 + \sum_{n=1}^{\infty}\varepsilon^n g_n(z,t)] \tag{2.5}$$

$$F = 1 + \sum_{n=1}^{\infty}\varepsilon^n f_n(z,t) \tag{2.6}$$

2.3 One-soliton solution

The dark one-soltion solution can be derived from the truncated power series of G and F in ε as follows, $G = g_0(1 + g_1)$ and $F = 1 + f_1$. Then, back to bilinear equations (2.3)-(2.4), we obtain

$$g_0 = ae^{i\psi}, \qquad g(z) = e^{-\int p(z)dz}$$

$$g_1 = \alpha_1 e^{\theta_1}, \qquad f_1 = e^{\theta_1}$$

$$\psi = k_0 t - \omega_0 \int D(z)dz, \qquad \theta_1 = k_1 t - \omega_1 \int D(z)dz + \phi_1$$

$$\lambda = \frac{1}{2}\delta a^2 D(z), \qquad \omega_0 = -\frac{\lambda}{D(z)} - \frac{k_0^2}{2}$$

$$\alpha_1 = \frac{2\omega_1 + 2k_0k_1 + ik_1^2}{2\omega_1 + 2k_0k_1 - ik_1^2}, \qquad \omega_1 = \frac{k_1}{2}(-2k_0 \pm \sqrt{2\delta a^2 - k_1^2})$$

Then, the final form of dark one-soliton solution is obtained as,

$$q(z,t) = \frac{a[(1+\alpha_1) + (\alpha_1 - 1)tanh\left(\frac{\theta_1}{2}\right)]}{2e^{\int p(z)dz}e^{-i\psi}} \tag{2.7}$$

The a and ψ are real functions representing the amplitudes and phase of the background wave. To get the real value of ω_1, k_1 should satisfy the condition $-\sqrt{2\delta a^2} \leq k_1 \leq \sqrt{2\delta a^2}$. Here δ can be introduced as, $\delta = \frac{2R(z)}{D(z)}e^{-2\int p(z)dz}$. From the Eq. (2.7), one can analyze the dynamics of dark one-soliton pulse in inhomogeneous fibers. The propagation of dark one-solitons through homogeneous fiber is depicted in the Fig. 2.1.

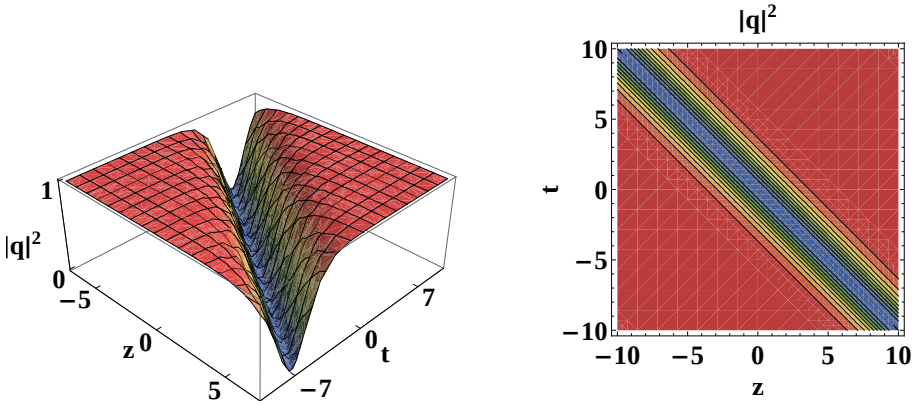

(a) (b)

Figure 2.1: (a) The dark one-soliton propagation through homogenous fiber for parameters $k_1 = k_0 = a = D(z) = 1$, $p = 0$ and $\delta = 1$.(b) Corresponding contour plot

To explore the dynamics of dark soliton propagation given by Eq. (2.7), some of the physical quantities such as velocity $\left(V = \frac{\omega_1}{k_1}D(z)\right)$, amplitude $\left(A = |\frac{a(1+\alpha_1)}{2e^{\int p(z)dz}}|\right)$ and blackness factor $\left(B = |\frac{a(\alpha_1-1)}{2e^{\int p(z)dz}}|\right)$ are important. It is interesting to note that, $p(z)$ affects the soliton amplitude and $D(z)$ affects the soliton velocity. The energy E and power P, in terms of the background amplitude a,

can be written as $E = \int_{-\infty}^{\infty} Pdt$ and $P(z,t) = a^2 - |q|^2$, respectively. Here, the instantaneous power is obtained as a difference between the total power and the corresponding value for the background [40]. The energy, in terms of blackness factor, can be written as

$$E = \int_{-\infty}^{\infty} (a^2 - \mid q \mid^2) dt = \frac{2 - \alpha_1 - \alpha_1^*}{a^{-2} e^{2\int p(z)dz} k_1} = \frac{4B^2}{e^{2\int p(z)dz} k_1} \tag{2.8}$$

The above Eq. (2.8) indicates that blackness factor is directly proportional to the energy associated with the dark soliton.

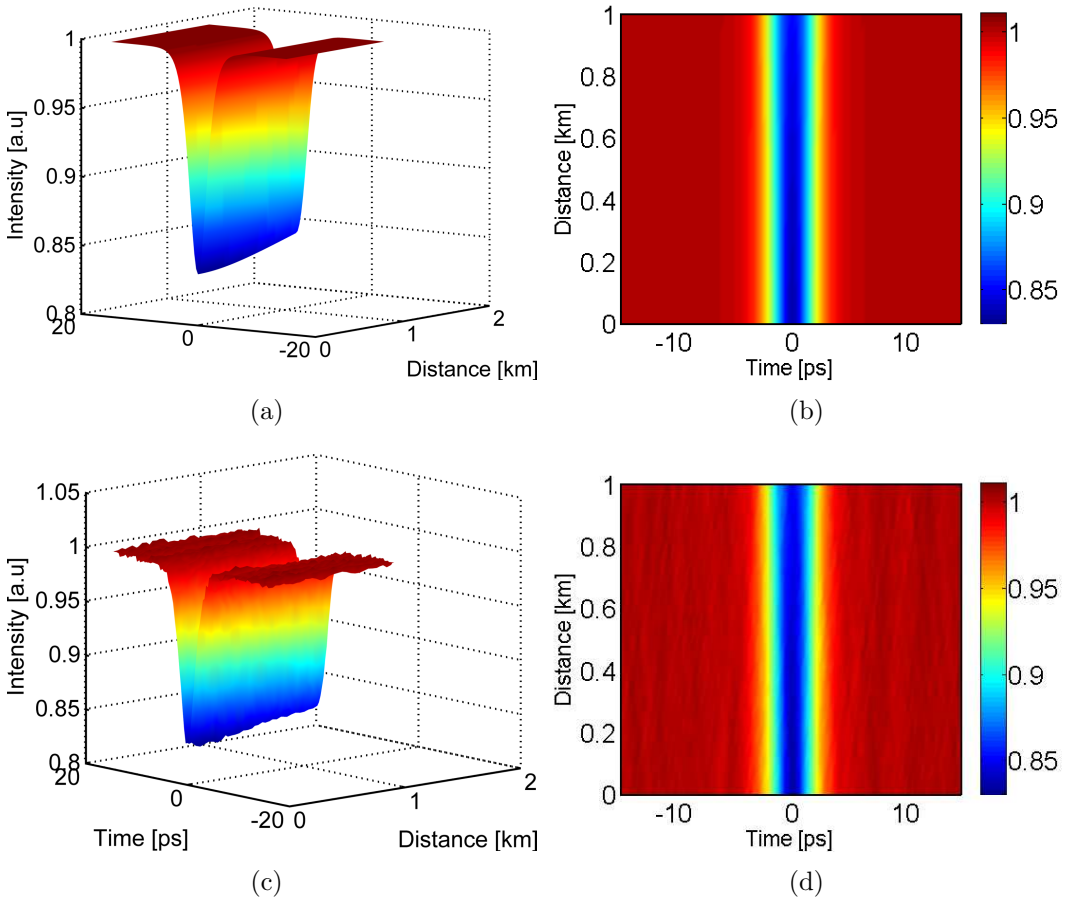

Figure 2.2: Figs (a) and (b) show the dark soliton evolution. Figs (c) and (d) shows the stable propagation of the soliton in the presence of strong photon noise. The parameters of relevant physical quantities are $k_1 = k_0 = a = 1$ $\delta = 2$, $\gamma = 1$and $p(z) = 0$.

2.3.1 Direct numerical simulation

The essential aspect of the soliton concept is its stability against perturbation over long propagation distance. To validate the signature of soliton, such as stable propagation over appreciable distance, and the stability against perturbation, we perform numerical simulation using split-step Fourier method. As a representative case, we consider the one soliton solution given by Eq. (2.7), and perform the stability analysis in two parts, (i) numerical simulation of soliton propagation using Vc-NLSE, and (ii) the propagation subject to perturbation such as the photon noise. Fig. 2.2 shows the numerical simulation of stable propagation of the dark soliton in the continuous back ground. Fig. 2.2(a) show the stable propagation of soliton pulse given by Eq. (2.7). It can be more clearly noticed from the contour map shown in Fig. 2.2(b), the soliton propagates without any intensity fluctuation or deformation of pulse profile.

So far, the propagation of soliton pulse has been considered in an ideal environment. However, there are numerous effects can contribute to instability in the soliton propagation. Therefore, it becomes essential to investigate the stability of the soliton in an environment subject to external noise or perturbations. For our purpose, we assumed a photon noise, which corresponds to 0.40% of the continuous background. This is indeed an appreciable noise level, which can potentially perturb any propagation dynamics, as evident from the smooth pulse shown in Fig. 2.2(b) and the noisy pulse depicted in Fig. 2.2(d). So, the initial condition for the simulation is the soliton profile with strong perturbation. Fig. 2.2(c) shows the simulation results of the perturbed soliton propagation for the same set of parameters. It is very evident that the dark soliton show remarkable stability against strong perturbation, which can be clearly noticed from the contour map shown in the Fig. 2.2(d). Thus, the soliton solution constructed in the current system is very robust and show excellent stability even against strong perturbation.

2.3.2 Parametric region for Black and gray soliton

Here, we classify the dark solitons into the black and gray mode based on the amplitude (A) or blackness (B) of the obtained soliton solution. The parameters A, B and background wave amplitude (a) are connected by a simple relation $A^2 + B^2 = a^2$ [5]. Generally, the dark soliton with zero intensity at its center is referred as black soliton ($B^2 = a^2$), otherwise ($B^2 < a^2$) as gray solitons. In Fig. 2.3(a), we have plotted the black soliton for $B^2 = 1$ and gray solitons for $B^2 = 0.5$ and 0.25.

Fig. 2.3(b) shows the variation of energy as a function of SPM parameter R. Similarly, we have demonstrated the blackness and intensity variation as a function of R in Fig. 2.3(c). It is evident that, the energy (E) and blackness (B^2) of the pulse is maximum for least value of R and decreases gradually with increase in R. But the intensity (A^2) increases gradually with increase in R. It shows that black mode solitons have maximum energy with zero intensity in a continuous wave background. The relations between E, B^2 and A^2 are depicted in Fig. 2.3(d).

2.3.3 Phase profile of dark soliton

In order to study the phase of dark soliton, we introduce the solution q of the form [30]

$$q(z,t) = \sqrt{\rho(z,t)}e^{i\psi(z,t)} \tag{2.9}$$

Substituting this expression into Eq. (2.1) and separating the real and imaginary parts, we obtain

$$\rho_z - D(z)\frac{\partial}{\partial t}(\rho\psi_t) + 2p(z)\rho = 0 \tag{2.10}$$

$$R(z)\rho + \frac{D(z)}{8\rho^2}\rho_t^2 - \frac{D(z)}{4\rho}\rho_{tt} + \frac{D(z)}{2}\psi_t^2 - \psi_z = 0 \tag{2.11}$$

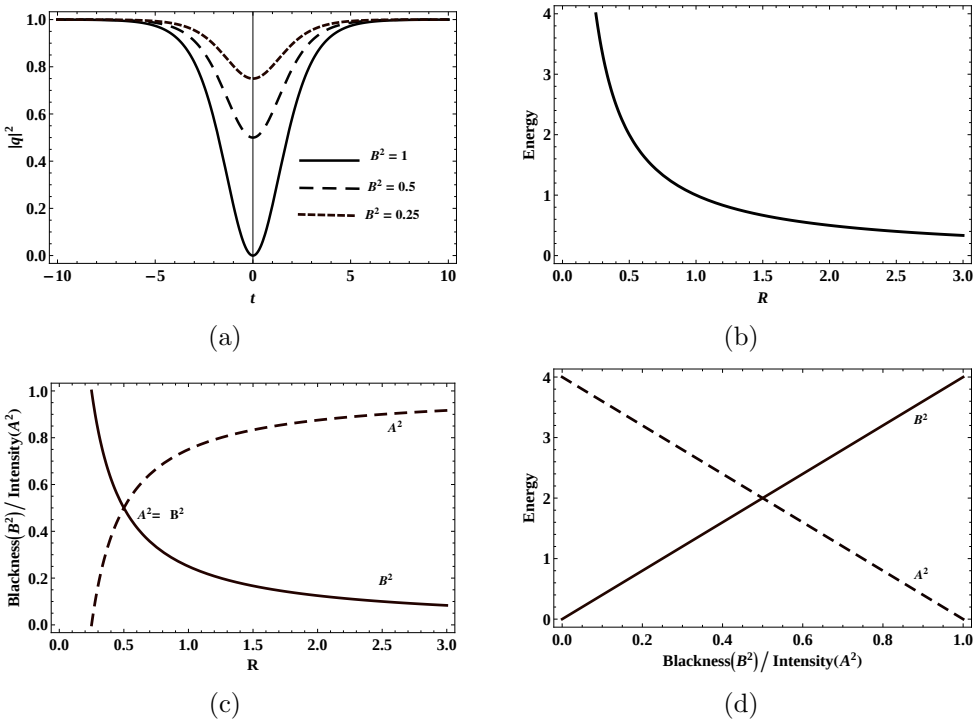

Figure 2.3: (a) The dark soliton with different values of blackness factor. (b) Soliton energy as a function of R. (c) Blackness/intensity variation due to the parameter R. (d)Energy variation due to the blackness/intensity factor. The parameters of relevant physical quantities are $k_1 = k_0 = a = 1$ and $p(z) = 0$.

The stationary condition for $|q|^2$ gives us an expression $\rho_z + 2p(z)\rho = 0$, from which one can deduce $\rho = \rho_0 e^{-2\int p(z)dz}$. Further, by using Eq. (2.10), we obtain $\psi = \int \frac{c_1(z)}{\rho_0} dt + A(z)$, where $c_1(z)$ and $A(z)$ are integration constants. Assuming, $\frac{dA}{dz}$ as a constant Ω, the expression for phase can be written as

$$\psi = \int \frac{c_1(z)}{\rho_0} dt + \Omega z \tag{2.12}$$

Substituting this expression into (2.11), we obtain the following equation for $\rho_0(t)$

$$(\frac{d\rho_0}{dt})^2 = 4\gamma\rho_0^3 - \frac{8\Omega}{D(z)}\rho_0^2 - c_2\rho_0 - 4c_1^2 \tag{2.13}$$

where $\gamma = \frac{R(z)}{D(z)} e^{-2\int p(z)dz}$. The above expression can be cast into the form

$$(\frac{d\rho_0}{dt})^2 = 4\gamma(\rho_0 - \rho_1)^2(\rho_0 - \rho_2) \tag{2.14}$$

Here, ρ_1 and ρ_2 correspond to the double root and the single root of (2.14), respectively. By integrating Eq.(2.14), we have

$$\rho_0 = \rho_1(1 - m^2 sech^2(\sqrt{\gamma\rho_1}mt) \tag{2.15}$$

Hence, from (2.9) the intensity profile of dark one-soliton solution for Vc-NLSE can be written as

$$|q|^2 = \rho = \rho_1 e^{-2\int p(z)dz}(1 - m^2 sech^2(\sqrt{\gamma\rho_1}mt)) \tag{2.16}$$

where we set $m^2 = \frac{\rho_1 - \rho_2}{\rho_1}$. By equating (2.14) and (2.13), we get the following set of equations

$$\Omega = \frac{\gamma}{2}\rho_1(3 - m^2)D(z),\ c_1^2 = \gamma\rho_1^3(1 - m^2),\ c_2 = -4\gamma(\rho_1^2 + 2\rho_1\rho_2) \tag{2.17}$$

Applying the expressions (2.15) and (2.17) into (2.12), we obtain the phase of dark soliton as

$$\psi = \sqrt{\gamma\rho_1^3(1 - m^2)}t + tan^{-1}[\frac{m\ tanh(\sqrt{\gamma\rho_1}mt)}{\sqrt{1 - m^2}}] + \frac{\gamma}{2}\rho_1(3 - m^2)D(z)z \tag{2.18}$$

It is worth mentioning that the Eq. (2.16) is almost same with dark one-soliton solution (2.7) that derived by HB method. The intensity of dark soliton via Eq.(2.7) can be written as

$$|q|^2 = \rho_0 e^{-2\int p(z)dz} = a^2 e^{-2\int p(z)dz}(1 - \frac{B^2}{a^2} sech^2(\frac{k_1}{2})) \tag{2.19}$$

where $a^2 = \rho_1$, $e^{2\int p(z)dz}\frac{B^2}{a^2} = m^2$, $-\sqrt{2\delta a^2} \leq k_1 \leq \sqrt{2\delta a^2}$ and $\gamma = \frac{\delta}{2}$(Refer Sec.3). By using the expression (2.19), we obtain the phase as

$$\psi = \sqrt{\gamma\rho_1^3(1-m^2)}t + \frac{2m\sqrt{\gamma\rho_1}}{k_1}tan^{-1}[\frac{m\ tanh(\frac{k_1}{2}t)}{\sqrt{1-m^2}}] + \frac{\gamma}{2}\rho_1(3-m^2)D(z)z \quad (2.20)$$

Here, we observed that the given expressions for intensity (Eqs. (2.16) and (2.19)) and for phase (Eqs. (2.18) and (2.20)) of dark solitons are exactly same with conditions $k_1 = \sqrt{4\gamma\rho_1}$ and $m = 1$.

Its interesting to note that the phase of the dark soliton changes across the width, which is in accordance with the results of the ref.[31]. Fig. 2.4 shows the intensity and corresponding phase profiles for different values of blackness factor m. It is evident that the phase of dark soliton changes with a total phase shift of $2sin^{-1}(m)$. For a black soliton ($m = 1$), a phase shift of π occurs exactly at the center of the dip. For the gray solitons ($m < 1$), phase varies gradually between $0 - \pi$. Fig. 2.5 depicts the influence of gain/loss coefficient $p(z)$ on phase profile of dark soliton and it is quite evident that gain/loss significantly influences the soliton phase.

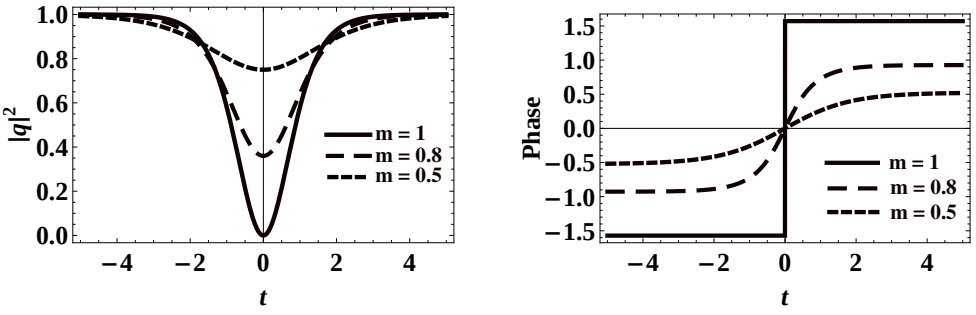

(a) (b)

Figure 2.4: (a) The dark soliton with different values of blackness factor via solution(2.16). (b) corresponding phase profiles. The parameters of relevant physical quantities are $R = D = \rho_1 = 1$ and $p(z) = 0$.

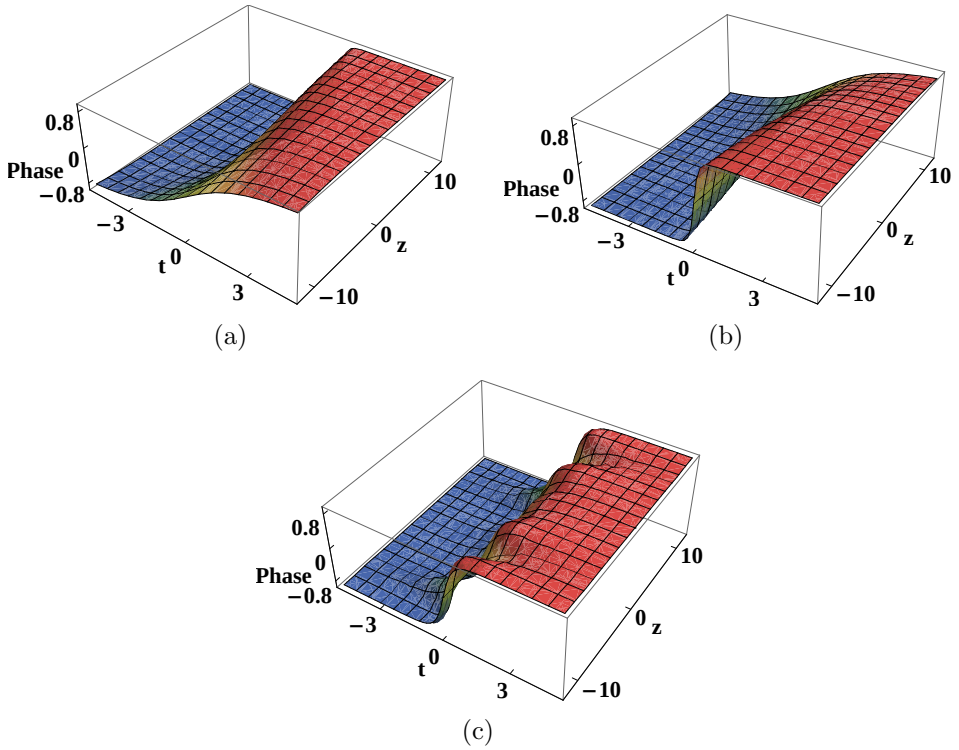

Figure 2.5: (a) The phase profiles via solution(2.16) with gain $p = -0.1$ (b) with loss $p = 0.1$ (c) with periodic background as $p = 0.1sin(z)$. Other relevant physical quantities are $R = D = \rho_1 = 1$ and $m = 0.8$.

2.4 Two-soliton solutions

The dark two-soliton solution can be derived from the truncated power series expansions of G and F as follows, $G = g_0(1 + g_1 + g_2)$ and $F = 1 + f_1 + f_2$. Then, back to bilinear Eqs. (2.3)-(2.4), we get

$$
\begin{aligned}
g_0 &= a e^{i\psi} & g(z) &= e^{-\int p(z)dz} \\
\lambda &= \frac{1}{2}\delta a^2 D(z) & \omega_0 &= -\frac{\lambda}{D(z)} - \frac{k_0^2}{2} \\
g_1 &= \alpha_1 e^{\theta_1} + \alpha_2 e^{\theta_2} & f_1 &= e^{\theta_1} + e^{\theta_2} \\
g_2 &= A_{12}\alpha_1\alpha_2 e^{\theta_1+\theta_2} & f_2 &= A_{12} e^{\theta_1+\theta_2} \\
\psi &= k_0 t - \omega_0 \int D(z)dz & \theta_i &= k_i t - \omega_i \int D(z)dz + \phi_i \\
\alpha_i &= \frac{2\omega_i + 2k_0k_i + ik_i^2}{2\omega_i + 2k_0k_i - ik_i^2} & \omega_i &= \frac{k_i}{2}(-2k_0 \pm \sqrt{2\delta a^2 - k_i^2})
\end{aligned}
$$

where $i = 1, 2$.

$$A_{12} = -\frac{2i(\alpha_1 - \alpha_2)(\omega_2 - \omega_1 - k_0k_1 + k_0k_2) - (\alpha_1 + \alpha_2)(k_1 - k_2)^2}{2i(1 - \alpha_1\alpha_2)(\omega_1 + \omega_2 + k_0k_1 + k_0k_2) - (\alpha_1\alpha_2 + 1)(k_1 + k_2)^2}$$

The two-soliton solution can be written as,

$$q(z,t) = e^{-\int p(z)dz} \frac{g_0(1 + g_1 + g_2)}{(1 + f_1 + f_2)} \tag{2.21}$$

Using Eq. (2.21), the propagation of two-soliton through homogeneous fiber is depicted in the Fig. 2.6. The collision between the solitons can be achieved by launching the solitons in opposite direction or in same direction with different velocities. Fig. 2.6(a) represents the two solitons propagation in same direction without any interactions. Fig. 2.6(c) depicts the propagation of dark solitons in opposite direction. The interaction between black and gray mode dark solitons are studied with different values of blackness factor. The resultant intensity profiles during the collision appears to reach zero only at a single time for lower blackness parameter, while for larger value of blackness the intensity drops twice to zero [27] as shown in Fig. 2.7. By using the obtained two-soliton solution, one can investigate many inhomogeneous behavior of dark soliton with its interactive or non-interactive propagation mode. In the section of results and discussions, we have studied the soliton dynamics with the assumption of same direction of propagation.

2.4.1 Two-soliton collision

The elastic collision between dark solitons can be analyzed by the asymptotic states of soliton solution. The asymptotic analysis of two-dark soliton solution are conducted as follows:

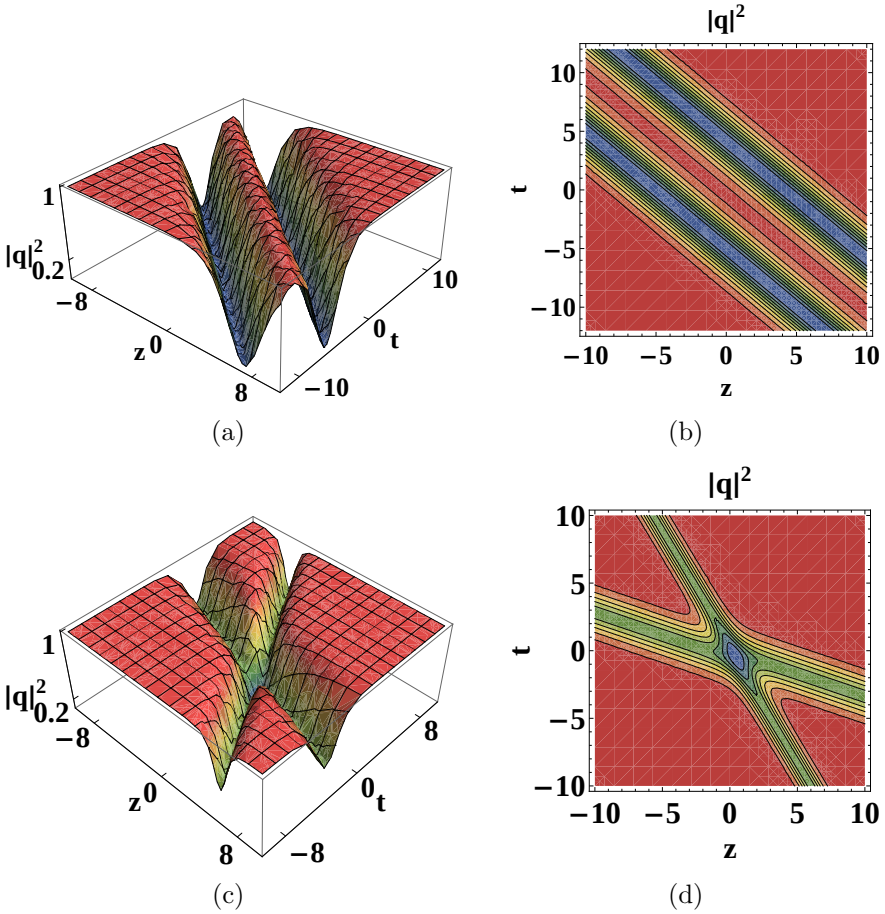

Figure 2.6: The dark two-soliton through homogeneous fiber with (a) same direction of propagation for parameter $k_1 = k_2 = 1$, $k_0 = a = D(z) = 1$, $p = 0$,$\delta = 0.5$, $\phi_1 = 5$ and$\phi_2 = -5$.(b) Corresponding contour plot. (c) opposite direction of propagation for parameter $k_1 = -1.5$, $k_2 = 1.5$, $k_0 = a = D(z) = 1$, $p = 0$, $\delta = 2$ and $\phi_1 = \phi_2 = 0$.(d) Corresponding contour plot.

1) Before collision

(a)$S_1^-(\theta_1 \sim 0, \theta_2 \to -\infty)$

$$q(z,t) \to S_1^- = \frac{ae^{i\psi_1^-}}{2e^{\int p(z)dz}}[(1+\alpha_1) + (\alpha_1 - 1)tanh(\frac{\theta_1}{2})] \tag{2.22}$$

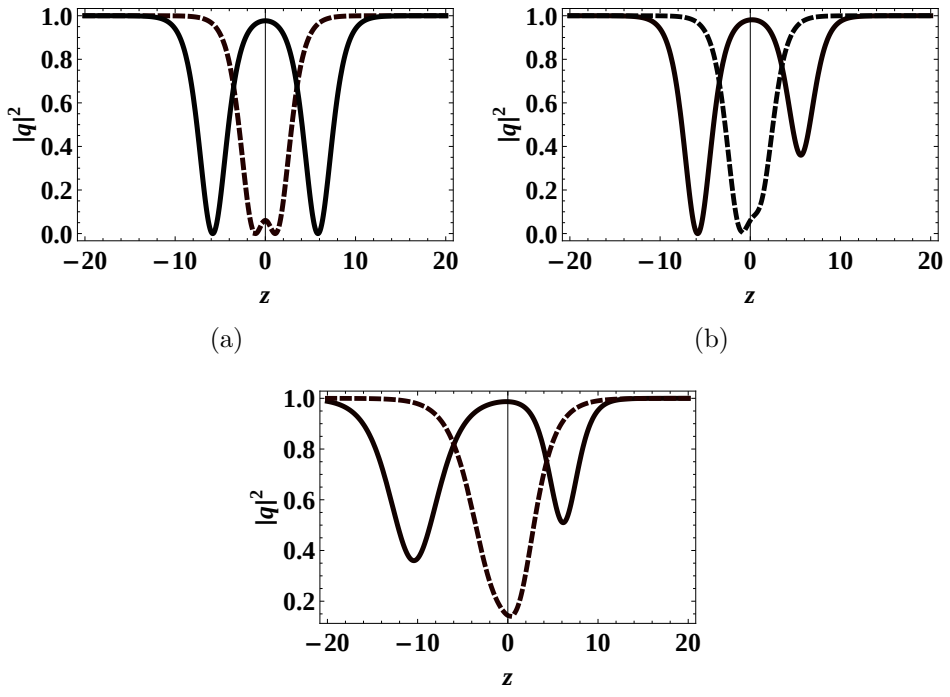

(a) (b)

(c)

Figure 2.7: The resultant intensity of dark soliton before collision (solid profile) and during collision (dashed profile)(a) black-black mode for $k_1 = -1$ and $k_2 = 1$ (b) black-gray mode for $k_1 = -1$ and $k_2 = 0.8$ (c) gray-gray mode for $k_1 = -0.7$ and $k_2 = 0.8$. Other physical parameters are $k_0 = a = D(z) = 1$, $p = 0$, $\delta = 0.5$ $\phi_1 = \phi_2 = 5$.

(b)$S_2^-(\theta_2 \sim 0, \theta_1 \to \infty)$

$$q(z,t) \to S_2^- = \frac{a\alpha_1 e^{i\psi_2^-}}{2e^{\int p(z)dz}}[(1+\alpha_2) + (\alpha_2 - 1)tanh(\frac{\theta_2}{2} + \ln(\sqrt{A_{12}}))] \quad (2.23)$$

2)After collision

(a)$S_1^+(\theta_1 \sim 0, \theta_2 \to \infty)$

$$q(z,t) \to S_1^+ = \frac{a\alpha_2 e^{i\psi_1^+}}{2e^{\int p(z)dz}}[(1+\alpha_1) + (\alpha_1 - 1)tanh(\frac{\theta_1}{2} + \ln(\sqrt{A_{12}}))] \quad (2.24)$$

(b)$S_2^+(\theta_2 \sim 0, \theta_1 \to -\infty)$

$$q(z,t) \to S_2^+ = \frac{ae^{i\psi_2^+}}{2e^{\int p(z)dz}}[(1+\alpha_2)+(\alpha_2-1)tanh(\frac{\theta_2}{2})] \tag{2.25}$$

By comparing the asymptotic expressions before collision (2.22)- (2.23) and after collision (2.24)- (2.25), we can observe the particle like behavior through the elastic collision of dark solitons S_1 and S_2 with the condition $|\alpha_i| = 1(i = 1, 2)$. The intensity profiles of black-black interactions are depicted in Fig. 2.7(a). The corresponding phase can be derived as

$$\psi_1^- = c_1 t + \frac{2m\sqrt{\gamma\rho_1}}{k_1} tan^{-1}[\frac{m\ tanh(\frac{k_1}{2}t+\phi_1)}{\sqrt{1-m^2}}] + \Omega z \tag{2.26}$$

$$\psi_2^- = c_1 t + \frac{2m\sqrt{\gamma\rho_1}}{k_2} tan^{-1}[\frac{m\ tanh(\frac{k_2}{2}t+\phi_2+\ln(\sqrt{A_{12}})}{\sqrt{1-m^2}}] + \Omega z \tag{2.27}$$

$$\psi_1^+ = c_1 t + \frac{2m\sqrt{\gamma\rho_1}}{k_1} tan^{-1}[\frac{m\ tanh(\frac{k_1}{2}t+\phi_1+\ln(\sqrt{A_{12}})}{\sqrt{1-m^2}}] + \Omega z \tag{2.28}$$

$$\psi_2^+ = c_1 t + \frac{2m\sqrt{\gamma\rho_1}}{k_2} tan^{-1}[\frac{m\ tanh(\frac{k_2}{2}t+\phi_2)}{\sqrt{1-m^2}}] + \Omega z \tag{2.29}$$

By using above set of above relations, we have studied the phase profile of two-soliton interaction between two oppositely moving black solitons as shown in the Fig.2.8. Fig. 2.8(a) represents the phase profile before the collision while, Fig. 2.8(c) depicts the recovered phase after collision. It is evident that the solitons recover the phase after collision and maintains a phase shift of π. The resultant phase profile during the collision is given by $-\psi + \psi$, and it is quite evident that the phase of the solitons cancel each other as shown in the Fig. 2.8(b).

2.5 Results and discussions

As an attempt to make the discussion self-explanatory, we first consider the propagation dynamics of dark soliton pulse in the absence of varying coefficients. In such system, the coefficient corresponding to dispersion and nonlinearity remains constant. Using Hirota Bilinear method, the analytical dark soliton

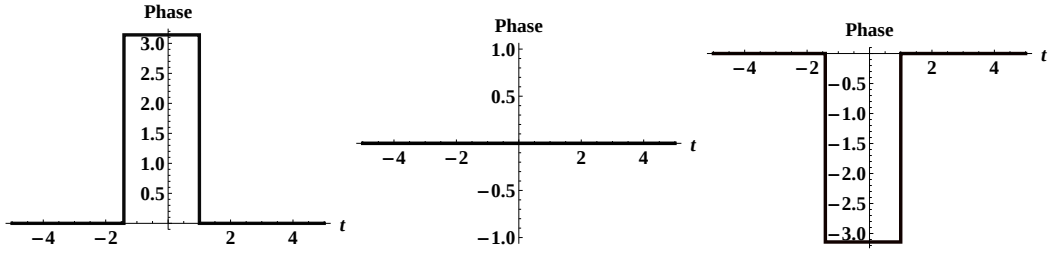

(a) (b) (c)

Figure 2.8: The resultant phase of two black soliton (a)before collision (b)at collision (c) after collision. The relevant physical parameters are $k_1 = 1$ and $k_2 = 1$, $k_0 = a = D(z) = 1$, $p = 0$, $\delta = 0.5$, $\phi_1 = -1$ and $\phi_2 = 1$.

Table 2.1: Physical quantities of solitons S_1 and S_2 before and after the collision.

Solitons	Velocities(V)	Amplitudes(A)	Energies(E)	Blackness(B)
s_1^-	$\frac{\omega_1}{k_1}D(z)$	$\lvert\frac{a(1+\alpha_1)}{2e^{\int p(z)dz}}\rvert$	$\frac{a^2(2-\alpha_1-\alpha_1^*)}{k_1 e^{2\int p(z)dz}}$	$\lvert\frac{a(\alpha_1-1)}{2e^{\int p(z)dz}}\rvert$
s_2^-	$\frac{\omega_2}{k_2}D(z)$	$\lvert\frac{a\alpha_1(1+A_{12}\alpha_2)}{e^{\int p(z)dz}(1+A_{12})}\rvert$	$\frac{a^2(2-\alpha_2-\alpha_2^*)}{k_2 e^{2\int p(z)dz}}$	$\lvert\frac{a\sqrt{A_{12}}(\alpha_2-1)}{(A_{12}+1)e^{\int p(z)dz}}\rvert$
s_1^+	$\frac{\omega_1}{k_1}D(z)$	$\lvert\frac{a\alpha_2(1+A_{12}\alpha_1)}{e^{\int p(z)dz}(1+A_{12})}\rvert$	$\frac{a^2(2-\alpha_1-\alpha_1^*)}{k_1 e^{2\int p(z)dz}}$	$\lvert\frac{a\sqrt{A_{12}}(\alpha_1-1)}{(A_{12}+1)e^{\int p(z)dz}}\rvert$
s_2^+	$\frac{\omega_2}{k_2}D(z)$	$\lvert\frac{a(1+\alpha_2)}{2e^{\int p(z)dz}}\rvert$	$\frac{a^2(2-\alpha_2-\alpha_2^*)}{k_2 e^{2\int p(z)dz}}$	$\lvert\frac{a(\alpha_2-1)}{2e^{\int p(z)dz}}\rvert$

solution corresponding to one- and two-solitons are presented in Eqs. (2.7) and (2.21) and graphically in Figs. 2.1 and 2.6, respectively. It is found that the dark soliton propagates without deformation in such homogeneous system whose amplitude and velocity remain constant. In the following section, we will consider the variable coefficients for inhomogeneous fiber and intended to study the dynamical evolutions of dark soliton for different physical effects.

To investigate the propagation of soliton in inhomogeneous fiber described by the model (2.1), we consider the GVD parameter $D(z)$ and nonlinearity parameters $R(z)$ as a trigonometric periodic function. In this case, the solitons are exhibiting oscillatory nature without any energy variation. But in the presence of medium with gain(or loss), the pulse undergoes the amplifications (or absorption). In such a way the medium with gain increases the energy while the loss

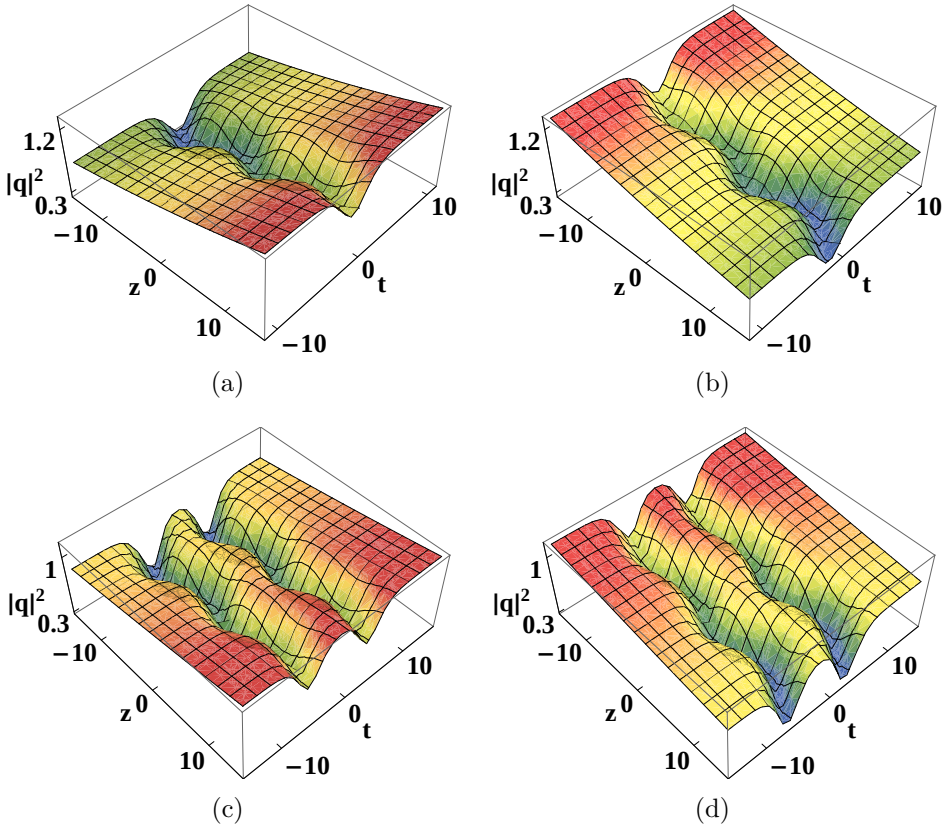

Figure 2.9: The dispersion and nonlinearity managed dark solitons with constant gain/loss (a) One-soliton gain with $p = -0.01$ (b) One-soliton loss with $p = 0.01$ (c) Two-soliton gain with $p = -0.01$ (d) Two-soliton loss with $p = 0.01$. Other physical parameters are $D(z) = Cos(0.5z)$, $k_0 = a = 1$ and $\delta = 1$.

decreases the same. Fig. 2.9 represent the one and two periodically varying dark soliton in the presence of linear gain (loss).

The pulse background variation due to the influence of gain/loss coefficient $p(z)$ are depicted in Fig. 2.10. As reported in Refs. [41, 42], different type of background profiles are possible in inhomogeneous medium. Here, the periodic oscillation of background are portrayed in the Figs. 2.10(a) and 2.10(b) for the one- and two- solitons, respectively. Similarly, intensity variation with exponentially increasing background are studied in the Figs. 2.10(c) and 2.10(d). It is evident that the gain/loss coefficient $p(z)$ directly influences the shape of the background.

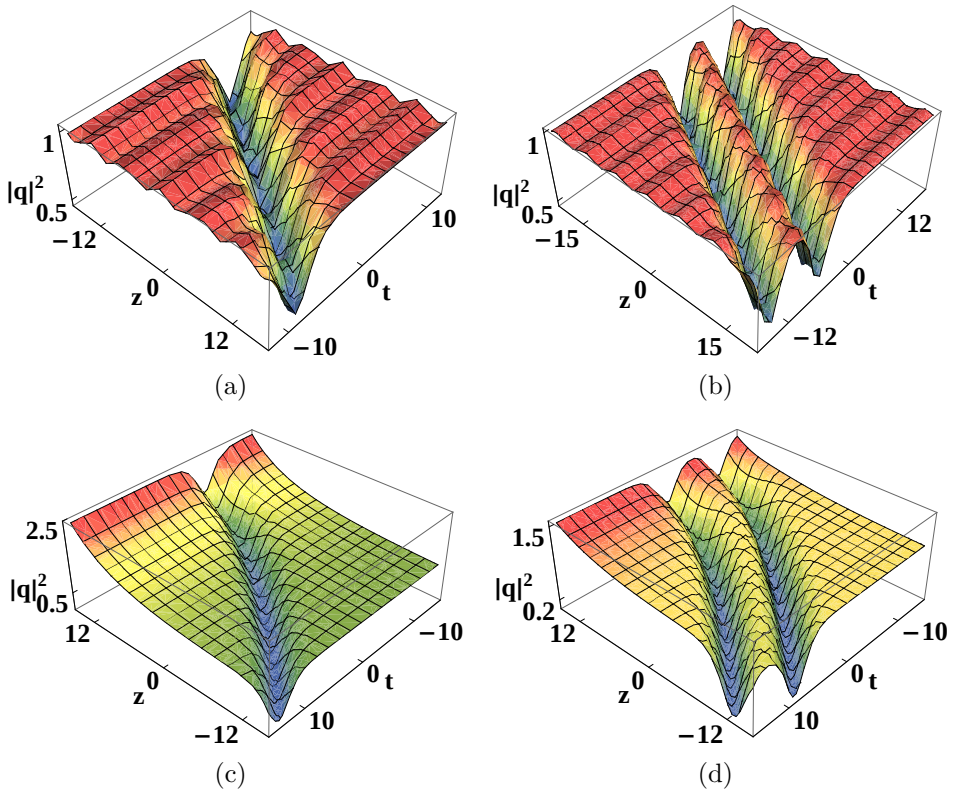

Figure 2.10: The dark solitons propagation with periodic background as $p = 0.02sin(z)$ for (a) One-soliton (b) Two-soliton. Propagation with exponential gain factor as $p = -0.01Exp(0.1z)$ for (c) One-soliton (d) Two-soliton. The other physical quantities are $k_0 = a = D(z) = 1$ and $R(z) = 0.5$.

2.5.1 Nonlinear tunneling and cascade compression

Recently, the nonlinear (NL) tunneling effect of solitons in different physical systems have been investigated in many pioneering research works [33–35, 37–39]. The first experimental observation of soliton tunneling phenomena through a potential barrier has been reported in Ref. [36]. All these theoretical and experimental works have shown that the soliton can pass through the barrier/well without any considerable power attenuation under a special conditions which depends on the ratio between the height of the barrier and the amplitude of the soliton. To investigate the NL tunneling phenomena of dark soliton through the dispersion barrier (DB) or well (DW), we choose the dispersion and nonlinear parameter as follows [35]:

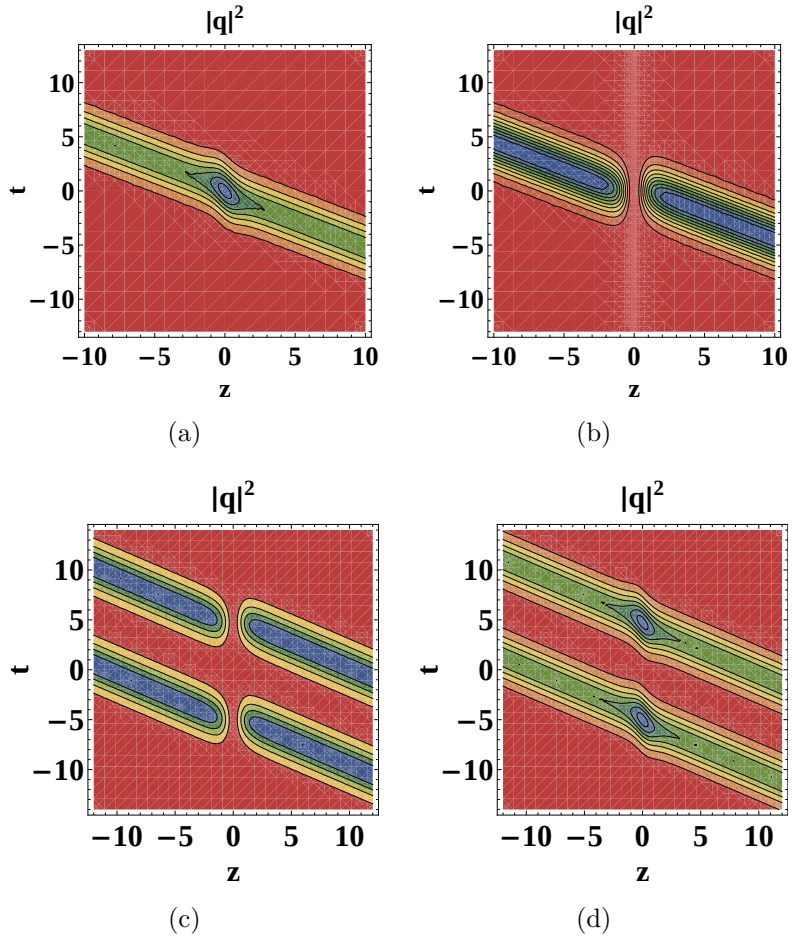

Figure 2.11: Contour plot of nonlinear tunneling of dark one-soliton (a) Dispersion barrier with $D(z) = 1 + hsech[z - z_0]^2$, $R = 0.5$ and $h = 0.5$.(b) Dispersion well with $h = -1$.(c) Nonlinear barrier with $D(z) = 1$,$R = 0.5(1+hsech[z-z_0]^2)$ and $h = 1$.(d) Nonlinear well with $h = -0.5$. Other physical quantities are $k_0 = k_1 = a = 1$ and $z_0 = 0$.

$$D(z) = D_0 exp[-rz] \pm h \sum_{j=1}^{n} sech^2[c(z - jz_0)] \qquad R(z) = R_0 exp(-rz) \quad (2.30)$$

In the above expressions, h indicates the height of the barrier, c is related to its width, z_0 represents the location of the DB/DW, r represent a decaying parameter, n is a integer indicating the number of the barrier, D_0 and R_0 are constant parameters. Here the positive (negative) sign of $\pm h$ denotes the barrier (well).

Here, we first consider the NL tunneling without exponential background

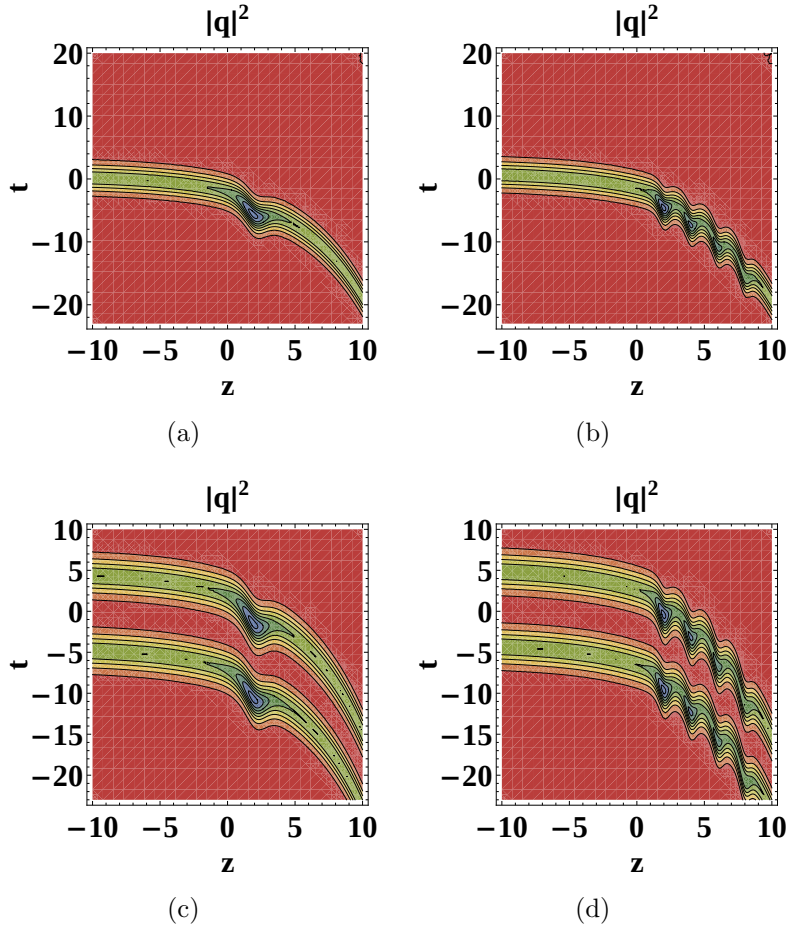

Figure 2.12: Contour plot of nonlinear tunneling with exponential background. (a)Dispersion barrier of one-soliton with $h = 1$,$k_1 = 1$,$n = 4$ and $z = 2$. (b)Dispersion barrier of two-soliton with $h = 0.7$,$k_1 = 1.5$, $k_2 = -1.5$,$n = 4$ and $z = 2$. Other physical quantities are $D(z) = d_0 e^{-rz} + h \sum_{j=1}^{n} sech[z - z_0]^2$,$R = R_0 e^{-rz}$, $d_0 = k_0 = 1$, $R_0 = 0.5$,$r = -0.2$ and $p = 0$.

($r = 0$). It shows that, when the dark soliton pass through DB, the blackness of the soliton grows and forms a peak at $z = z_0$. After passing through the DB, the pulse regains its original form as shown in Fig. 2.11(a). Similarly, when dark solitons pass through DW the blackness of the solitons vanishes and a valley is formed at $z = z_0$; and restored to its original shape after passing through DW as shown in Fig. 2.11(b). In similar lines, the NL tunneling effect of corresponding to two-solitons are shown in the Figs. 2.11(c) and 2.11(d).

Then, we consider the NL tunneling effect with exponential background ($r \neq 0$). When a dark soliton passes through the DB with exponential decay, the

blackness of the soliton increases at $z = z_0$, and after tunneling through the DB, the width of the soliton gradually decreases during propagation. It is evident that, tunneling of soliton through the exponential background generally exhibits pulse compression. Figs. 2.12(a) and 2.12(c) clearly show that soliton undergoes compression when it propagate through DB.

Finally, we report the so called cascaded compression resulting from the propagation of soliton through number of successive potential barrier. The compression of the pulse gradually increases with the number of barriers along the propagation distance. Generally, this process is called cascades compression. Here, z_0 stands for the spacing between two consecutive barriers. To observe the cascade compression in one and two soliton solutions, we have considered four successive dispersion barrier ($n = 4$) with separation value $z_0 = 2$. As a result, the pulse keep compressing whenever it crosses a barrier, and the height of the barriers are gradually decreased along the propagation distance. The above behavior is illustrated in the Figs. 2.12(b) and 2.12(d).

The cascaded compression of soliton can also be studied with the nonlinear barrier (NB) or well (NW). In this case, the dispersion and nonlinear parameter can be choose as follows:

$$D(z) = D_0 exp[-rz] \qquad R(z) = R_0 exp(-rz) \pm h \sum_{j=1}^{n} sech^2[c(z - jz_0)] \quad (2.31)$$

Here, the soliton grows and forms a peak when it is passing through NW and a valley is formed when it crosses NB, just opposite to the case of soliton propagation in DB and DW.

The height of the barrier (h) exhibits a relation with blackness parameter (B) such that, $h > 0$ indicates the DB/NB, and $-1 < h < 0$ represents the DW/NW. We arrive at this suitable choice of h by the existing region of dark soliton with B as $0 \leq B^2 \leq a^2$. Similar type of restriction on value of h for the NL similariton tunneling are reported in Ref.[38]. Here, due to the dependence between h and B, the study of tunneling through DB/NW is possible only in the case of gray soliton solutions, however the propagation through DW/NB can be studied in

the both cases of black and gray mode of dark soliton solutions.

2.6 Conclusion

In this chapter, we have investigated the dark soliton dynamics in the Vc-NLSE with distributed dispersion, SPM and linear gain/loss. The one and two dark soliton solutions have been derived using Hirota's bilinear method. Through the derived soliton expressions and graphical illustration, the dispersion managed pulse with amplification/absorption and the influence of gain/loss coefficient on the shape of the background have been discussed. Numerically, we have studied the dark soliton propagation in the continuous wave background, and our simulations confirm that the obtained soliton solution is very stable and robust against perturbations. We have derived an exact solution for the phase of dark soliton and reported the effect of blackness parameter and gain/loss coefficient on soliton phase profiles.

Black and gray soliton interactions and elastic collision between dark solitons are exclusively studied via the asymptotic analysis. We have also studied the nonlinear tunneling of dark soliton through barrier/well. It has been found that the intensity of the tunneling soliton either forms a peak or valley and retains its shape after tunneling through barrier/well. We also identified that the tunneling of dark soliton with exponential background tends to compress the pulse. Moreover, a cascaded compression of dark soliton has been investigated by considering a soliton passing through multiple nonlinear tunneling barrier. The most conventional studies on HB method for constructing soliton solution focuses primarily on the intensity part and the stability of the solution. In contrast, here we have added a new insight and extended the capability of HB method in understanding the phase profile of the obtained solutions. As it is known, the phase profile plays a vital role in multi-soliton solutions, especially in the bound state solution, where relative phase plays a very deterministic role in explaining the nature of interaction, such as attractive or repulsive.

Bibliography

[1] A. Hasegawa, and F.D. Tappert, Appl. Phys. Lett. 23 (1973) 142144.

[2] L.F. Mollenauer, R.H. Stolen, and J.P. Gordon, Phys. Rev. Lett. 45 (1980) 10951098.

[3] G.P. Agrawal, Nonlinear Fiber Optics, Academic, New York, 2013.

[4] F. Abdullaev, S. Darmanyan, and P. Khabibullaev, Optical Solitons, Springer-Verlag, Berlin, 1991.

[5] Yuri S. Kivshar and Barry Luther-Davies, Phys. Rep. 298 (1998) 81197.

[6] P. Emplit, J.P. Hamaide, F. Reynaud, and A. Barthelemy, Opt. Commun. 62 (1987) 374379.

[7] A.M. Weiner, J.P. Heritage, R.J. Hawkins, R.N. Thurston, E.M. Kirschner, D.E. Leaird, and W.J. Tomlinson, Phys. Rev. Lett. 61 (1988) 2445-2448.

[8] Yuri S. Kivshar and Xiaoping Yang, Chaos, Solitons Fractals 4 (1994) 17451758.

[9] M. Mitchell, Z. Chen, M. Shih, and M. Segev, Phys. Rev. Lett. 77 (1996) 490493.

[10] V.N. Serkin and A. Hasegawa, Phys. Rev. Lett. 85 (2000) 45024505.

[11] I. Gabitov, E.G. Shapiro, and S.K. Turitsyn, Phys. Rev. E 55 (1997) 3624

[12] Lakoba T I and Kaup D J, Phys. Rev. E 58 (1998)6728

[13] V.I. Kruglov, A.C. Peacock, and J.D. Harvey, Phys. Rev. Lett. 90 (2003) 113902.

[14] S.H. Chen and L. Yi, Phys. Rev. E 71(2005)016606

[15] W.J. Liu, B. Tian, and H.Q. Zhang, Phys. Rev. E 78(2008) 066613 .

[16] Rongcao Yang, Lu. Ruiyu Hao, Xiaojuan Shi Li, Zhonghao Li, and Guosheng Zhou, Opt. Commun. 253 (2005) 177185.

[17] K. Nithyanandan, and K. Porsezian, Laser Physics 26 (2015) 015401.

[18] R. Hirota, The Direct Method in Soliton Theory, Cambridge University Press, Cambridge, 2004.

[19] R. Radhakrishnan, M. Lakshmanan, and J. Hietarinta, Phys. Rev. E 56(1997)2213

[20] T. Kanna and M. Lakshmanan, Phys. Rev. Lett. 86 (2001) 50435046.

[21] W.J. Liu, B. Tian, H.Q. Zhang, L.L. Li, and Y.S. Xue, Phys. Rev. E 77 (2008) 066605.

[22] N.M. Musammil, K. Porsezian, and K. Nithyanandan, P.A. Subha and P. Tchofo Dinda, Optical Fiber Technology 37(2017)11-20

[23] R. Radhakrishnan and M. Lakshmanan, J. Phys. A: Math. Gen. 28 (1995) 26832692.

[24] K. Porsezian and K. Nakkeeran, Phys. Rev. Lett. 76 (1996) 3955.

[25] N.M. Musammil, K. Porsezian, P.A. Subha, and K. Nithyanandan, Chaos 27(2017)023113 (112).

[26] W.J. Liu, B. Tian, H.Q. Zhang, T. Xu, and H. Li, Phys. Rev. A 79 (2009)063810.

[27] R. N. Thurston and Andrew M. Weiner, J. Opt. Soc. Am. B 8(1991)471

[28] Dmitri Foursa and Philippe Emplit, Phys. Rev. Lett.77 (1996)4011

[29] Mark J. Ablowitz and Ziad H. Musslimani, Phys. Rev. E 67(2006)025601(R)

[30] A.Hasegawa and M.Matsumoto, Springer, New York, 2003

[31] G.P. Agrawal. Fiber-Optic Communication Systems, John Wiley and sons, New York, 2012

[32] A. Chabchoub, O. Kimmoun, H. Branger, N. Hoffmann, D. Proment, M. Onorato, and N. Akhmediev, Phys. Rev. Lett. 110(2013)124101.

[33] A.C. Newell, Nonlinear tunnelling, J. Math. Phys. 19 (1978) 11261133.

[34] V.N. Serkin and T.L. Belyaeva, J. Exp. Theor. Phys. Lett. 74 (2001) 573577.

[35] Guangye Yang, Ruiyu Hao, Lu Li , Zhonghao Li, and Guosheng Zhou, Optics Communications 260 (2006)282

[36] Assaf Barak, Or Peleg, Chris Stucchio, Avy Soffer, and Mordechai Segev, Phys. Rev. Lett. 100 (2008) 153901(14).

[37] W.P. Zhong and M.R. Belic, Phys. Rev. E 81(2010) 056604

[38] C.Q. Dai, G.Q. Zhou, and J.F. Zhang, Phys. Rev. E 85 (2012) 016603.

[39] M.S. Mani Rajan, J. Hakkim, A. Mahalingam, and A. Uthayakumar, Eur. Phys. J. D 67 (150) (2013) 18.

[40] M.J. Ablowitz, S.D. Nixon, T.P. Horikis, and D.J. Frantzeskakis, J. Phys. A: Math. Theor. 46 (2013)095201 (118).

[41] Yu-Jie Feng, Yi-Tian Gao, Zhi-Yuan Sun, Da-Wei Zuo, Yu-Jia Shen, Yu-Hao Sun, Long Xue, Yu. Xin, Phys. Scr. 90(2015)045201 (18).

[42] K Aysha Muhsina and P A Subha, Phys. Scr.89 (2014)075205

Chapter 3

Bright solitons dynamics in the Vc-NLS equation

3.1 Introduction

In this chapter, we focus on the following variable coefficient model for the anomalous dispersion regime, which governs the bright soliton pulse propagation in an inhomogeneous fiber with the distributed dispersion, kerr nonlinearity and linear gain/loss [1–8]:

$$iq_z + \frac{1}{2}D(z)q_{tt} + R(z)(q|q|^2) + ip(z)q = 0 \tag{3.1}$$

where, $q(z,t)$ is the complex amplitude of the pulse envelope, the variables z and t represent the normalized spatial and temporal coordinates. The group velocity dispersion, kerr nonlinearity and amplification/absorption effects are related to the respective coefficient functions $D(z)$, $R(z)$ and $p(z)$.

To construct the exact bright soliton solution for the model (3.1), we have used Hirota's bilinear method. The important physical quantities and interaction behaviors can be well understood with the use of this method [9–12]. By using this approach, we report an exact form of bright soliton solutions for Vc-NLSE model.

Here, in addition to the intensity based explanations, we have been investigated the phase dynamics of bright soliton for the first time to the best of our knowledge. The influence of inhomogeneity, such as varying GVD, pulse compression and medium gain/loss, on soliton intensity and corresponding phase change of bright solitons are presented in this chapter. Moreover, with a particular interest of nonlinear tunneling in the context of optical switching, we exclusively investigated the bright soliton tunneling and corresponding phase change when it pass through dispersion barrier or well. Recently, many leading works are extensively reported the tunneling effect of soliton in different nonlinear media [13–16]. In this work, we also investigate the nonlinear(NL)tunneling of the bright with exponential background via Hirota bilinear method. Additionally, we have reported the cascaded compression of bright solitons with two successive dispersion barrier.

The organization of the chapter is as follows. Sec.1 features an introduction about bright soliton and Vc-NLSE. Sec. 2 presents the bright soliton solutions by Hirota's method. The dark one-soliton, two-soliton, and the collision behavior of solitons via asymptotic analysis is also presented in Sec. 2. A brief discussion about the NL tunneling of soliton through barrier/well is presented in Sec. 3, and the paper concludes with a summary of results in Sec. 4.

3.2 Bright soliton solutions

In this section, we use Hirota's bilinear method to investigate the analytical bright soliton solutions of equation (3.1). Here, we use the transformation as followed in Refs. [10, 11] and is set to give a exact form of bright soliton solution. In order to construct the bright soliton solutions, we apply the following form of Hirota bilinear transformation;

$$q(z,t) = g(z)\frac{G}{F} \tag{3.2}$$

where G is a complex functions and F is a real function. By substituting this transformation into Eq. (3.1), the following bilinear equations can be obtained,

$$g_z(z) + g(z)p(z) = 0 \tag{3.3a}$$

$$[iD_z + \frac{1}{2}D(z)D_t^2](G.F) = 0 \tag{3.3b}$$

$$D_t^2(F.F) = \delta|G|^2 \tag{3.3c}$$

where D_m^n represent the hirota bilinear operator, the δ can be introduced as $\delta = \frac{2R(z)}{D(z)}g(z)^2$ The Bright multi-soliton solutions of equation (3.1) can be generated by solving the above set of equations (3.3) with the power series expansions of G and F as

$$G = \varepsilon^1 g_1 + \varepsilon^3 g_3 + \varepsilon^5 g_3 + ...$$
$$F = 1 + \varepsilon^2 f_2 + \varepsilon^4 f_4 + \varepsilon^6 f_6 + ...$$

with ε as the formal expansion parameter.

3.2.1 Bright one-soliton solutions

In order to get the bright one-soliton solution, the power series expansions for G and F are truncated series of lowest order in ϵ as follows, $G = g_1$ and $F = 1 + f_2$. Then, back to bilinear equations (3.3), we get

$$g(z) = e^{-\int p(z)dz}$$
$$g_1 = \alpha_1 e^{\theta_1}$$
$$f_2 = \varrho_1 e^{\theta_1 + \theta_1^*}$$
$$\theta_1 = k_1 t + ik_1^2 \int D(z)dz$$
$$\varrho_1 = \frac{\delta|\alpha_1|^2}{2(k_1 + k_1^*)^2}$$

The one-soliton solution can be written as,

$$q(z,t) = \frac{e^{-\int p(z)dz}\alpha_1}{2\sqrt{\rho_1}} e^{-i\theta_{1I}} sech(\theta_{1R} + \frac{\ln \varrho_1}{2}) \tag{3.4}$$

From the Eq. (3.4) , we can study the bright one-soliton pulse propagation through constant or inhomogeneous fibers.

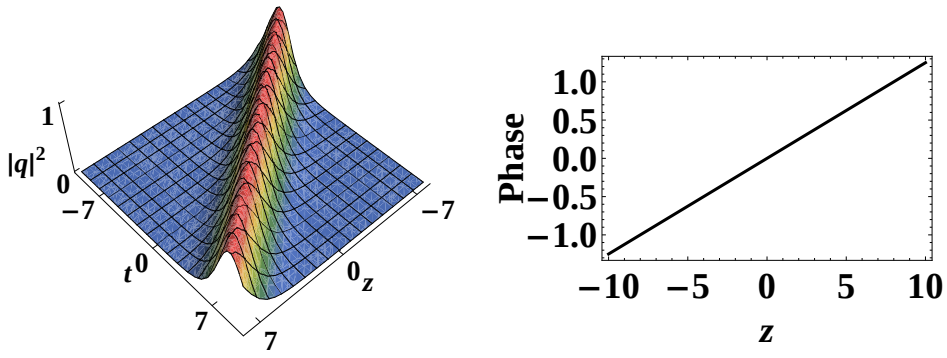

(a) (b)

Figure 3.1: The bright one-soliton propagation through homogenous fiber for parameters, (a)$k_1 = 0.5 + 0.5i$, $D(z) = 1$, $R = 0.5$,$\alpha_1 = 1 + i$ and $p = 0$. (b)Corresponding contour plot.

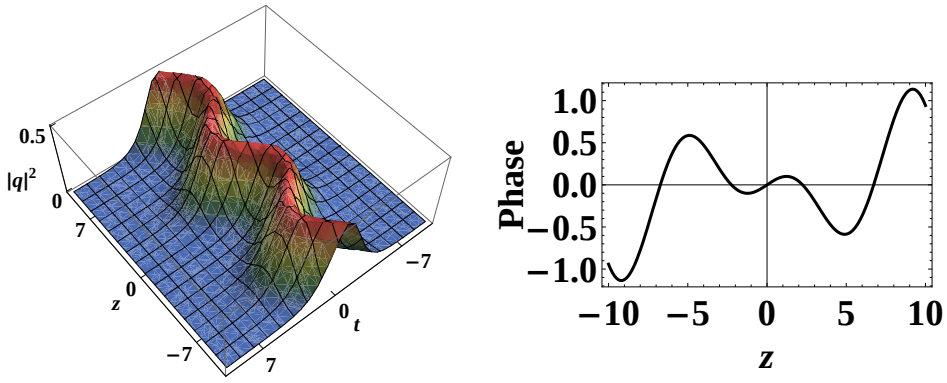

(a) (b)

Figure 3.2: The bright one-soliton propagation through homogenous fiber for parameters, (a)$k_1 = 0.5 + 0.5i$, $D(z) = cos(0.7z)$, $R = 0.5$,$\alpha_1 = 1 + i$ and $p = 0$. (b)Corresponding phase

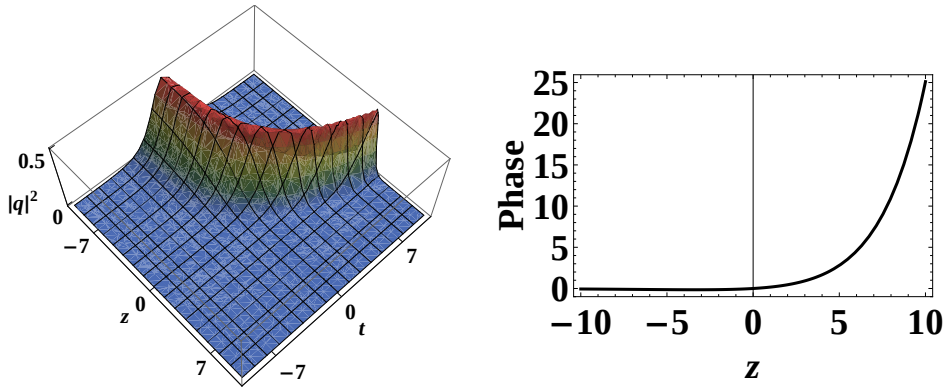

(a) (b)

Figure 3.3: The bright one-soliton propagation through homogenous fiber for parameters, (a)$k_1 = 0.5+0.5i$, $D(z) = Exp(0.3z)$, $R = 0.5$,$\alpha_1 = 1+i$ and $p = 0$. (b)Corresponding phase

3.2.2 Phase of bright soliton

To obtain the exact phase of bright soliton, we introduce an ansatz method. Thus, we can assume the solution q of the form [17]

$$q(z,t) = \rho(z,t)e^{i\psi(z,t)} \tag{3.5}$$

Substituting this expression into Eq. (3.1) and separating the real and imaginary parts, we obtain

$$\rho_z + p(z)\rho + D(z)\rho_t\psi_t + \frac{D(z)}{2}\psi_{tt} = 0 \tag{3.6}$$

$$2R(z)\rho^3 + D(z)\rho_{tt} - D(z)\rho\psi_t^2 - 2\rho\psi_z = 0 \tag{3.7}$$

Here, $\rho_z + 2p(z)\rho = 0$ is the stationary condition for $|q|^2$ from which one can assume the form $\rho = \rho_0 e^{-2\int p(z)dz}$. Further, by using Eq. (3.6), we obtain the expression for phase as

$$\psi = \int \frac{c_1(z)}{\rho_0}dt + \Omega z \tag{3.8}$$

where $\Omega = \frac{dA}{dz}$, $c_1(z)$ and $A(z)$ are integration constants. Substituting the expression (3.8) into (3.7), we obtain the following equation for intensity $I_0 = |\rho_0|^2$ as

$$(\frac{dI_0}{dt})^2 = -2\delta I_0^3 + \frac{8\Omega}{D(z)} I_0^2 + 4KI_0 - 4c_1^2 \tag{3.9}$$

where $\delta = \frac{2R(z)}{D(z)} e^{-2\int p(z)dz}$ and K is an integration constant. For the bright soliton the c_1 and K can be considered as zero. Hence the above expression can be cast into the form

$$(\frac{dI_0}{dt})^2 = -2\delta I_0^2 (I_0 - \rho_s) \tag{3.10}$$

where $\rho_s = \frac{4\Omega}{\delta D(z)}$. By integrating Eq.(3.10), we obtain the final form intensity($I = I_0 e^{-2\int p(z)dz}$) for the Vc-NLSE model as follows

$$I = \rho_s e^{-2\int p(z)dz} Sech^2(\sqrt{\frac{\delta}{2}\rho_s}\ \ t) \tag{3.11}$$

comparing with exact bright soliton intensity Eq.(3.4) that obtained by the HB method, we have $\rho_s = \frac{|\alpha_1|^2}{4\varrho_1}$. Therefore, the phase for bright soliton with this condition can be written as;

$$\psi = \frac{\delta |\alpha_1|^2 D(z)}{16\varrho_1} z \tag{3.12}$$

It is evident that, the phase of bright soliton is a time independent physical quantity which exhibit a constant phase along the spatial co-ordinate for the homogeneous systems. In the variable coefficient models, the GVD parameter $D(z)$ plays an important role on phase evolution which gives the idea of dispersion managed phase of soliton.

3.2.3 Bright two-soliton solutions

In order to get the bright two-soliton solution, the power series expansions of G and F can be truncated as follows, $G = g_1 + g_3$ and $F = 1 + f_2 + f_4$. Then, back

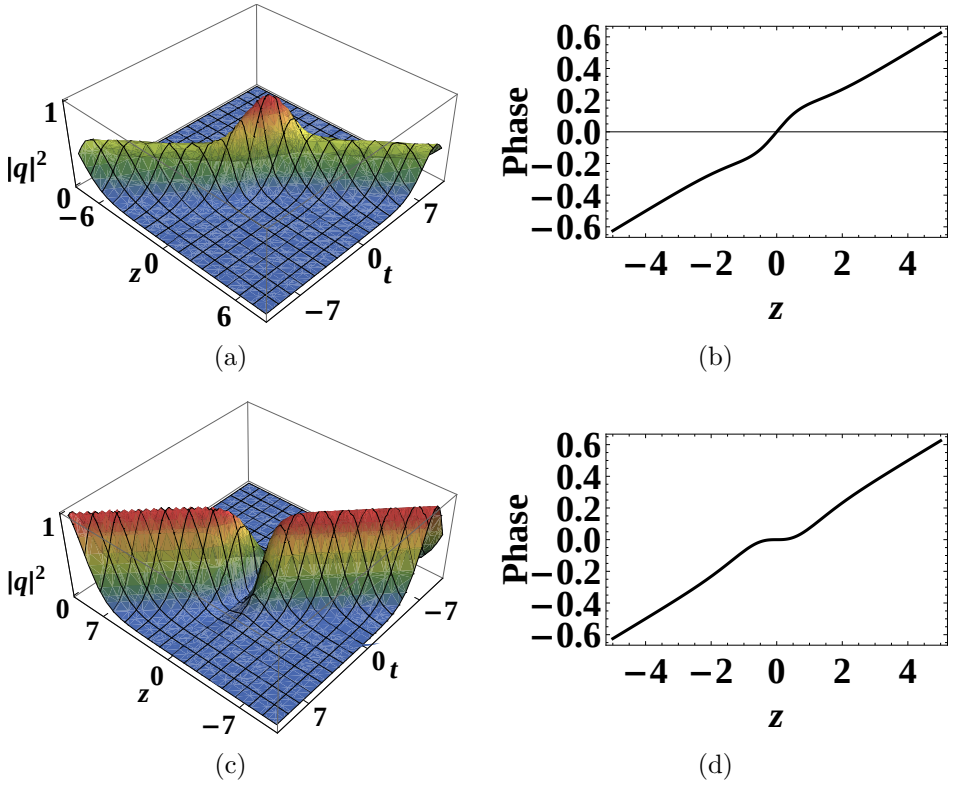

Figure 3.4: Nonlinear tunneling of bright one-soliton. (a) Dispersion barrier with $D(z) = 1 + hsech[z - z_0]^2$, $R = 0.5$ and $h = 1$.(b)Corresponding phase, (c) Dispersion well with $h = -1$.(d)Corresponding phase. Other physical quantities are $k_1 = 0.5 + 0.5i$,$\alpha_1 = 1 + i$, $p = 0.$ and $z_0 = 0.$

to bilinear equations (3.3), we obtain

$$g(z) = e^{-\int p(z)dz}$$

$$g_1 = \alpha_1 e^{\theta_1} + \alpha_2 e^{\theta_2}$$

$$g_3 = \beta_1 e^{\theta_1+\theta_1^*+\theta_2} + \beta_2 e^{\theta_2+\theta_2^*+\theta_1}$$

$$f_2 = \varrho_1 e^{\theta_1+\theta_1^*} + \varrho_2 e^{\theta_1+\theta_2^*} + \varrho_3 e^{\theta_2+\theta_1^*} + \varrho_4 e^{\theta_2+\theta_2^*}$$

$$f_4 = \varrho_5 e^{\theta_1+\theta_1^*+\theta_2+\theta_2^*}$$

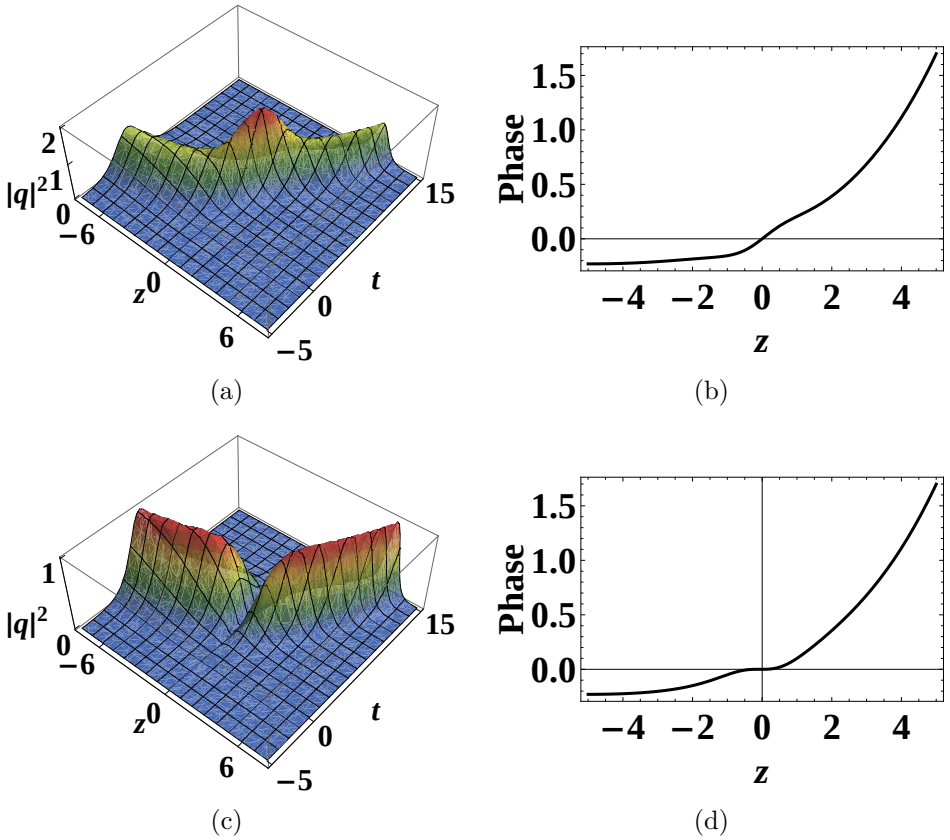

Figure 3.5: Tunneling with exponential background (a) Dispersion barrier of one-soliton with $k_1 = 0.5+0.5i$ and $h = 1$.(b)Corresponding phase (c)Dispersion well of one-soliton with $k_1 = 0.5 + 0.5i$ and $h = -1$.(d) Corresponding phase. Other physical quantities are $D(z) = d_0 e^{-rz} + h sech[z - z_0]^2$,$R = R_0 e^{-rz}$, $d_0 = 1$, $R_0 = 0.5$,$r = -0.2$,$z_0 = 0$ and $p = 0$.

$$\theta_1 = k_1 t + i k_1^2 \int D(z) dz$$

$$\theta_2 = k_2 t + i k_2^2 \int D(z) dz$$

$$\varrho_1 = \frac{\delta \alpha_1 \alpha_1^*}{2(k_1 + k_1^*)^2}$$

$$\varrho_2 = \frac{\delta \alpha_1 \alpha_2^*}{2(k_1 + k_2^*)^2}$$

$$\varrho_3 = \frac{\delta \alpha_1^* \alpha_2}{2(k_1^* + k_2)^2}$$

$$\varrho_4 = \frac{\delta \alpha_2 \alpha_2^*}{2(k_2 + k_2^*)^2}$$

$$\beta_1 = (k_1 - k_2)(\frac{\alpha_1 \varrho_3}{k_1 + k_1^*} - \frac{\alpha_2 \varrho_1}{k_2 + k_1^*})$$

$$\beta_2 = (k_1 - k_2)(\frac{\alpha_1 \varrho_4}{k_1 + k_2^*} - \frac{\alpha_2 \varrho_2}{k_2 + k_2^*})$$

$$\varrho_5 = \frac{|\alpha_1|^2|\alpha_2|^2|k_1 - k_2|^4}{4(k_1 + k_1^*)(k_2 + k_2^*)|k_1 + k_2|^4}$$

$$q_1(z,t) = e^{-\int p(z)dz}\frac{(g_1 + g_3)}{(1 + f_2 + f_4)} \tag{3.13}$$

3.2.4 Bright soliton collision

The collision behaviors between bright solitons in fibers can be revealed by analyzing the asymptotic states of soliton solution. Based on the two-soliton solution, we discussed the elastic collision between dark solitons in inhomogeneous fibers. The asymptotic analysis of two- soliton solution (3.13) has been studied as follows.

1) Before collision

(a)$S_1^-(\theta_1 + \theta_1^* \sim 0, \theta_2 + \theta_2^* \to -\infty)$

$$q(z,t) \to S_1^- = \frac{e^{-\int p(z)dz}\alpha_1}{2\sqrt{\varrho_1}}e^{-i\theta_{1I}}sech(\theta_{1R} + \frac{\ln \varrho_1}{2}) \tag{3.14}$$

(b)$S_2^-(\theta_2 + \theta_2^* \sim 0, \theta_1 + \theta_1^* \to \infty)$

$$q(z,t) \to S_2^- = \frac{e^{-\int p(z)dz}\beta_1}{2\sqrt{\varrho_1}\sqrt{\varrho_5}}e^{-i\theta_{2I}}sech(\theta_{2R} + \frac{1}{2}\ln(\varrho_5/\varrho_1)) \tag{3.15}$$

2)After collision

(a)$S_1^+(\theta_1 + \theta_1^* \sim 0, \theta_2 + \theta_2^* \to \infty)$

$$q(z,t) \to S_1^+ = \frac{e^{-\int p(z)dz}\beta_2}{2\sqrt{\varrho_4}\sqrt{\varrho_5}}e^{-i\theta_{1I}}sech(\theta_{1R} + \frac{\ln \varrho_5 - \ln \varrho_4}{2}) \tag{3.16}$$

(b)$S_2^+(\theta_2+\theta_2^*\sim 0, \theta_1+\theta_1^*\to -\infty)$

$$q(z,t)\to S_2^+ = \frac{e^{-\int p(z)dz}\alpha_2}{2\sqrt{\varrho_4}}e^{-i\theta_{2I}}sech(\theta_{2R}+\frac{\ln\varrho_4}{2}) \quad (3.17)$$

Similar way to the construct one-soliton phase with HB method, here, the individual soliton phase for the before and after collision can be written as

$$\psi^{1-} = \frac{\delta|\alpha_1|^2 D(z)}{16\varrho_1}z \quad (3.18)$$

$$\psi^{2-} = \frac{\delta|\beta_1|^2 D(z)}{16\varrho_1\varrho_5}z \quad (3.19)$$

$$\psi^{1+} = \frac{\delta|\beta_2|^2 D(z)}{16\varrho_4\varrho_5}z \quad (3.20)$$

$$\psi^{2+} = \frac{\delta|\alpha_2|^2 D(z)}{16\varrho_4}z \quad (3.21)$$

3.3 Results and discussions

In the presented work, firstly, we have investigated the constant mode of propagation. In such systems, the coefficient corresponding to GVD and nonlinearity taken as constant. The bright soliton propagation and corresponding phase evolution through homogeneous fiber is depicted in Fig. 3.1, where, the soliton amplitude, velocity and phase remains constant along the spatial dimension. By taking the varying GVD parameter as $D(z) = Cos(0.7z)$ the snaking phenomenon of dispersion managed solitons can be observed [18–21]. The corresponding phase are exhibiting an oscillating nature along the spatial axis as shown in Fig. 3.2.

To observe the pulse compression of bright soliton , we choose the dispersion and nonlinearity parameters are taken in the form of $\exp(0.3z)$[22]. It is observed that the soliton gets compressed during the propagation of the pulse down the fiber and corresponding phase also exhibiting an exponentially increasing nature as shown in Fig. 3.3 . It is evident that, unlike the concept of constant phase of bright soliton in NLSE [23], the $D(z)$ plays a important role on the evolution dynamics of soliton phase in the Vc-NLSE models.

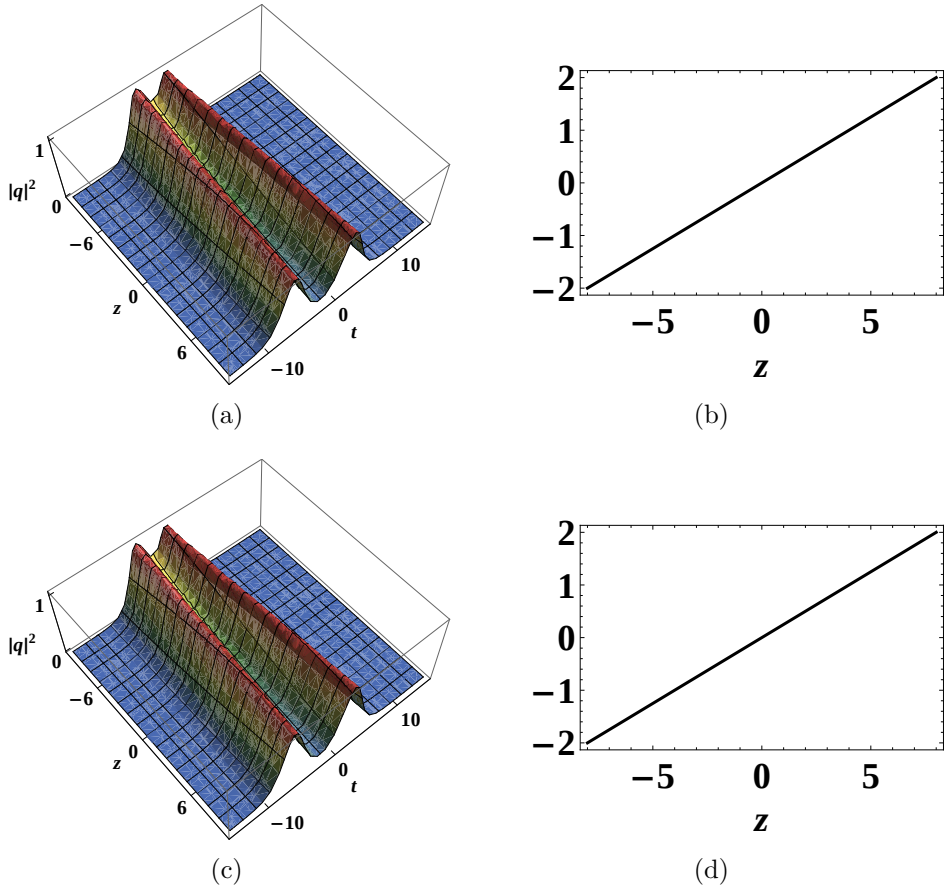

Figure 3.6: Elastic collision between two-soliton via asymptotic expression. (a)Before collision (b) Corresponding phase (c)after collision (d) Corresponding phase . Where $k_1 = 0.5 + 0.1i$and$k_2 = -0.5 - 0.1i$, $\alpha_1 = 1$,$\alpha_2 = -1$,$R = 0.5$ and $p = 0$

It is interesting to note that, the resultant phase of two-soliton remains constant during the time elastic collisions, see Fig. 3.6. That is, the phase study of two-soliton does not give any much more insight on evolution dynamics, therefor we have investigated the effect of inhomogeneity only on one-soliton cases. But the intensity based observation are conducted up to two-soliton level.

3.3.1 Nonlinear tunneling effect

We investigate the Nonlinear tunneling(NLT) effect of bright solitons through dispersion barrier. Recently, many leading research works have been investigated the tunneling effect of solitons in different physical systems [13–16]. All such

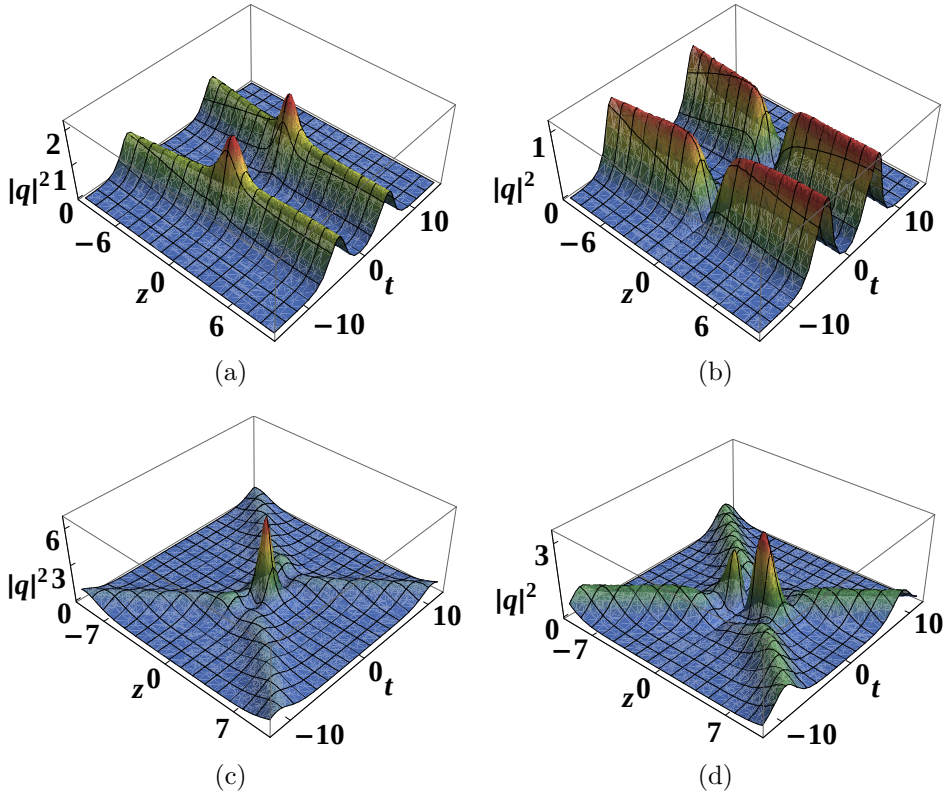

Figure 3.7: Nonlinear tunneling of Bright two-soliton. (a) Dispersion barrier with $D(z) = 1 + hsech[z - z_0]^2$, $R = 0.5$ and $h = 1$.(b) Dispersion well with $h = -1$. Where $k_1 = 0.5 + 0.1i$and$k_2 = -0.5 - 0.1i$.(c) Dispersion barrier (d) Dispersion well. Where $k_1 = 0.5 - 0.5i$ and $k_2 = -0.5 + 0.5i$. Other physical quantities are $\alpha_1 = 1 + i$, $p = 0.$ and $z_0 = 0.$

pioneering work has shown that the soliton can pass through the barrier without any loss

3.3.2 Nonlinear tunneling without exponential background

To investigate the NLT of Vc-NLS bright soliton propagating through the dispersion barrier or well, we choose the dispersion and nonlinear parameter as follows:

$$D(z) = r_0 \pm h\, sech^2(c(z - z_0))$$
$$R(z) = R_0$$

In the above expression h indicates the height of the barrier. The parameter c is related to its width and z_0 represents the longitudinal co-ordinate indicating the location of the dispersion barrier or dispersion well, and D_0, R_0 and S_0 are constant parameters. Here the positive (negative) sign of $\pm h$ denotes the barrier (well).

When the soliton is passing through the dispersion barrier, the intensity of the soliton grows and forms a peak at the location $z = z_0$. After passing through the barrier, the pulse will maintains its original shape . Similarly, when solitons pass through the dispersion well the amplitudes of solitons diminishes and a valley is formed at $z = z_0$; after the tunneling, solitons are regained to their original shapes as shown in Fig. 3.4. Similarly, the two-solitons tunneling are reported in Fig. 3.7

3.3.3 Nonlinear tunneling with exponential background

When pulse passing through the tunnel with exponential background, pulse compression is occur. To investigate dispersion barrier or well with exponential decay, we choose the dispersion and nonlinear parameter as shown below:

$$D(z) = D_0 exp(-rz) \pm h\, sech^2(c(z - z_0))$$
$$R(z) = R_0 exp(-rz)$$

Here, r represent the decaying parameter. From the above expressions with suitable parameter, we can conclude that when a bright soliton passes through the dispersion barrier/well with exponential decay the soliton will get compressed as shown in Fig. 3.5 It clearly shows that when solitons propagate through the dispersion barrier/well, after emerging from the well, the width of the soliton

gradually decreases along the propagation. From this result, the input pulse can be compressed to a desired extent in a controllable manner by the choice of barrier or well parameters of special form.

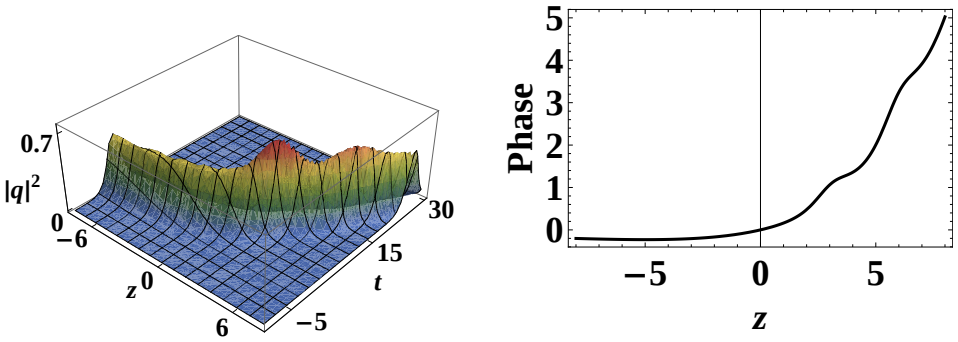

(a) (b)

Figure 3.8: Nonlinear tunneling and cascaded compression. (a) Dispersion barrier with $h = 1$ and $z = 3$.(b) Corresponding contour plot. Other physical quantities are $D(z) = d_0 e^{-rz} + h \sum_{j=1}^{n} sech[z - z_0]^2$, $R = R_0 e^{-rz}$, $k_1 = 0.5 + 0.5i$,$\alpha_1 = 1 + i$, $d_0 = 1$, $r = -0.2$ and $p = 0$.

3.3.4 Cascade compression

Based on the property of compression caused by pulse propagation through tunneling barrier or well with exponential background, we have studied the cascade compression through two successive potential barrier as shown in Fig. 3.8. To examine the cascaded compression of bright soliton, dispersion and nonlinear parameter are considered as follows;

$$D(z) = D_0 exp(-rz) \pm h\, sech^2(c(z - z_0))$$

$$R(z) = R_0 exp(-rz)$$

3.4 Conclusion

we have investigated the dynamics of bright soliton in the variable coefficient nonlinear Schrödinger (Vc-NLS)equation. Many fascinating results underlying spatial dependent bright soliton phase, which provides important insights into well-

known inhomogeneous phenomena, such as dispersion managed system, pulse compression and especially nonlinear tunneling effect, have been reported. By connecting an ansatz method with Hirota bilinear technique, we have introduced an explicit form of bright soliton phase. Exact bright two-soliton solution has also been derived by using the Hirota bilinear method. The elastic collision behavior of the bright solitons are observed by means of asymptotic analysis. Two-soliton phase are studied by the asymptotic expression which gives the description of individual solitons that exist before and after collision. Moreover, with a particular interest, we have investigated the tunneling effect through the dispersion barrier or well. Soliton intensity either forms a peak or valley and regains its shape after the tunneling through the barrier/well. For the case of exponential background, the soliton tends to compress after tunneling. Corresponding phase evolutions are illustrated in detail. For better insight, we have reported the cascade compression of solitons with multiple successive dispersion barriers. Overall, a comprehensive study of bright soliton dynamics and its phase evolution in Vc-NLS equation is presented.

Bibliography

[1] V.N. Serkin, A. Hasegawa, Phys. Rev. Lett. 85, 4502(2000)

[2] I. Gabitov, E.G. Shapiro, S.K. Turitsyn, Phys. Rev. E 55, 3624(1997)

[3] Lakoba T I and Kaup D J, Phys. Rev. E 58, 6728(1998)

[4] Kruglov V I, Peacock A C and Harvey J D, Phys. Rev. Lett. 90, 113902(2003)

[5] S.H. Chen, L. Yi, Phys. Rev. E 71, 016606 (2005)

[6] J.P. Tian, G.S. Zhou, Opt. Commun. 262, 257 (2006)

[7] Liu W J, B Tian and H Q Zhang, Phys. Rev. E 78, 066613(2008)

[8] T. Xu et al., Phys. Lett. A 372, 1990 (2008)

[9] R. Hirota, The Direct Method in Soliton Theory (Cambridge University Press, Cambridge, 2004)

[10] R. Radhakrishnan, M. Lakshmanan, J. Hietarinta, Phys. Rev. E 56, 2213 (1997)

[11] T. Kanna, M. Lakshmanan, Phys. Rev. Lett. 86, 5043(2001)

[12] W.J. Liu, B. Tian, H.Q. Zhang, L.L. Li, Y.S. Xue, Phys. Rev. E 77, 066605 (2008)

[13] A.C. Newell, J. Math. Phys. 19, 1126 (1978)

[14] V.N. Serkin, T.L. Belyaeva, J. Exp. Theor. Phys. Lett. 74, 573 (2001)

[15] V.N. Serkin, V.M. Chapela, J. Percino, T.L. Belyaeva, Opt. Commun. 192, 237 (2001)

[16] T.L. Belyaeva, V.N. Serkin, Eur. Phys. J. D 66, 153 (2012)

[17] A.Hasegawa and M.Matsumoto. Optical Solitons in Fibers, Springer, New York, 2003

[18] Malomed B A 2006 Soliton Management in Periodic Systems (Berlin: Springer)

[19] A. Mahalingam, A. Uthayakumar and P. Anandhi, J Opt (2013).

[20] K. Porsezian et al.,Physics Letters A 361, 504(2007)

[21] Yu-Jie Feng et al., Phys. Scr. 90, 045201 (2015)

[22] . M.S. Mani Rajan, A. Mahalingam, A. Uthayakumar, J. Opt. 14, 105204 (2012)

[23] G.P. Agrawal, Nonlinear Fiber Optics, Academic, New York, 2013.

Chapter 4

Dynamics of vector dark solitons propagation and tunneling effect in the Vc-CNLS equation

4.1 Introduction

The robust propagation of bright and dark solitons and its interaction behavior in multi-component optical fibers has been verified in a number of elegant experiments. In comparison to the bright soliton, the dark solitons have better stability against the influence of noise and fiber loss. Eversince the first investigation of the optical soliton propagation in the multimode fibers, coupled NLS equation (CNLSE) takes the lead role to describe the co-propagation of two or more optical fields via the cross-phase modulation (XPM) mechanism. In the birefringent fibers, which have two principal transmission axes within the fiber known as the fast and slow axes, solitons can co-propagate as one unit without splitting due to the phenomenon of soliton trapping. [1, 2] The unsplit two-component soliton by the soliton trapping mechanism are generally referred to as vector solitons. The different kind of vector soliton pair are possible in nonlinear fiber, which may have multiple distinct polarization components. The generalized CNLS equations are

widely used to describe the propagation of the bright vector solitons, dark-bright vector solitons and dark vector solitons. Recently, the Manakov vector-soliton received much attention from researchers because it was observed experimentally in different nonlinear mediums. [2–8]

In all the earlier investigations, the CNLS considered was for the ideal optical fiber with constant coefficients. However, in the realistic optical fiber under practical condition, the medium exhibits inhomogeneous behavior, which is inevitable. The generalized CNLS equations with variable coefficient (Vc-CNLSE) serves as the practical model to describe the vector soliton dynamics in an inhomogeneous systems. In this work, we focus on the following inhomogeneous Manakov model with distributed dispersion and nonlinearity, which governs the vector dark soliton propagation in the generalized 2-coupled NLS equations with varying coefficients [9–12]:

$$iq_{1z} - \frac{1}{2}D(z)q_{1tt} + R(z)(|q_1|^2 + |q_2|^2)q_1 + ip(z)q_1 = 0 \tag{4.1a}$$

$$iq_{2z} - \frac{1}{2}D(z)q_{2tt} + R(z)(|q_2|^2 + |q_1|^2)q_2 + ip(z)q_2 = 0 \tag{4.1b}$$

where, $q_1(z,t)$ and $q_2(z,t)$ are the slowly varying envelopes for the two polarization components in the electric fields. The variables z and t represent the normalized spatial and temporal coordinates. The group velocity dispersion, Kerr nonlinearity and amplification/absorption effects are related to the respective coefficient functions $D(z)$, $R(z)$ and $p(z)$.

Many mathematical techniques have been proposed to study the dynamics of the pulse evolution in nonlinear optical fibers. Here, we used Hirota's bilinear (HB) method. Compared with the numerical method, HB method involves perturbation technique to get the soliton solution and it provides explicit analytical expressions for the soliton pulses [13–18]. By using this approach, we report a more general form of vector dark soliton solutions for Vc-CNLSE. To the best of our knowledge, the dark soliton solutions of the model (4.1) have not been

reported before. In addition to that, we studied the vector dark solitons energies and its dependance with some important physical parameters. Moreover, collision dynamics of the dark vector solitons of Eq.(4.1)have been studied up to three soliton level, with various possible inhomogeneous effect, which also have not been reported so far, in the context of Vc-CNLSE.

In this chapter, we theoretically reveal the possible influence of inhomogeneity on the dynamical properties of vector dark solitons. Based on Eq.(4.1), one can investigate many inhomogeneous behaviors such as, pulse amplification/absorption, compression/broadening, dispersion-managed transmission systems and nonlinear tunneling. In many leading research works, they investigated the NL tunneling effect of solitons in different physical systems [19–22]. Recently, NL of bright and dark soliton in the nonlinear Schrödinger equation (NLSE) with variable coefficients and an external harmonic potential was reported in [23]. NL effects of rogue wave has been investigated in [24, 25]. Tunneling of bright and dark similariton in the birefringent fiber was reported in [12]. The wave-particle duality nature of soliton was revealed through tunneling of potential barrier/well in [26]. Tunneling of bright soliton in inhomogeneous CNLS equation with higher order effects was considered in [27, 28]. The NL tunneling of the higher-order breathers and rogue waves have been studied by the variable-coefficient derivative nonlinear Schrödinger (Vc-DNLS) equation in [29]. For the better insight, we also discussed the nonlinear tunneling of vector dark soliton in Vc-CNLS model for the first time to the best of our knowledge.

The organization of the chapter is as follows. Sec.1 features a detailed introduction to Vc-CNLSE. Sec. 2 presents the exact dark soliton solutions by Hirota's method. Sec 3 - 5 describe the dynamics of one, two and three soliton solutions respectively. Asymptotic analysis to study the collision behavior is also presented in Sec.4 and 5. A brief discussion about the various physical effects in the dynamics of dark soliton propagation through inhomogenous fiber is presented in Sec. 6. The NL tunneling of dark soliton through barrier/well is

presented in Sec. 7, and the paper concludes with a summary of results in Sec. 8.

4.2 Dark soliton solutions by Hirota method

We employ the Hirota's bilinear (HB) method to investigate the exact analytical dark soliton solutions of Eq. (4.1). We follow the transformation as used in the Refs. [16–18], which is expected to give an exact form of dark soliton solutions. Such study has not been discussed in the context of Vc-CNLSE. By using this transformation, one can transform the nonlinear differential equations into bilinear differential equations. Then, with the different levels of perturbation expansions, one can derive the exact form of dark soliton solutions up to the corresponding order through this bilinear equations.

To construct the vector dark soliton solutions, we apply the following form of Hirota bilinear transformations;

$$q_1(z,t) = g(z)\frac{G}{F} \tag{4.2a}$$

$$q_2(z,t) = g(z)\frac{H}{F} \tag{4.2b}$$

where, G and H are complex functions and F is a real function. By substituting this transformation into Eq. (4.1), the following bilinear equations can be obtained,

$$[iD_z - \frac{1}{2}D(z)D_t^2 + \lambda(z)](G.F) = 0 \tag{4.3a}$$

$$[iD_z - \frac{1}{2}D(z)D_t^2 + \lambda(z)](H.F) = 0 \tag{4.3b}$$

$$\delta(|G|^2 + |H|^2) + D_t^2(F.F) = \frac{2\lambda(z)}{D(z)}F^2 \tag{4.3c}$$

With the condition $g_z(z) + g(z)p(z) = 0$. Here, $\lambda(z)$ is an analytic function to be determined, the δ can be introduced as $\delta = \frac{2R(z)}{D(z)}g(z)^2$ and D_z and D_t are the bilinear differential operators [13] defined by

$$D_z^m D_t^n(g.f) = (\frac{\partial}{\partial z} - \frac{\partial}{\partial z'})^m(\frac{\partial}{\partial t} - \frac{\partial}{\partial t'})^n g(z,t)f(z,t)|_{z'=z,t'=t}$$

By solving the above set of Eqs. (4.3) , we take the power series expansion of G, H and F as,

$$G = g_0[1 + \sum_{n=1}^{\infty} \varepsilon^n g_n(z,t)]$$
$$H = h_0[1 + \sum_{n=1}^{\infty} \varepsilon^n h_n(z,t)]$$
$$F = 1 + \sum_{n=1}^{\infty} \varepsilon^n f_n(z,t)$$

with ε as the formal expansion parameter. In regular perturbation expansion, the effect of the small amplitude parameter ε is small. For all sufficiently small ε ($\varepsilon \ll 1$) and the coefficients g_n, h_n and f_n are independent of ε. Substituting this expansion series (G, H and F) into Eqs. (4.3) and collecting terms of each order of ε, we obtain

$$\varepsilon^0 : [iD_z - \frac{1}{2}D(z)D_t^2 + \lambda(z)](g_0.1) = 0,$$
$$[iD_z - \frac{1}{2}D(z)D_t^2 + \lambda(z)](h_0.1) = 0,$$
$$\delta(g_0 g_0^* + h_0 h_0^*) + D_t^2(1.1) = \frac{2\lambda(z)}{D(z)}1^2$$

$$\varepsilon^1 : [iD_z - \frac{1}{2}D(z)D_t^2 + \lambda(z)](g_0 g_1.1 + 1.f_1) = 0$$
$$[iD_z - \frac{1}{2}D(z)D_t^2 + \lambda(z)](h_0 h_1.1 + 1.f_1) = 0$$
$$\delta(g_0 g_0^*(g_1 + g_1^*) + h_0 h_0^*(h_1 + h_1^*)) + D_t^2(1.f_1 + f_1.1) = \frac{2\lambda(z)}{D(z)}(f_1 + f_1)$$

In the same way, we can find out the coefficient of ε^2,ε^3 etc. One of the solution of Eqs. (4.3) are exponential function. Hence,while applying Hirota Direct method,we assume g_n,h_n and f_n as,

$$\begin{aligned}
g_0(h_0) &= a(b)\exp[i\psi] \\
g_n &= \sum_{j_n>..j_2>j_1}^{n} A_{j_1 j_2..j_n}(\prod_{j_1=1}^{n}\alpha_{j_n})\exp[\sum_{j=1}^{n}\theta_j] \\
h_n &= \sum_{j_n>..j_2>j_1}^{n} A_{j_1 j_2..j_n}(\prod_{j_1=1}^{n}\beta_{j_n})\exp[\sum_{j=1}^{n}\theta_j] \\
f_n &= \sum_{j_n>..j_2>j_1}^{n} A_{j_1 j_2..j_n}\ \exp[\sum_{j=1}^{n}\theta_j]
\end{aligned}$$

Where,

$$A_{j_1...j_n} = \prod_{j_i<j_k}^{(n)} A_{j_i j_k}$$

Here, (n) indicates the product of all possible combinations of n elements with $(j_i < j_k)$. Note that $A_{j_m} = 1 \quad \text{for} \quad m = 1, 2, ...n$.

By the unique properties of D-operator, the perturbation expansions may be truncated as finite sums while solving the bilinear Eqs. (4.3). Such a truncated series will provide an exact analytical solution for the Vc-CNLSE. It would not be possible by a normal derivative [13]. Thus, while we are constructing n-soliton solution for the Eq. (4.1) we will assume that $g_N = h_N = f_N = 0$ for all $N \geq n + 1$. In this way, the G,H and F can be written as finite series for each level of soliton solutions. further details are discussed in the following sections.

4.3 One-soliton solutions

One can obtain the dark one-soltion solution by truncating the power series expansion for G, H and F to the first order in ε as follows, $G = g_0(1 + \varepsilon g_1)$, $H = h_0(1 + \varepsilon h_1)$ and $F = 1 + \varepsilon f_1$. Where the higher order terms in ε can be neglected. Then we assume,

$$g_0 = ae^{i\psi} \qquad h_0 = be^{i\psi}$$
$$g_1 = \alpha_1 e^{\theta_1} \qquad h_1 = \beta_1 e^{\theta_1}$$
$$f_1 = e^{\theta_1} \qquad g(z) = e^{-\int p(z)dz}$$
$$\psi = kt - \omega \int D(z)dz \qquad \theta_1 = k_1 t - \omega_1 \int D(z)dz$$

Then, back to bilinear Eqs. (4.3), we obtain some associated parameters related to one- soliton solution as

$$\lambda = \frac{1}{2}\delta(a^2 + b^2)D(z) \qquad \omega = -\frac{\lambda}{D(z)} - \frac{k^2}{2}$$

$$\alpha_1 = \frac{2\omega_1 + 2kk_1 + ik_1^2}{2\omega_1 + 2kk_1 - ik_1^2} \qquad \alpha_1 = \beta_1$$
$$\omega_1 = \frac{k_1}{2}(-2k \pm \sqrt{2\delta(a^2 + b^2) - k_1^2})$$

After absorbing ε, the final form of Eqn. (4.2) for the one-soliton solutions can be written as,

$$q_1(z,t) = \frac{a[(1 + \alpha_1) + (\alpha_1 - 1)tanh(\frac{\theta_1}{2})]}{2e^{\int p(z)dz}e^{-i\psi}} \tag{4.4a}$$

$$q_2(z,t) = \frac{b[(1 + \beta_1) + (\beta_1 - 1)tanh(\frac{\theta_1}{2})]}{2e^{\int p(z)dz}e^{-i\psi}} \tag{4.4b}$$

Where, a, b and ψ are real functions denoting the amplitudes and phase of the background wave. From the Eq. (4.4), one can analyze the dynamics of vector dark one-soliton pulse in inhomogeneous fibers. The propagation of dark one-solitons through homogenous fiber is depicted in the Fig. 4.1.

In order to get the suitable parametric region of soliton solution, we consider the real dispersion relation for the dark soliton solution. Thus, the frequency ω_1 is real, if the k_1 satisfies the condition $-\sqrt{2\delta(a^2+b^2)} < k_1 < \sqrt{2\delta(a^2+b^2)}$ with $2\delta(a^2+b^2) > 0$. which are the basic conditions to ensure the existence of soliton solution.

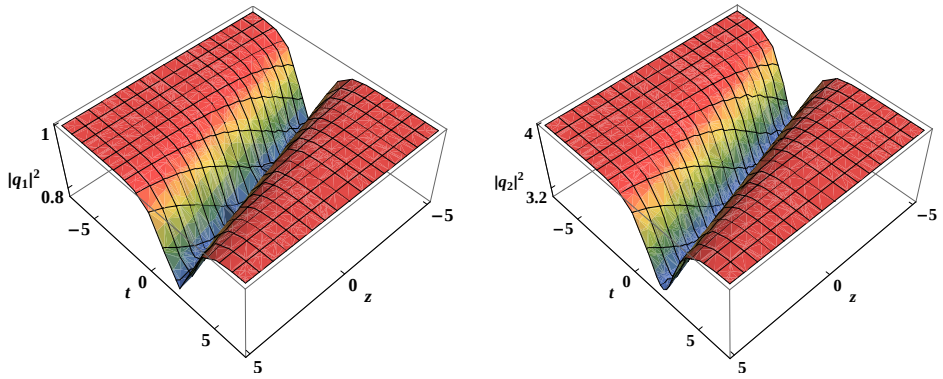

Figure 4.1: The dark one-soliton propagation through homogenous fiber for parameters, (a) a=1 ,(b)b=2. Other physical quantities are $k = D(z) = \delta = 1$, $k_1 = -1.5$ and $p = 0$

4.3.1 Physical quantities of dark solitons

To study the dynamics of dark soliton and to characterize the impact of inhomogeneous features of propagating optical dark soliton, some of the physical quantities such as velocity, width, amplitude and energy are important. Such quantities can be defined as follows,

$$V = \frac{\omega_1}{\kappa_1} D(z), \quad W = \frac{1}{\kappa_1}$$

$$A_1 = |\frac{a(1+\alpha_1)}{2e^{\int p(z)dz}}|, \quad A_2 = |\frac{b(1+\beta_1)}{2e^{\int p(z)dz}}|$$

The energy E and power P, in terms of the background amplitudes a and b can be expressed as $E_i = \int_{-\infty}^{\infty} P_i dt$ with $P_1(z,t) = a^2 - |q_1|^2$ and $P_2(z,t) = b^2 - |q_2|^2$, respectively. Here, the instantaneous power is obtained as a difference between the total power and the corresponding value for the background [30]. The energy, corresponding to the one-soliton solution as given by Eq. (4.4), can be written as

$$E_1 = \int_{-\infty}^{\infty} (a^2 - |q_1|^2)dt = \frac{2 - \alpha_1 - \alpha_1^*}{a^{-2}e^{2\int p(z)dz}k_1} \tag{4.5a}$$

$$E_2 = \int_{-\infty}^{\infty} (b^2 - |q_2|^2)dt = \frac{2 - \beta_1 - \beta_1^*}{b^{-2}e^{2\int p(z)dz}k_1} \tag{4.5b}$$

From the above set of equations, one can analyze the effect of inhomogeneity on the physical quantities of dark soliton. It is interesting to note that, $p(z)$ affects the soliton amplitude and energy, $D(z)$ affects the soliton velocity. The width of solitons are related to the wave number k_1.

4.4 Two-soliton solutions

To construct the dark two-soliton solutions, the power series expansions for G, H and F are truncated as follows, $G = g_0(1 + g_1 + g_2)$, $H = h_0(1 + h_1 + h_2)$ and $F = 1 + f_1 + f_2$. Then, from bilinear equations Eq.(4.3), we obtain

$$g_0 = ae^{i\psi} \qquad h_0 = be^{i\psi}$$

$$\psi = k\tau - \omega \int D(z)dz, \qquad g(z) = e^{-\int p(z)dz}$$

$$\lambda = \frac{1}{2}\delta(a^2+b^2)D(z) \qquad \omega = -\frac{\lambda}{D(z)} - \frac{k^2}{2}$$

$$g_1 = \alpha_1 e^{\theta_1} + \alpha_2 e^{\theta_2}, \qquad h_1 = \beta_1 e^{\theta_1} + \beta_2 e^{\theta_2}$$

$$g_2 = A_{12}\alpha_1\alpha_2 e^{\theta_1+\theta_2}, \qquad h_2 = A_{12}\beta_1\beta_2 e^{\theta_1+\theta_2}$$

$$f_1 = e^{\theta_1} + e^{\theta_2} \qquad f_2 = A_{12}e^{\theta_1+\theta_2}$$

$$\theta_1 = k_1 t - \omega_1 \int D(z)dz$$

$$\theta_2 = k_2 t - \omega_2 \int D(z)dz$$

$$\alpha_1 = \beta_1 = \frac{2\omega_1 + 2kk_1 + ik_1^2}{2\omega_1 + 2kk_1 - ik_1^2},$$

$$\alpha_2 = \beta_2 = \frac{2\omega_2 + 2kk_2 + ik_2^2}{2\omega_2 + 2kk_2 - ik_2^2},$$

$$\omega_1 = \frac{k_1}{2}(-2k \pm \sqrt{2\delta(a^2+b^2) - k_1^2})$$

$$\omega_2 = \frac{k_2}{2}(-2k \pm \sqrt{2\delta(a^2+b^2) - k_2^2})$$

$$A_{12} = -\frac{2i(\alpha_1-\alpha_2)(\omega_2-\omega_1-kk_1+kk_2) - (\alpha_1+\alpha_2)(k_1-k_2)^2}{2i(1-\alpha_1\alpha_2)(\omega_1+\omega_2+kk_1+kk_2) - (\alpha_1\alpha_2+1)(k_1+k_2)^2}$$

Then, the final form of two-soliton solutions can be written as,

$$q_1(z,t) = e^{-\int p(z)dz}\frac{g_0(1+g_1+g_2)}{(1+f_1+f_2)} \tag{4.6a}$$

$$q_2(z,t) = e^{-\int p(z)dz}\frac{h_0(1+h_1+h_2)}{(1+f_1+f_2)} \tag{4.6b}$$

Using Eqs. (4.6), the propagation of dark two-solitons through homogenous fiber is depicted in the Fig. 4.2.

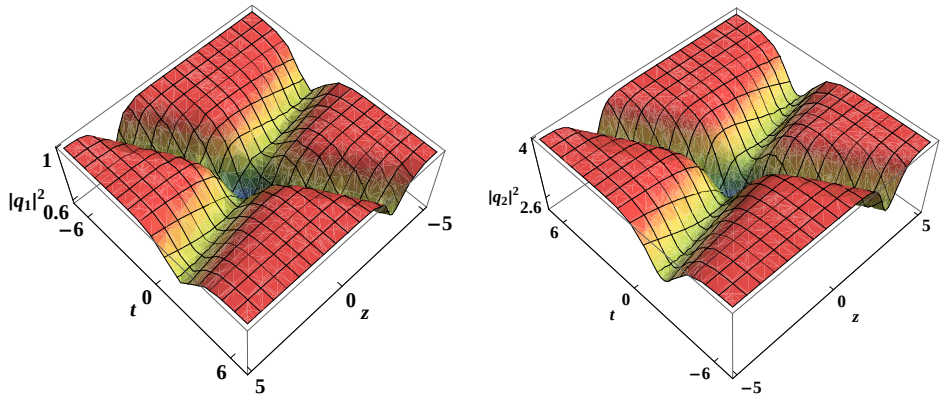

(a) (b)

Figure 4.2: The dark two-soliton propagation through homogenous fiber for parameters , (a) a=1 ,(b)b=2. Other physical quantities are $k = D(z) = \delta = 1$, $k_1 = -1.5$, $k_2 = 1.5$ and $p = 0$

4.4.1 Two-soliton collision

The collision behavior between dark solitons in fibers can be studied by analyzing the asymptotic states of soliton solution. Based on the two-soliton solutions, we discussed the elastic collision between dark solitons in inhomogeneous fibers. The asymptotic analysis of two-dark soliton solutions given by Eq. (4.6) are conducted as follows.

1) Before collision

(a)$S^{1-}(\theta_1 \sim 0, \theta_2 \to -\infty)$

$$q_1 \to S_1^{1-} = \frac{ae^{i\psi}}{2e^{\int p(z)dz}}[(1+\alpha_1) + (\alpha_1 - 1)tanh(\frac{\theta_1}{2})] \quad (4.7a)$$

$$q_2 \to S_2^{1-} = \frac{be^{i\psi}}{2e^{\int p(z)dz}}[(1+\beta_1) + (\beta_1 - 1)tanh(\frac{\theta_1}{2})] \quad (4.7b)$$

(b)$S^{2-}(\theta_2 \sim 0, \theta_1 \to \infty)$

$$q_1 \to S_1^{2-} = \frac{a\alpha_1 e^{i\psi}}{2e^{\int p(z)dz}}[(1+\alpha_2) + (\alpha_2 - 1)tanh(\frac{\theta_2}{2} + ln\sqrt{A_{12}})] \quad (4.8a)$$

$$q_1 \to S_2^{2-} = \frac{b\beta_1 e^{i\psi}}{2e^{\int p(z)dz}}[(1+\beta_2)+(\beta_2-1)tanh(\frac{\theta_2}{2}+ln\sqrt{A_{12}}))] \quad (4.8b)$$

2)After collision

(a)$S^{1+}(\theta_1 \sim 0, \theta_2 \to \infty)$

$$q_1 \to S_1^{1+} = \frac{a\alpha_2 e^{i\psi}}{2e^{\int p(z)dz}}[(1+\alpha_1)+(\alpha_1-1)tanh(\frac{\theta_1}{2}+ln\sqrt{A_{12}})] \quad (4.9a)$$

$$q_2 \to S_2^{1+} = \frac{b\beta_2 e^{i\psi}}{2e^{\int p(z)dz}}[(1+\beta_1)+(\beta_1-1)tanh(\frac{\theta_1}{2}+ln\sqrt{A_{12}})] \quad (4.9b)$$

(b)$S^{2+}(\theta_2 \sim 0, \theta_1 \to -\infty)$

$$q_1 \to S_1^{2+} = \frac{ae^{i\psi}}{2e^{\int p(z)dz}}[(1+\alpha_2)+(\alpha_2-1)tanh(\frac{\theta_2}{2})] \quad (4.10a)$$

$$q_1 \to S_2^{2+} = \frac{be^{i\psi}}{2e^{\int p(z)dz}}[(1+\beta_2)+(\beta_2-1)tanh(\frac{\theta_2}{2})] \quad (4.10b)$$

By comparing the asymptotic expressions (4.7)-(4.8) with (4.9)-(4.10), one can infer the particle like behavior of solitons during the time of collisions between dark solitons S_1 and S_2. The above expressions, also illustrate that the collision between the two-dark solitons are elastic for the condition $|\alpha_i| = |\beta_i| = 1(i = 1, 2)$. The exchange of energy in the dark solitons collision provides a useful way on how to manipulate and utilize dark soliton in optical communication systems. The relevant physical quantities of solitons S_1 and S_2 before and after collisions are mentioned in Table 1.

Table 4.1: Physical quantities of solitons S_1 and S_2 before and after the collision.

Solitons	Velocities	Widths	Amplitudes	Energies
s_1^{1-}	$\frac{\omega_1}{k_1}D(z)$	$\frac{1}{k_1}$	$\lvert\frac{a(1+\alpha_1)}{2e^{\int p(z)dz}}\rvert$	$\frac{a^2(2-\alpha_1-\alpha_1^*)}{k_1 e^{2\int p(z)dz}}$
s_2^{1-}	$\frac{\omega_1}{k_1}D(z)$	$\frac{1}{k_1}$	$\lvert\frac{b(1+\beta_1)}{2e^{\int p(z)dz}}\rvert$	$\frac{b^2(2-\beta_1-\beta_1^*)}{k_1 e^{2\int p(z)dz}}$
s_1^{2-}	$\frac{\omega_2}{k_2}D(z)$	$\frac{1}{k_2}$	$\lvert\frac{a\alpha_1(1+A_{12}\alpha_2)}{e^{\int p(z)dz}(1+A_{12})}\rvert$	$\frac{a^2(2-\alpha_2-\alpha_2^*)}{k_2 e^{2\int p(z)dz}}$
s_2^{2-}	$\frac{\omega_2}{k_2}D(z)$	$\frac{1}{k_2}$	$\lvert\frac{b\beta_1(1+A_{12}\beta_2)}{e^{\int p(z)dz}(1+A_{12})}\rvert$	$\frac{b^2(2-\beta_2-\beta_2^*)}{k_2 e^{2\int p(z)dz}}$
s_1^{1+}	$\frac{\omega_1}{k_1}D(z)$	$\frac{1}{k_1}$	$\lvert\frac{a\alpha_2(1+A_{12}\alpha_1)}{e^{\int p(z)dz}(1+A_{12})}\rvert$	$\frac{a^2(2-\alpha_1-\alpha_1^*)}{k_1 e^{2\int p(z)dz}}$
s_2^{1+}	$\frac{\omega_1}{k_1}D(z)$	$\frac{1}{k_1}$	$\lvert\frac{b\beta_2(1+A_{12}\beta_1)}{e^{\int p(z)dz}(1+A_{12})}\rvert$	$\frac{b^2(2-\beta_1-\beta_1^*)}{k_1 e^{2\int p(z)dz}}$
s_1^{2+}	$\frac{\omega_2}{k_2}D(z)$	$\frac{1}{k_2}$	$\lvert\frac{a(1+\alpha_2)}{2e^{\int p(z)dz}}\rvert$	$\frac{a^2(2-\alpha_2-\alpha_2^*)}{k_2 e^{2\int p(z)dz}}$
s_2^{2+}	$\frac{\omega_2}{k_2}D(z)$	$\frac{1}{k_2}$	$\lvert\frac{b(1+\beta_2)}{2e^{\int p(z)dz}}\rvert$	$\frac{b^2(2-\beta_2-\beta_2^*)}{k_2 e^{2\int p(z)dz}}$

4.5 Three-soliton solutions

The three-soliton solutions can be obtained by truncating G, H and F as follows, $G = G_0(1 + g_1 + g_2 + g_3)$,$G = G_0(1 + h_1 + h_2 + h_3)$ and $F = 1 + f_1 + f_2 + f_3$. Then, back to bilinear equations (4.3), we obtain

$$g_0 = ae^{i\psi} \qquad h_0 = be^{i\psi}$$

$$\psi = k\tau - \omega\int D(z)dz, \qquad g(z) = e^{-\int p(z)dz}$$

$$\lambda = \frac{1}{2}\delta(a^2+b^2)D(z) \qquad \omega = -\frac{\lambda}{D(z)} - \frac{k^2}{2}$$

$$g_1 = \alpha_1\, e^{\theta_1} + \alpha_2\, e^{\theta_2} + \alpha_3\, e^{\theta_3}$$

$$h_1 = \beta_1\, e^{\theta_1} + \beta_2\, e^{\theta_2} + \beta_3\, e^{\theta_3}$$

$$f_1 = e^{\theta_1} + e^{\theta_2} + e^{\theta_3}$$

$$g_2 = A_{12}\alpha_1\alpha_2\, e^{\theta_1+\theta_2} + A_{13}\alpha_1\alpha_3 e^{\theta_1+\theta_3} + A_{23}\alpha_2\alpha_3 e^{\theta_2+\theta_3}$$

$$h_2 = A_{12}\beta_1\beta_2\, e^{\theta_1+\theta_2} + A_{13}\beta_1\beta_3 e^{\theta_1+\theta_3} + A_{23}\beta_2\beta_3 e^{\theta_2+\theta_3}$$

$$f_2 = A_{12}e^{\theta_1+\theta_2} + A_{13}e^{\theta_1+\theta_3} + A_{23}e^{\theta_2+\theta_3}$$

$$g_3 = A_{123}\alpha_1\alpha_2\alpha_3 e^{\theta_1+\theta_2+\theta_3}$$

$$h_3 = A_{123}\beta_1\beta_2\beta_3 e^{\theta_1+\theta_2+\theta_3}$$

$$f_3 = A_{123}e^{\theta_1+\theta_2+\theta_3}$$

with

$$\theta_i = k_i t - \omega_i \int D(z)dz$$

$$\alpha_i = \frac{2\omega_i + 2kk_i + ik_i^2}{2\omega_i + 2kk_i - ik_i^2}$$

$$\omega_i = \frac{k_i}{2}(-2k \pm \sqrt{2\delta(a^2+b^2) - k_i^2})$$

where $i = 1, 2\text{and } 3$

$$A_{12} = -\frac{2i(\alpha_1-\alpha_2)(\omega_2-\omega_1-kk_1+kk_2) - (\alpha_1+\alpha_2)(k_1-k_2)^2}{2i(1-\alpha_1\alpha_2)(\omega_1+\omega_2+kk_1+kk_2) - (\alpha_1\alpha_2+1)(k_1+k_2)^2}$$

$$A_{13} = -\frac{2i(\alpha_1-\alpha_3)(\omega_3-\omega_1-kk_1+kk_3) - (\alpha_1+\alpha_3)(k_1-k_3)^2}{2i(1-\alpha_1\alpha_3)(\omega_1+\omega_3+kk_1+kk_3) - (\alpha_1\alpha_3+1)(k_1+k_3)^2}$$

$$A_{23} = -\frac{2i(\alpha_2-\alpha_3)(\omega_3-\omega_2-kk_2+kk_3) - (\alpha_2+\alpha_3)(k_2-k_3)^2}{2i(1-\alpha_2\alpha_3)(\omega_2+\omega_3+kk_2+kk_3) - (\alpha_2\alpha_3+1)(k_2+k_3)^2}$$

$$A_{123} = A_{12}A_{13}A_{23}$$

The three-soliton solutions can be written as,

$$q_1(z,t) = e^{-\int p(z)dz} \frac{g_0(1+g_1+g_2+g_3)}{(1+f_1+f_2+f_3)} \tag{4.11a}$$

$$q_2(z,t) = e^{-\int p(z)dz} \frac{h_0(1+h_1+h_2+h_3)}{(1+f_1+f_2+f_3)} \tag{4.11b}$$

Using Eqs.(4.11), the propagation of dark three-solitons through homogenous fiber is illustrated in the Fig. 4.3.

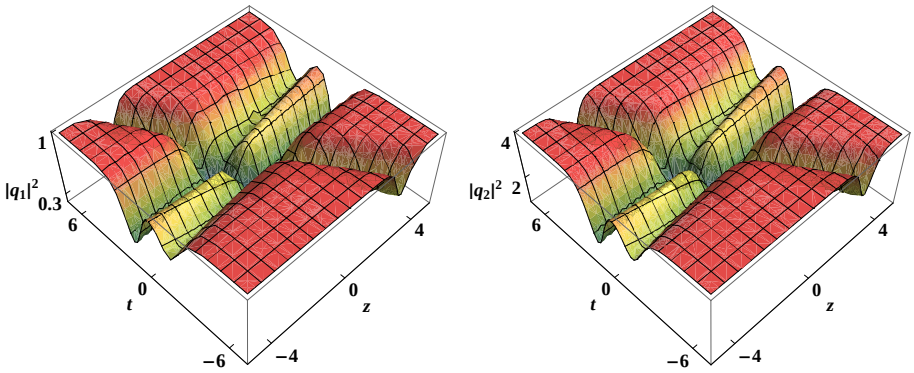

Figure 4.3: The dark three-soliton propagation through homogenous fiber for parameters , (a)a=1 ,(b)b=2. Other physical quantities are $k = D(z) = \delta = 1$, $k_1 = 2$, $k_2 = 2.5$, $k_3 = -2$ and $p = 0$.

4.5.1 Three-soliton collisions

The asymptotic analysis of three-dark solitons S_1, S_2 and S_3 before and after collision are elucidated as follows.

1) Before collision

(a) $S^{1-}(\theta_1 \sim 0, \theta_2 \to -\infty, \theta_3 \to -\infty)$

$$q_1 \to S_1^{1-} = \frac{ae^{i\psi}}{2e^{\int p(z)dz}}[(1+\alpha_1) + (\alpha_1 - 1)tanh(\frac{\theta_1}{2})] \tag{4.12a}$$

$$q_2 \to S_2^{1-} = \frac{be^{i\psi}}{2e^{\int p(z)dz}}[(1+\beta_1) + (\beta_1 - 1)tanh(\frac{\theta_1}{2})] \quad (4.12b)$$

(b) $S^{2-}(\theta_2 \sim 0, \theta_1 \to \infty, \theta_3 \to -\infty)$

$$q_1 \to S_1^{2-} = \frac{a\alpha_1 e^{i\psi}}{2e^{\int p(z)dz}}[(1+\alpha_2) + (\alpha_2 - 1)tanh(\frac{\theta_2}{2} + ln\sqrt{A_{12}})] \quad (4.13a)$$

$$q_2 \to S_2^{2-} = \frac{b\beta_1 e^{i\psi}}{2e^{\int p(z)dz}}[(1+\beta_2) + (\beta_2 - 1)tanh(\frac{\theta_2}{2} + ln\sqrt{A_{12}})] \quad (4.13b)$$

(c) $S^{3-}(\theta_3 \sim 0, \theta_1 \to \infty, \theta_2 \to \infty)$

$$q_1 \to S_1^{3-} = \frac{a\alpha_1\alpha_2 e^{i\psi}}{2e^{\int p(z)dz}}[(1+\alpha_3) + (\alpha_3 - 1)tanh(\frac{\theta_3}{2} + ln\sqrt{A_{13}A_{23}})] \quad (4.14a)$$

$$q_2 \to S_2^{3-} = \frac{b\beta_1\beta_2 e^{i\psi}}{2e^{\int p(z)dz}}[(1+\beta_3) + (\beta_3 - 1)tanh(\frac{\theta_3}{2} + ln\sqrt{A_{13}A_{23}})] \quad (4.14b)$$

2)After collision

(a)$S^{1+}(\theta_1 \sim 0, \theta_2 \to \infty, \theta_3 \to \infty)$

$$q_1 \to S_1^{1+} = \frac{a\alpha_2\alpha_3 e^{i\psi}}{2e^{\int p(z)dz}}[(1+\alpha_1) + (\alpha_1 - 1)tanh(\frac{\theta_1}{2} + ln\sqrt{A_{12}A_{13}})] \quad (4.15a)$$

$$q_2 \to S_2^{1+} = \frac{b\beta_2\beta_3 e^{i\psi}}{2e^{\int p(z)dz}}[(1+\beta_1) + (\beta_1 - 1)tanh(\frac{\theta_1}{2} + ln\sqrt{A_{12}A_{13}})] \quad (4.15b)$$

(b)$S^{2+}(\theta_2 \sim 0, \theta_1 \to -\infty, \theta_3 \to \infty)$

$$q_1 \to S_1^{2+} = \frac{a\alpha_3 e^{i\psi}}{2e^{\int p(z)dz}}[(1+\alpha_2) + (\alpha_2 - 1)tanh(\frac{\theta_2}{2} + ln\sqrt{A_{23}})] \quad (4.16a)$$

$$q_2 \to S_2^{2+} = \frac{b\beta_3 e^{i\psi}}{2e^{\int p(z)dz}}[(1+\beta_2) + (\beta_2 - 1)tanh(\frac{\theta_2}{2} + ln\sqrt{A_{23}})] \quad (4.16b)$$

(c)$S^{3+}(\theta_3 \sim 0, \theta_1 \to -\infty, \theta_2 \to -\infty)$

$$q_1 \to S_1^{3+} = \frac{ae^{i\psi}}{2e^{\int p(z)dz}}[(1+\alpha_3) + (\alpha_3 - 1)tanh(\frac{\theta_3}{2})] \quad (4.17a)$$

$$q_1 \to S_2^{3+} = \frac{be^{i\psi}}{2e^{\int p(z)dz}} \times [(1+\beta_3) + (\beta_3 - 1)tanh(\frac{\theta_3}{2})] \quad (4.17b)$$

It is evident from the above expressions (4.15)-(4.17), and in comparison with two-soliton case as given by (4.12)-(4.14), the collision between three-dark solitons also exhibits elastic interaction behavior. The relevant physical quantities of solitons S_1, S_2 and S_3 before and after collisions are listed in Table 2.

4.6 Results and discussions

In our present work, we first consider the propagation dynamics of vector dark soliton pulse in the absence of varying coefficients. In this case, the dispersion and nonlinear coefficients remain constant. In such system, the dark soliton propagates without deformation and its amplitude and velocity remains unchanged during the propagation. Figs. 4.1, 4.2 and 4.3 depict the evolution plot of one, two and three dark soliton pulses propagation in homogeneous fibers, via the solutions (4.4), (4.6) and (4.11), respectively. From the above set of equations, we can observe that q_2 satisfies the relation with q_1 as $q_2 = \frac{b}{a}q_1$. Thus we plotted only q_1 field in the following sections.

4.6.1 Periodically varying dispersion and nonlinearity

To study the dispersion-managed vector dark soliton by the periodical perturbations, we consider a system with GVD parameter $D(z)$ and nonlinearity parameters $R(z)$ as a trigonometric periodic functions of the form of $a\,cos(bz)$, where a and b are integers. It is noted in such case, the soliton peak position and the velocity vary periodically during the propagation without any compression or

Table 4.2: Physical quantities of solitons S_1,S_2 andS_3 before and after the collision.

Solitons	Velocities	Widths	Amplitudes	Energies
s_1^{1-}	$\frac{\omega_1}{k_1}D(z)$	$\frac{1}{k_1}$	$\lvert\frac{a(1+\alpha_1)}{2e^{\int p(z)dz}}\rvert$	$\frac{a^2(2-\alpha_1-\alpha_1^*)}{k_1e^{2\int p(z)dz}}$
s_2^{1-}	$\frac{\omega_1}{k_1}D(z)$	$\frac{1}{k_1}$	$\lvert\frac{b(1+\beta_1)}{2e^{\int p(z)dz}}\rvert$	$\frac{b^2(2-\beta_1-\beta_1^*)}{k_1e^{2\int p(z)dz}}$
s_1^{2-}	$\frac{\omega_2}{k_2}D(z)$	$\frac{1}{k_2}$	$\lvert\frac{a\alpha_1(1+A_{12}\alpha_2)}{e^{\int p(z)dz}(1+A_{12})}\rvert$	$\frac{a^2(2-\alpha_2-\alpha_2^*)}{k_2e^{2\int p(z)dz}}$
s_2^{2-}	$\frac{\omega_2}{k_2}D(z)$	$\frac{1}{k_2}$	$\lvert\frac{b\beta_1(1+A_{12}\beta_2)}{e^{\int p(z)dz}(1+A_{12})}\rvert$	$\frac{b^2(2-\beta_2-\beta_2^*)}{k_2e^{2\int p(z)dz}}$
s_1^{3-}	$\frac{\omega_3}{k_3}D(z)$	$\frac{1}{k_3}$	$\lvert\frac{a\alpha_1\alpha_2(A_{12}+A_{123}\alpha_3)}{e^{\int p(z)dz}(A_{12}+A_{123})}\rvert$	$\frac{a^2(2-\alpha_3-\alpha_3^*)}{k_3e^{2\int p(z)dz}}$
s_2^{3-}	$\frac{\omega_3}{k_3}D(\xi)$	$\frac{1}{k_3}$	$\lvert\frac{b\beta_1\beta_2(A_{12}+A_{123}\beta_3)}{e^{\int p(z)dz}(A_{12}+A_{123})}\rvert$	$\frac{b^2(2-\beta_3-\beta_3^*)}{k_3e^{2\int p(z)dz}}$
s_1^{1+}	$\frac{\omega_1}{k_1}D(z)$	$\frac{1}{k_1}$	$\lvert\frac{a\alpha_2\alpha_3(A_{23}+A_{123}\alpha_1)}{e^{\int p(z)dz}(A_{23}+A_{123})}\rvert$	$\frac{a^2(2-\alpha_1-\alpha_1^*)}{k_1e^{2\int p(z)dz}}$
s_2^{1+}	$\frac{\omega_1}{k_1}D(z)$	$\frac{1}{k_1}$	$\lvert\frac{b\beta_2\beta_3(A_{23}+A_{123}\beta_1)}{e^{\int p(z)dz}(A_{23}+A_{123})}\rvert$	$\frac{b^2(2-\beta_1-\beta_1^*)}{k_1e^{2\int p(z)dz}}$
s_1^{2+}	$\frac{\omega_2}{k_2}D(z)$	$\frac{1}{k_2}$	$\lvert\frac{a\alpha_3(1+A_{23}\alpha_2)}{e^{\int p(z)dz}(1+A_{23})}\rvert$	$\frac{a^2(2-\alpha_2-\alpha_2^*)}{k_2e^{2\int p(z)dz}}$
s_2^{2+}	$\frac{\omega_2}{k_2}D(z)$	$\frac{1}{k_2}$	$\lvert\frac{b\beta_3(1+A_{23}\beta_2)}{e^{\int p(z)dz}(1+A_{23})}\rvert$	$\frac{b^2(2-\beta_2-\beta_2^*)}{k_2e^{2\int p(z)dz}}$
s_1^{3+}	$\frac{\omega_1}{k_3}D(z)$	$\frac{1}{k_3}$	$\lvert\frac{a(1+\alpha_3)}{2e^{\int p(z)dz}}\rvert$	$\frac{a^2(2-\alpha_3-\alpha_3^*)}{k_3e^{2\int p(z)dz}}$
s_2^{3+}	$\frac{\omega_1}{k_3}D(z)$	$\frac{1}{k_3}$	$\lvert\frac{b(1+\beta_3)}{2e^{\int p(z)dz}}\rvert$	$\frac{b^2(2-\beta_3-\beta_3^*)}{k_1e^{2\int p(z)dz}}$

broadening. Such type of solitons are called as snaking soliton [31–35]. Similar type of inhomogeneous behavior is observed in two and three-soliton solutions as well. The Fig. 4.4 represents the one, two and three dark solitons pulse evolutions with periodically varying effects. It shows that the amplitude, energy and pulse width remain constants during the propagation of the pulse down the fiber.

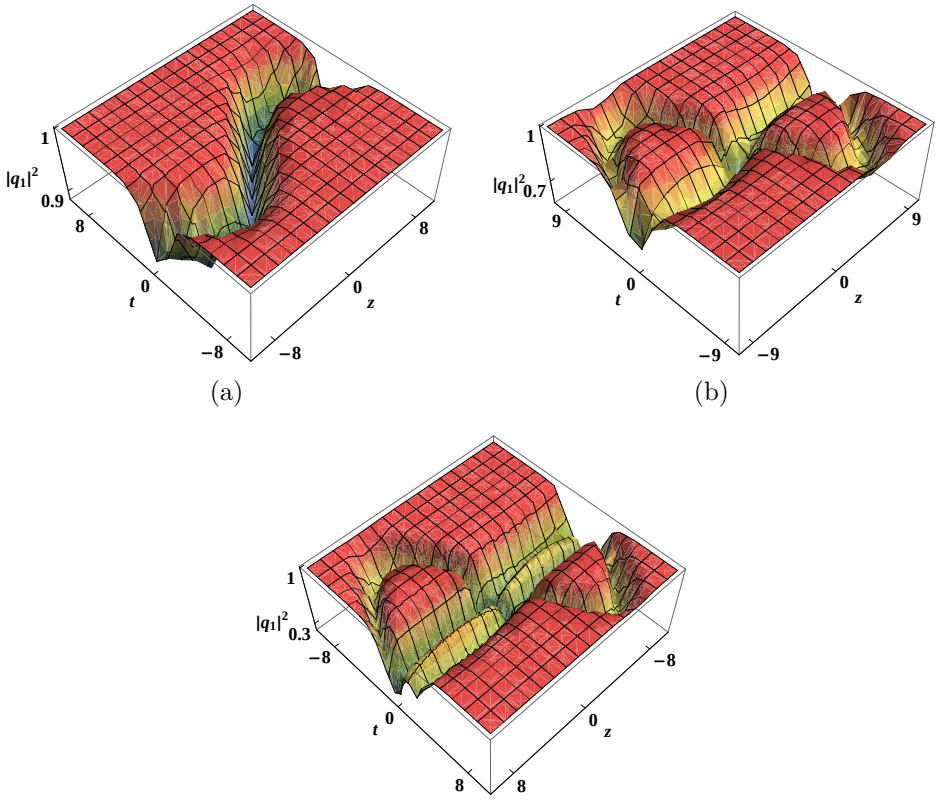

Figure 4.4: The periodically varying dark solitons, (a)One-soliton with a=1 and $k_1 = 1.5$ (b)two-soliton with a=1, $k_1 = 1.5$, and $k_2 = -1.5$ (c)Three-soliton with a=1, $k_1 = 2$, $k_2 = 2.5$ and $k_3 = -2$. Other physical quantities are $k = \delta = 1$, $D(z) = Cos(0.3z)$ and $p = 0$.

4.6.2 Pulse compression

The pulse compression (PC) is an important technique to produce ultrashort pulse in nonlinear fiber, which reduces the duration of the pulse along the fiber. Techniques like soliton effect, adiabatic pulse compression, self-similar methods are few of the most populary known pulse compression techniques. Out of the different nonlinear and dispersion profile, exponential varying dispersion and nonlinearity is found to be a good contender for soliton compression, as it compresses the soliton with better compression factor. In similar lines with the earlier report, we consider the dispersion and nonlinearity parameters of the form $c\exp(dz)$, where c is the initial peak power and d is an integer. The PC will

occur, when the leading edge of the pulse is delayed by just the right amount to arrive nearly with the trailing edge [36, 37]. The PC of one, two and three solitons are shown in the Fig.4.5.

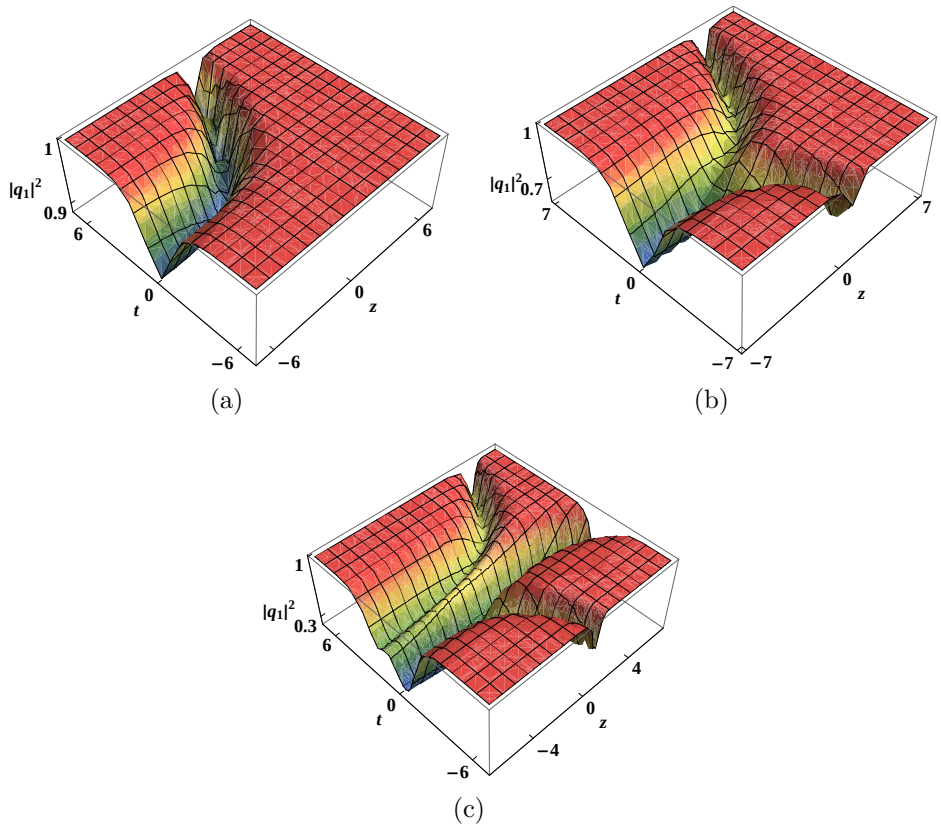

Figure 4.5: The pulse compression of vector dark solitons, (a)One-soliton with a=1 and $k_1 = 1.5$ (b)two-soliton with a=1, $k_1 = 1.5$ and $k_2 = -1.5$, (c)Three-soliton with a=1, $k_1 = 2$, $k_2 = 2.5$ and $k_3 = -2$. Other physical quantities are $k = \delta = 1$, $D(z) = Exp(0.5z)$and $p = 0$.

4.6.3 Gain/loss

The fiber loss plays a crucial role in the long haul optical communications system, as a result of which, the pump power depletes and the propagation soliton will deform progressively during the propagation. The coefficient $p(z)$ plays an important role in determining the amplification or absorption of the soliton pulse. The coefficient $p(z) = 0$ corresponds to the case of zero loss and for any finite value of σ, the solution represents the propagation of soliton pulse in a medium with constant gain or loss.

Figs.4.6 and 4.7 represent the soliton propagation in a medium with gain and loss, respectively. When $\sigma < 0 (\sigma > 0)$, the pulse undergoes the amplification (absorption), in such a case the amplitude of the pulse increases(decreases) as it propagates down the fiber. Thus, one can control the soliton amplification or absorption by varying the coefficient $p(z)$. It is obvious that the medium with gain increases the amplitude and energy in comparison to the case of lossy medium [32, 33] .

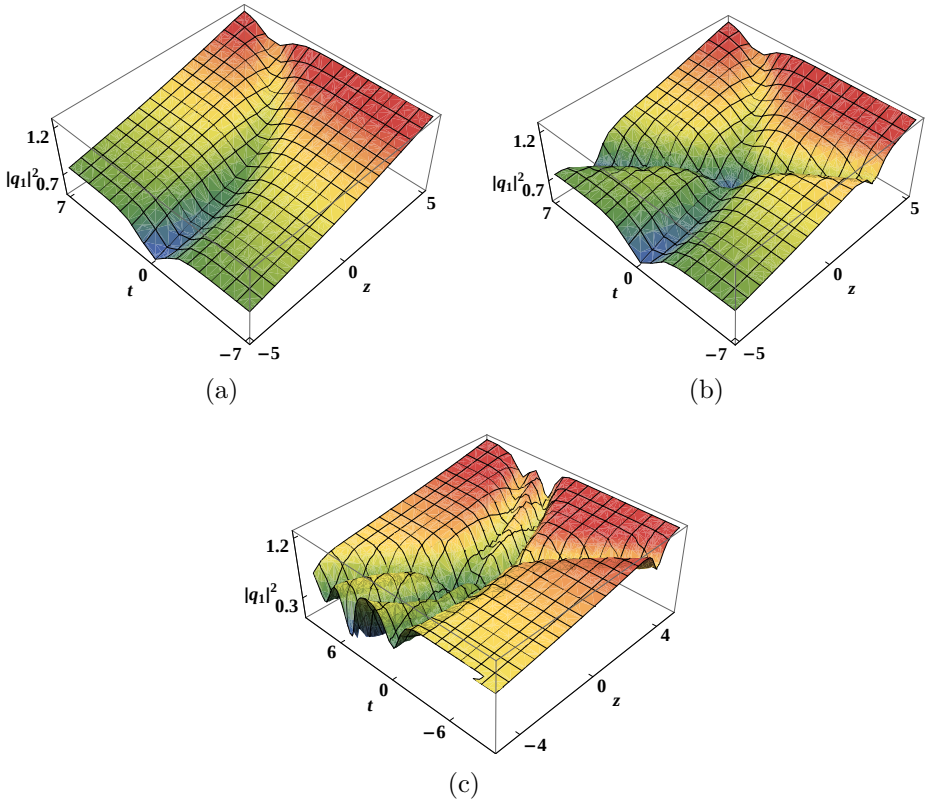

Figure 4.6: The vector dark solitons propagation with gain, (a)One-soliton with a=1 and $k_1 = 1.5$ (b)two-soliton with a=1, $k_1 = 1.5$, and $k_2 = -1.5$ (c)Three-soliton with a=1, $k_1 = 2$, $k_2 = 2.5$ and $k_3 = -2$. Other physical quantities are $k = \delta = D(z) = 1$ and $p = -0.05$.

4.7 Nonlinear tunneling effect

So far, we discussed the impact of various physical effects and inhomogenous parameters in the one, two and three solitons. We now extend our study to one of the dramatic nonlinear effects, known as the nonlinear tunneling (NL).

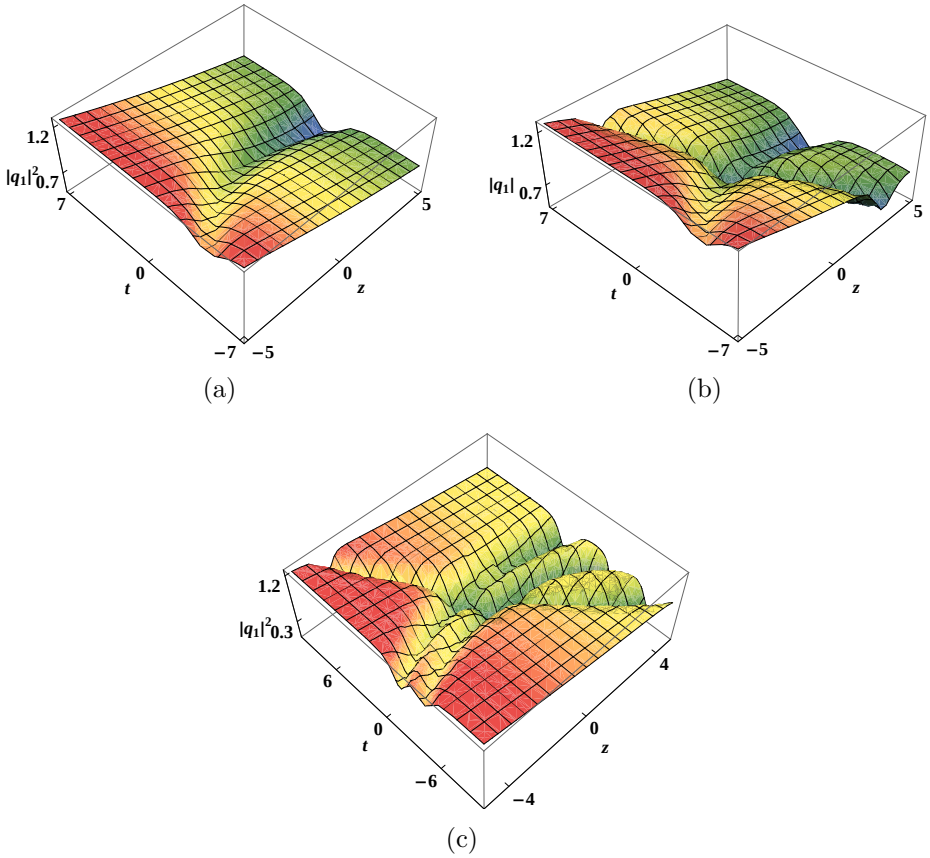

Figure 4.7: The vector dark solitons propagation with gain (a)One-soliton with a=1 and $k_1 = 1.5$ (b)two-soliton with a=1, $k_1 = 1.5$, and $k_2 = -1.5$ (c)Three-soliton with a=1, $k_1 = 2$, $k_2 = 2.5$ and $k_3 = -2$. Other physical quantities are $k = \delta = D(z) = 1$ and $p = 0.05$.

Recently, many leading research works have been devoted to study the tunneling effect of solitons in different physical systems [9, 19–21, 24–29]. All pioneering works have shown that the soliton can pass through the barrier without loss under a special conditions which depends on the height of the barrier and the amplitude of the soliton. The NL tunneling of soliton may create a new field of interest and feature wide applications in all-optical switches and logic circuits.

4.7.1 Nonlinear tunneling without exponential background

To investigate the NL tunneling of Vc-CNLS dark soliton propagating through the dispersion barrier or well, we choose the dispersion and nonlinear parameter

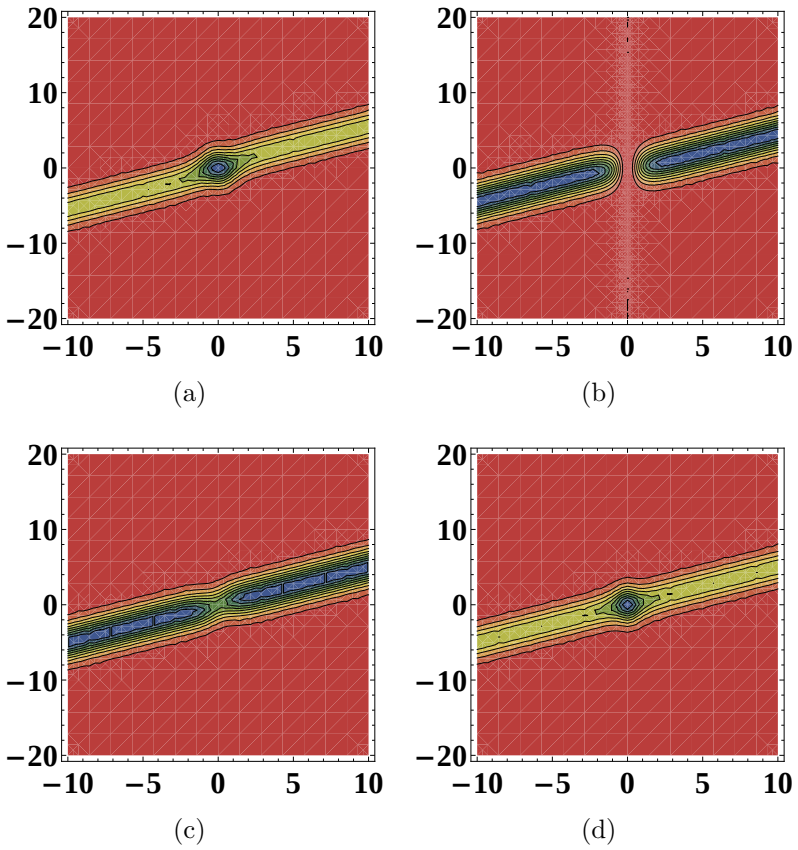

Figure 4.8: (Color online) Contour plot of nonlinear tunneling of vector dark one-soliton. (a) Dispersion barrier with $D(z) = 1 + hsech[z - z_0]^2$, $R = 0.5$ and $h = 1$.(b) Dispersion well with $h = -1$.(c) Nonlinear barrier with $D(z) = 1$,$R = 0.5(1 + hsech[z - z_0]^2)$ and $h = 0.5$.(d) Nonlinear well with $h = -0.5$. Other physical quantities are $k = k_1 = a = 1$ and $z_0 = 0$.

as follows:

$$D(z) = r_0 \pm h\, sech^2(c(z - z_0))$$

$$R(z) = R_0$$

In the above expression h indicates the height of the barrier. The parameter c is related to its width and z_0 represents the longitudinal co-ordinate indicating the location of the dispersion barrier or dispersion well, and D_0, R_0 and S_0 are constant parameters. Here the positive or the negative sign of $\pm h$ denotes the barrier or the well. If $h = 0$ it means that soliton propagation is through

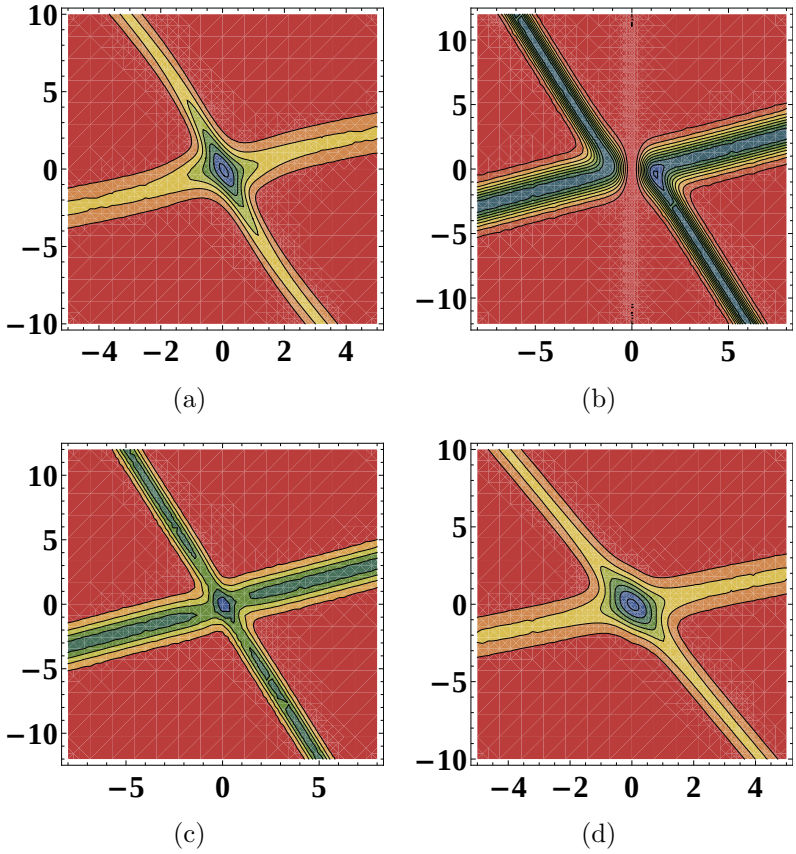

Figure 4.9: Contour plot of nonlinear tunneling of vector dark two-soliton. (a) Dispersion barrier with $D(z) = 1 + hsech[z - z_0]^2$, $R = 0.5$ and $h = 1$.(b) Dispersion well with $h = -1$.(c) Nonlinear barrier with $D(z) = 1$,$R = 0.5(1 + hsech[z - z_0]^2)$ and $h = 0.5$.(d) Nonlinear well with $h = -0.5$. Other physical quantities are $k = a = 1$,$k_1 = -1.5, k_2 = 1.5$ and $z_0 = 0$.

homogeneous fiber. To investigate the soliton propagation through the nonlinear barrier or well, we consider the variable coefficients as follows:

$$D(z) = D_0$$

$$R(z) = R_0(r_0 \pm h\, sech^2(c(z - z_0))$$

When the dark soliton pass through the dispersion barrier, the intensity of the soliton grows and forms a peak at $z = z_0$. After passing through the barrier, the pulse will get its original shape as shown in Fig.4.8(a). Similarly, when

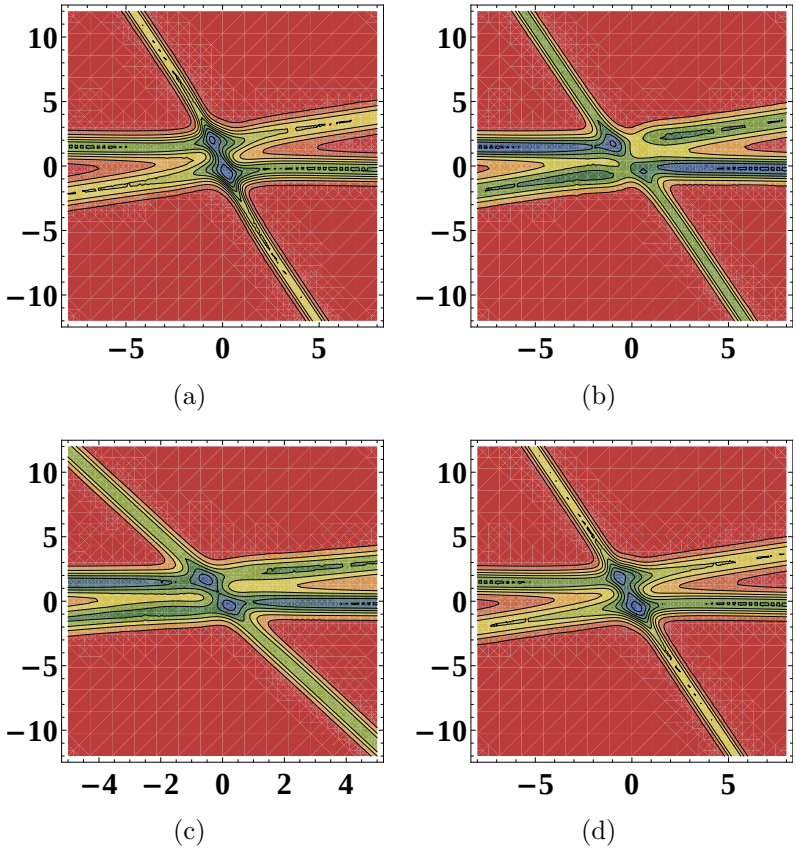

Figure 4.10: Contour plot of nonlinear tunneling of vector dark two-soliton. (a) Dispersion barrier with $D(z) = 1 + hsech[z - z_0]^2$, $R = 0.5$ and $h = 0.5$.(b) Dispersion well with $h = -0.5$.(c) Nonlinear barrier with $D(z) = 1$,$R = 0.5(1 + hsech[z - z_0]^2)$ and $h = 0.3$.(d) Nonlinear well with $h = -0.3$. Other physical quantities are $k = a = 1$,$k_1 = 2, k_2 = 2.5, k_3 = -2.5$ and $z_0 = 0$.

dark solitons pass through the dispersion well the amplitudes of solitons vanish and a valley is formed at $z = z_0$; after the tunneling, solitons are restored to their original shapes as shown in Fig.4.8(b). If solitons pass through a nonlinear barrier or well, the valley is formed for nonlinear barrier and peak is formed for well as evident from the Figs. 4.8. In similar lines with one-soliton case, the NL tunneling of two solitons are demonstrated in the Figs. 4.9 and three solitons are demonstrated in the Figs. 4.10 , respectively.

The height of the barrier (h) and amplitude of pulse (A) exhibit a relation in given soliton solutions. Thus we studied the tunneling effect with suitable parametric choice of h. To investigate the dark soliton propagation through the

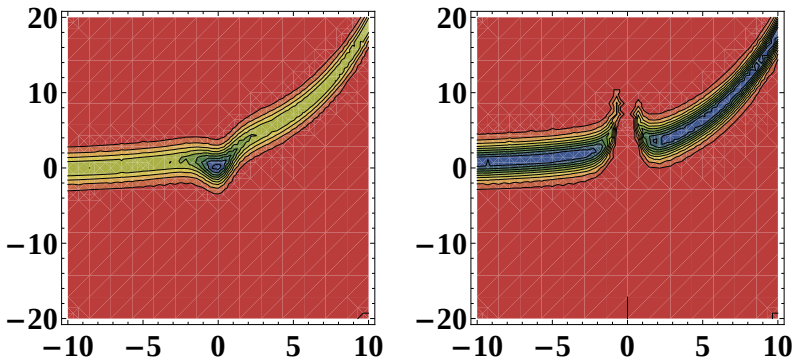

(a) (b)

Figure 4.11: Contour plot of nonlinear tunneling with exponential background. (a) Dispersion barrier of one soliton with $a = 1$ and $h = 0.9$. (b)Dispersion well of one soliton with $a = 1$ and $h = -0.9$. Other physical quantities are $D(z) = d_0 e^{-rz} + hsech[z - z_0]^2$,$R = R_0 e^{-rz}$, $d_0 = k_1 = 1$, $R_0 = 0.5$,$r = -0.2$,$z_0 = 0$ and $p = 0$.

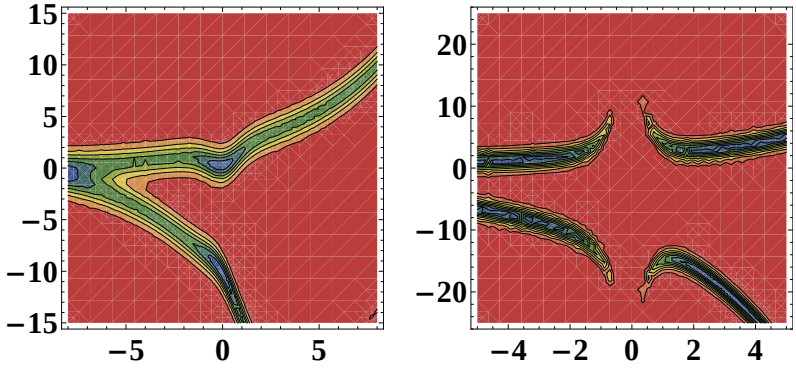

(a) (b)

Figure 4.12: Contour plot of nonlinear tunneling with exponential background. (a)Dispersion barrier of two-soliton with $a = 1$ and $h = 0.5$. (b)Dispersion well of two-soliton with $a = 1$ and $h = -0.9$. Other physical quantities are $D(z) = d_0 e^{-rz} + hsech[z - z_0]^2$,$R = R_0 e^{-rz}$, $d_0 = 1$, $k_1 = 1.5$,$k_2 = -1.5$, $R_0 = 0.5$,$r = -0.2$,$z_0 = 0$ and $p = 0$.

dispersion barrier or well, we obtained a condition, where $h > 0$ indicates the dispersion barrier, and $-1 < h < 0$ represents the dispersion well. Similarly, in the case of nonlinear barrier or well, we also obtained a condition, where $h > 0$ indicates the nonlinear barrier, and $-1 < h < 0$ represents the nonlinear well. We arrive at this suitable choice of h from the equation of soliton amplitude with

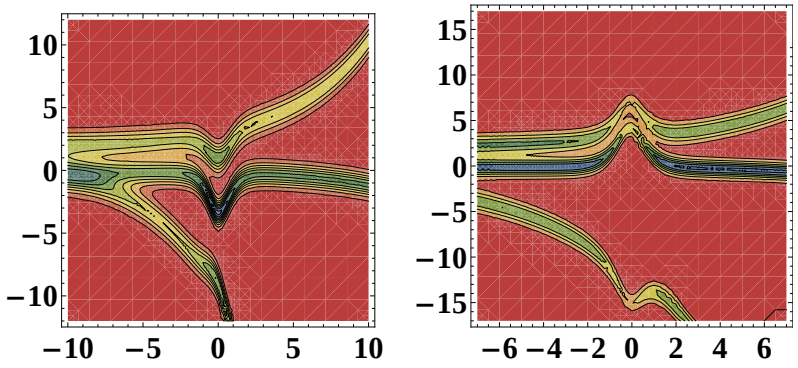

(a) (b)

Figure 4.13: Contour plot of nonlinear tunneling with exponential background. (a)Dispersion barrier of three-soliton with $a = 1$ and $h = 0.5$. (b) Dispersion well of three-soliton with $a = 1$ and $h = -0.5$. Other physical quantities are $D(z) = d_0 e^{-rz} + hsech[z - z_0]^2$,$R = R_0 e^{-rz}$, $d_0 = 1$, $k_1 = 2$,$k_2 = 2.5$,$k_= - 2$, $R_0 = 0.5$,$r = -0.2$,$z_0 = 0$ and $p = 0$.

the condition that $0 \leq A \leq a(b)$. where A represents the resultant amplitude of pulse with tunneling effect ($h \neq 0$).

4.7.2 Nonlinear tunneling with exponential background

Now, we consider the case of tunneling effect with exponential background. This case is of particular importance, because, pulse tunneling through the exponential background generally exhibits compression of the pulse. To investigate this special case, we consider the dispersion and nonlinear parameter as follows:

$$D(z) = D_0 exp(-rz) \pm h\, sech^2(c(z - z_0))$$
$$R(z) = R_0 exp(-rz)$$

In the above expression, the positive sign of h indicates the dispersion potential barrier and the negative sign indicates for the dispersion well. Here, r represents a decaying parameter. To consider the exponential decay, the decaying parameter r should not be equal to zero.

From the above expressions with suitable parameters, one can conclude that when a dark soliton passes through the dispersion barrier with exponential decay, the amplitude of the soliton increases at $z = z_0$, and after tunneling through the barriers, the width of the soliton decreases gradually during propagation. Figs. 4.11(a) clearly show that when solitons propagate through the dispersion barrier, they will naturally compress. Similarly, the amplitude of the soliton vanishes at $z = z_0$ and after emerging from the well, the width of the soliton gradually decreases along the propagation. Figs. 4.11(b) represent the dispersion well with decay effect. Similarly, the two and three solitons are studied in Figs. 4.12 and 4.13 respectively. From this result, one can control the compression of the input pulse by a proper choice of the barrier or well parameters.

4.8 Conclusion

In this chapter, we have investigated the dynamics of dark soliton pulse propagation in inhomogeneous fibers by employing Vc-CNLS model. The dark soliton solutions have been derived by Hirota's bilinear method. Through the analytical soliton solutions and detailed graphical illustration, the propagation dynamics and collision behaviors of the dark soliton pulses in inhomogeneous fibers have been discussed. Especially, we have studied the almost all dynamical related physical quantities up to the level of three-dark solitons interactions. The inhomogeneous effects on the evolution and interaction between dark solitons have also been considered. The shapes and velocities of the dark solitons can be controlled by modulating dispersion and gain/loss terms. The gain or loss term affects the amplitude and energy. Finally, we investigated the nonlinear tunneling effect of optical dark solitons with and without exponential background. It has been reported that tunneling of the soliton depends on a condition related to the height of the barrier and the soliton amplitude. The intensity of the tunneling soliton either forms a peak or valley and retains its shape after tunneling through barrier/well. We also identified the tunneling of dark soliton with exponential background tends to compress the pulse. Thus, in this work, we attempt

to give detailed study about the dark soliton dynamics in the Vc-CNLS model, by incorporating most of the physical effects.

Bibliography

[1] G.P. Agrawal, Nonlinear Fiber Optics (Academic, New York, 2013)

[2] S.V. Manakov, Sov. Phys. JETP **38**,248 (1974).

[3] C. R. Menyuk, IEEE J. Quantum Electron, **QE-25**, 2674(1989).

[4] J. U. Kang, G. I. Stegeman, J. S. Aitchison, and N. Akhmediev, Phys. Rev. Lett. **76**, 3699 (1996).

[5] B. Frisquet, B. Kibler, J. Fatome, P. Morin, F. Baronio, M. Conforti, G. Millot and S. Wabnitz , Phys. Rev. A **92**,053854(2015).

[6] B. Crosignani and P. Di Porto, Opt. Lett. **6**, 329 (1981).

[7] R. Radhakrishnan, M. Lakshmanan, J. Hietarinta, Phys. Rev. E **56**,2213 (1997).

[8] D. J. Kaup and B.A. Malomed, Phys. Rev. A **48**,599 (1993).

[9] C.Q. Dai, Y.Y. Wang, J.F. Zhang, Opt. Express **18**, 17548(2010)

[10] Jinping Tian, Jihong Li, Linsheng Kang and Guosheng Zhou,Physica Scripta. Vol. **72**, 394(2005)

[11] C.G. Latchio Tiofacka, Alidou Mohamadoub, Timoleon C. Kofane and K. Porsezian, J. Mod. Opt.**57**, 261(2010)

[12] Sushmita Chakraborty, Sudipta Nandy, and Abhijit Barthakur, Phys. Rev. E **91**, 023210 (2015)

[13] R. Hirota, The Direct Method in Soliton Theory (Cambridge University Press, Cambridge, 2004)

[14] T. Kanna, M. Lakshmanan, Phys. Rev. Lett. **86**, 5043 (2001).

[15] W.J. Liu, B. Tian, H.Q. Zhang, L.L. Li, Y.S. Xue, Phys. Rev. E **77**, 066605 (2008)

[16] R.Radhakrishnan and M.Lakshmanan J.Phys.A:Math.Gen.**28**, 2683(1995).

[17] K. Porsezian, K. Nakkeeran, Phys. Rev. Lett. **76**,3955 (1996).

[18] Liu W J, B Tian, H Q Zhang, T Xu and H Li, Phys. Rev. A **79**, 063810(2009)

[19] A.C. Newell, J. Math. Phys. **19**, 1126 (1978)

[20] V.N. Serkin, T.L. Belyaeva, J. Exp. Theor. Phys. Lett. **74**, 573 (2001)

[21] V.N. Serkin, V.M. Chapela, J. Percino, T.L. Belyaeva, Opt. Commun. **192**, 237 (2001)

[22] Assaf Barak, Or Peleg, Chris Stucchio, Avy Soffer, and Mordechai Segev, Phys. Rev. Lett. **100**, 153901(2008)

[23] W.P. Zhong, M.R. Belic, Phys. Rev. E **81**, 056604 (2010)

[24] C.Q. Dai, G.Q. Zhou, J.F. Zhang, Phys. Rev. E **85**, 016603 (2012)

[25] C.Q. Dai, Y.Y. Wang, Q. Tian, J.F. Zhang, Ann. Phys. **327**, 512 (2012)

[26] T.L. Belyaeva, V.N. Serkin, Eur. Phys. J. D **66**, 153 (2012)

[27] . J.D. He, J.F. Zhang, J. Phys. A:Math. Theor **44**, 205203 (2011)

[28] M.S. Mani Rajan et al., Eur. Phys. J. D **67**, 150(2013).

[29] Lei Wang, Min Li, Feng-Hua Qi and Chao Geng, Eur. Phys. J. D **69**, 108(2015).

[30] M J Ablowitz, S D Nixon, T P Horikis and D J Frantzeskakis. J. Phys. A: Math. Theor. **46**, 095201 (2013)

[31] Malomed B A 2006 Soliton Management in Periodic Systems (Berlin: Springer)

[32] A. Mahalingam, A. Uthayakumar and P. Anandhi, J Opt.**42(3)**,182 (2013).

[33] . M.S. Mani Rajan, A. Mahalingam, A. Uthayakumar, J. Opt.**14**, 105204 (2012).

[34] K.Porsezian, A.Hasegawa, V.N.Serkin, T.L. Belyaeva and R.Ganapathy, Phys. Lett. A., **361**, 504 (2007)

[35] Yu-Jie Feng, Yi-Tian Gao, Zhi-Yuan Sun, Da-Wei Zuo, Yu-Jia Shen, Yu-Hao Sun, Long Xue, and Xin Yu, Phys. Scr. **90**, 045201 (2015).

[36] M N Vinoj and V C Kuriakose, J. Opt. A: Pure Appl. Opt. **6**, 63 (2004).

[37] K. Nithyanandan, R. Vasantha Jayakantha Raja, and K. Porsezian, J. Opt. Soc. Am. B, **30**, 178 (2013).

Chapter 5

Phase dynamics of inhomogeneous Manakov vector solitons

5.1 Introduction

One of the most elegant and simplest forms of integrable coupled nonlinear Schrödinger (CNLS) equation describing the co-propagation of intense optical beams in two-components birefringent system is the so called Manakov Model[1–10]. The effect of birefringence in a single-mode fiber was first considered by Menyuk [2]. The existence of two-component vector soliton in birefringent Kerr medium was first proposed by Manakov [11]. The utility of these theoretical models can be employed under specific choice of nonlinear parameters, that is, the cross-coupling coefficient must be equal to unity and the self-phase modulation(SPM) coefficients need to be equal for the both polarizations. It is a well-known integrable model of CNLS equation, which yields explicit forms of stable multi-soliton solution in different fields ranging from nonlinear optics, hydrodynamics, plasma physics and Bose-Einstein condensates. Many practical ways to create Manakov solitons in realistic birefringence materials are known

today [12–15]. Recently, Manakov vector-soliton has attracted renewed interest among the researchers due to its important applications in optical fiber systems such as optical switching and soliton dragging logic gates [16, 17].

Based on the different signs of group velocity dispersion (GVD) parameter, Manakov model mainly admits two kinds of vector soliton propagation, bright and dark, respectively. The bright (dark) vector soliton intensity, in the anomalous (normal) dispersion regime, has been investigated in many pioneering works [18, 19]. The key features of Manakov bright-bright pair underlying the energy sharing collision between the components of the interacting vector solitons. But in the case of dark-dark pair, it always exhibit elastic mode of interactions [20, 21]. Interaction of such solitons pairs in two-component Bose-Einstein condensates have been exclusively studied by Rajendran *et al.*, [2–4]. To understand the scope of CNLS equation, the transformation of Gross-Pitaevskii(GP)equations into the well known completely integrable Manakov model has been presented in Appendix.

In most of the previous studies reported in the context of Manakov model, the interaction dynamics and the discussion was primarily based on the intensity description, only a little emphasize is paved on the phase dynamics. In the present context, in addition to the intensity based explanations, we highlight and discuss the phase dynamics of Manakov soliton for the first time to the best of our knowledge. For a complete understanding of the system dynamics, it would be interesting to reveal the distinct properties of intensity and corresponding phase profile of Manakov bright and dark solitons. We further extend the phase analysis to the case of multi-soliton interactions and highlight the variation of phase for different soliton types.

In this chapter, we focus on the following inhomogeneous Manakov model for the bright and dark vector soliton[21, 25–27]:

$$iq_{1z} \pm \frac{1}{2}D(z)q_{1tt} + R(z)(|q_1|^2 + |q_2|^2)q_1 + ip(z)q_1 = 0 \tag{5.1a}$$

$$iq_{2z} \pm \frac{1}{2}D(z)q_{2tt} + R(z)(|q_2|^2 + |q_1|^2)q_2 + ip(z)q_2 = 0 \tag{5.1b}$$

where, $q_1(z,t)$ and $q_2(z,t)$ are the complex envelopes for the two polarization components in Kerr medium. The variables z and t represent the normalized spatial and temporal coordinates. The group velocity dispersion, Kerr nonlinearity and gain/absorption effects are related to the respective coefficient functions $D(z)$, $R(z)$ and $p(z)$. By using Hirota's bilinear (HB) method, we analytically derived exact solutions for the model (5.1), which also provides explicit form of multi-soliton solutions. In this chapter, apart from the intensity, we reveal the influence of inhomogeneity on the phase of manakov solitons for the first time. The given model(5.1) has the capability to handle many inhomogeneous behaviors in fiber such as, pulse gain/absorption, background oscillation, pulse compression, dispersion-managed transmission systems and nonlinear tunneling. The vector soliton phase has not been studied analytically anywhere, being motivated by this fact, we paid particular attention on soliton propagation and corresponding phase change with constant or varying coefficients. Unlike the bright counter part, phase of dark vector soliton gives more intriguing results, and the interaction scenario provides interesting features which has not been reported so far.

The organization of the chapter is as follows. Following a detailed introduction about Manakov model(Vc-CNLSE). Sec. 2 presents the exact bright and dark vector soliton solutions by HB method. Sec. 3 describes the phase dynamics of Manakov one soliton solutions. Two soliton solution and soliton collision by employing asymptotic analysis is presented in Sec. 4. A brief discussion about the various physical effects in intensity and corresponding phase dynamics of vector soliton propagation through inhomogeneous medium is reported in Sec.

5. The chapter concludes with a summary of results in Sec. 6.

5.2 Exact soliton solutions by HB method

To obtain exact vector soliton solutions of model (5.1), we use the Hirota's bilinear (HB) method [28–31], which is expected to give an explicit form of bright and dark multi-soliton solutions, as follows

$$q_1(z,t) = g(z)\frac{G}{F} \tag{5.2a}$$

$$q_2(z,t) = g(z)\frac{H}{F} \tag{5.2b}$$

where, G and H are complex functions and F is a real function. By substituting this transformation into Eq. (5.1), the following bilinear equations can be obtained,

$$[iD_z \pm \frac{1}{2}D(z)D_t^2 + \lambda(z)](G.F) = 0 \tag{5.3a}$$

$$[iD_z \pm \frac{1}{2}D(z)D_t^2 + \lambda(z)](H.F) = 0 \tag{5.3b}$$

$$\delta(|G|^2 + |H|^2) \mp D_t^2(F.F) = \frac{2\lambda(z)}{D(z)}F^2 \tag{5.3c}$$

With the condition $g_z(z) + g(z)p(z) = 0$, we can choose $\lambda(z) = 0$ for the bright soliton solution. But, for the dark soliton case $\lambda(z)$ is an analytic function to be determined. Where $\delta = \frac{2R(z)}{D(z)}g(z)^2$ and D_z and D_t are the bilinear differential operators [28].

5.2.1 Bright one-soliton solutions

The Bright multi-soliton solutions of equation (5.1) can be generated by solving the above set of equations (5.3) with the power series expansions of G and F as

$$G = \varepsilon^1 g_1 + \varepsilon^3 g_3 + \varepsilon^5 g_3 + ...$$
$$H = \varepsilon^1 h_1 + \varepsilon^3 h_3 + \varepsilon^5 h_3 + ...$$
$$F = 1 + \varepsilon^2 f_2 + \varepsilon^4 f_4 + \varepsilon^6 f_6 + ...$$

with ε as the formal expansion parameter. In order to get the bright one-soliton solution, the power series expansions for G , H and F are truncated corresponding to the lowest order in ϵ as follows; $G = g_1$, $H = h_1$and $F = 1 + f_2$. Then, back to bilinear equations (5.3), we obtain

$$g(z) = e^{-\int p(z)dz} \qquad g_1 = \alpha_1 e^{\theta_1}$$
$$h_1 = \beta_1 e^{\theta_1} \qquad f_2 = \varrho_1 e^{\theta_1 + \theta_1^*}$$
$$\theta_1 = k_1 t - \omega_1 \int D(z)dz + \phi_1 \qquad \omega_1 = -\frac{1}{2} i k_1^2$$
$$\varrho_1 = \frac{\delta(|\alpha_1|^2 + |\beta_1|^2)}{2(k_1 + k_1^*)^2}$$

Thus, bright one-soliton solutions can be written as,

$$\begin{pmatrix} q_1 \\ q_2 \end{pmatrix} = \begin{pmatrix} \alpha_1 \\ \beta_1 \end{pmatrix} \frac{e^{-\int p(z)dz}}{2\sqrt{\varrho_1}} e^{-i\theta_{1I}} sech(\theta_{1R} + \frac{\ln \varrho_1}{2}) \tag{5.4}$$

From the Eq. (5.4), we can analyze the characteristics of bright one-soliton pulse in inhomogeneous fibers. The propagation through constant fiber is depicted in the Fig. 5.1(a).

5.2.2 Dark one-soliton solutions

We obtain the dark one-soltion solution by truncated series of G, H and F to the lowes order in ε as follows, $G = g_0(1+\varepsilon g_1)$, $H = h_0(1+\varepsilon h_1)$ and $F = 1+\varepsilon f_1$.

Here, we assume

$$g_0 = ae^{i\phi} \qquad h_0 = be^{i\phi}$$
$$g_1 = \mu_1 e^{\theta_1} \qquad h_1 = \nu_1 e^{\theta_1}$$
$$f_1 = e^{\theta_1} \qquad g(z) = e^{-\int p(z)dz}$$
$$\phi = k_0 t - \omega_0 \int D(z)dz \qquad \theta_1 = k_1 t - \omega_1 \int D(z)dz + \phi_1$$

Then, back to bilinear Eqs. (5.3), we obtain some associated parameters related to one- soliton solutions as

$$\lambda = \frac{1}{2}\delta(a^2 + b^2)D(z) \qquad \omega_0 = -\frac{\lambda}{D(z)} - \frac{k_0^2}{2}$$
$$\mu_1 = \frac{2\omega_1 + 2k_0k_1 + ik_1^2}{2\omega_1 + 2k_0k_1 - ik_1^2} \qquad \mu_1 = \nu_1$$
$$\omega_1 = \frac{k_1}{2}(-2k_0 \pm \sqrt{2\delta(a^2 + b^2) - k_1^2})$$

The dark one-soliton solutions can be written as,

$$\begin{pmatrix} q_1 \\ q_2 \end{pmatrix} = \begin{pmatrix} a \\ b \end{pmatrix} \frac{(1 + \mu_1) + (\mu_1 - 1)tanh(\frac{\theta_1}{2})}{2e^{\int p(z)dz} e^{-i\phi}} \tag{5.5}$$

From the Eq. (5.5), one can analyze the dynamics of vector dark one-soliton pulse in inhomogeneous fibers. The propagation of dark one-solitons through homogenous fiber is depicted in the Fig. 5.2.

Parametric region for Black and gray soliton

Based on the amplitude (A_j) or blackness (B_j) parameter of the obtained solution(where $j = 1, 2$), the dark solitons can be classified into black and gray mode of soliton. The A_j, B_j and background wave amplitude (a *or* b) are connected by a simple relation $A_j^2 + B_j^2 = a^2(b^2)e^{-2\int p(z)dz}$ [7, 34]. Generally, the dark soliton with zero intensity at its center is referred to as black soli-

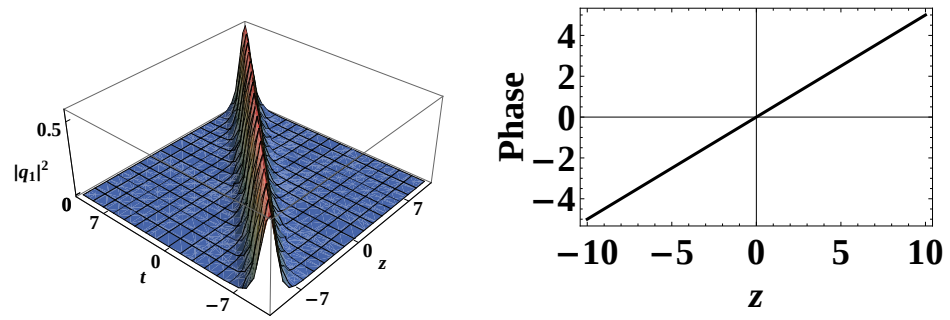

(a) (b)

Figure 5.1: The bright soliton propagation through a constant fiber medium for parameters (a) $k_1 = 1 + i$, $\alpha_1 = 1 + i$, $\beta_1 = 2 - i$, $D(z) = 1$, $R(z) = 0.5$ and $p = 0$. (b)Corresponding phase profile.

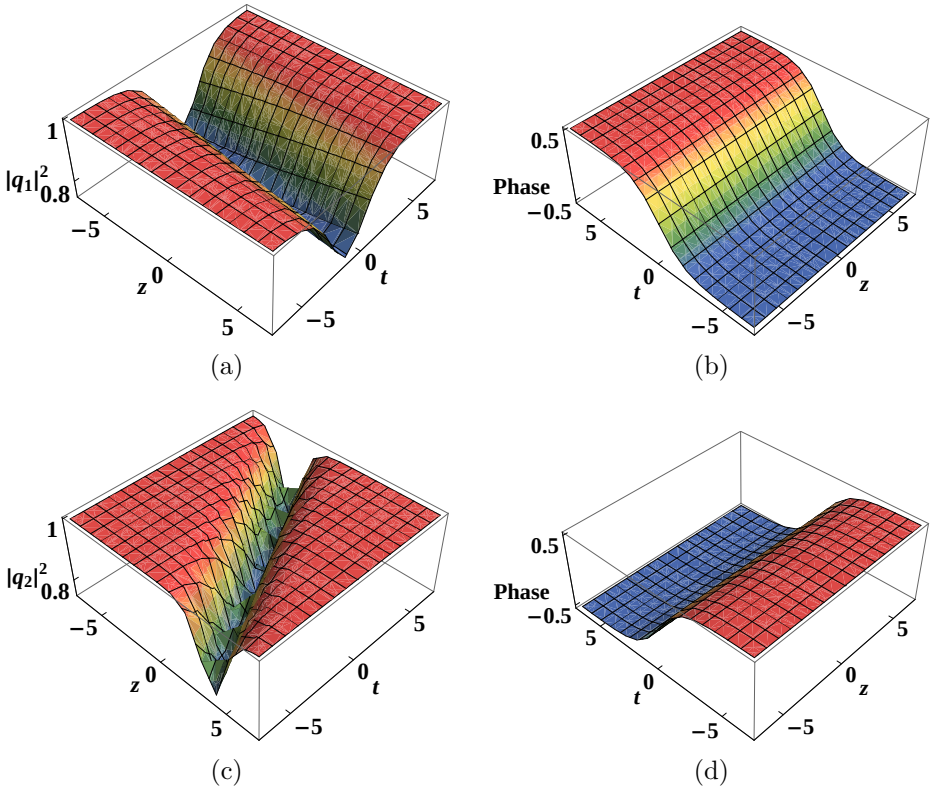

(a) (b)

(c) (d)

Figure 5.2: The dark soliton propagation through homogenous fiber for parameters , (a) $k_1 = 1$ (b)Corresponding phase profile. (c) $k_1 = -1$ (d)Corresponding phase profile. Other physical quantities are $a = b = 1 = k_0 = D(z) = \delta = 1$.

ton ($B_j^2 = a^2(b^2)e^{-2\int p(z)dz}$), otherwise ($B_j^2 < a^2(b^2)e^{-2\int p(z)dz}$) as gray solitons [32, 33]. In Fig. 5.3, we have plotted the black and gray soliton with different blackness parameter. To explore the dynamics of dark soliton propagation given

by Eq. (5.5), some of the physical quantities such as velocity $\left(V = \frac{\omega_1}{k_1} D(z)\right)$, amplitude $\begin{pmatrix} A_1 \\ A_2 \end{pmatrix} = \begin{pmatrix} a \\ b \end{pmatrix} |\frac{(1+\mu_1)}{2e^{\int p(z)dz}}|$ and blackness factor $\begin{pmatrix} B_1 \\ B_2 \end{pmatrix} = \begin{pmatrix} a \\ b \end{pmatrix} |\frac{(\mu_1 - 1)}{2e^{\int p(z)dz}}|$ are important. The dark vector soliton energy associated with blackness factor can be written as [34]

$$E_1 = \int_{-\infty}^{\infty} (a^2 - |\, q_1 \,|^2) dt = \frac{4B_1^2}{k_1 e^{2\int p(z)dz}} \tag{5.6a}$$

$$E_2 = \int_{-\infty}^{\infty} (b^2 - |\, q_2 \,|^2) dt = \frac{4B_2^2}{k_1 e^{2\int p(z)dz}} \tag{5.6b}$$

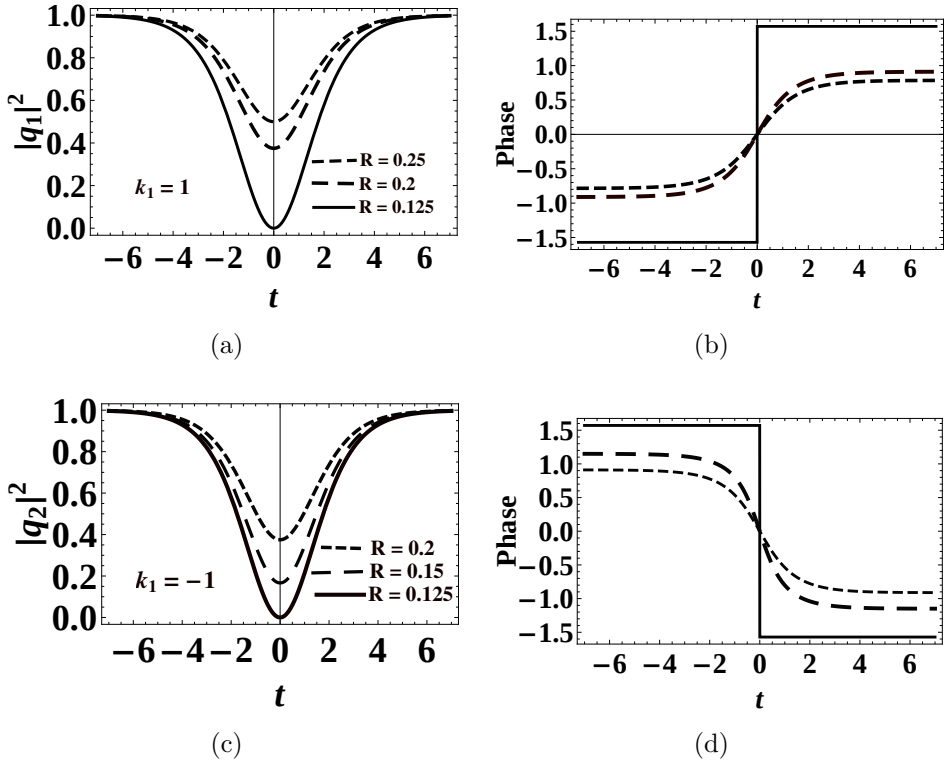

Figure 5.3: The black and gray soliton with different values of blackness factor (a) $k_1 = 1$ and $R = 0.125,\ 0.2,\ 0.25$ (b)Corresponding phase profile. (c) $k_1 = -1$ and $R = 0.125,\ 0.15,\ 0.2$ (d)Corresponding phase profile. Other physical quantities are $a = b = 1 = k_0 = D(z) = 1$.

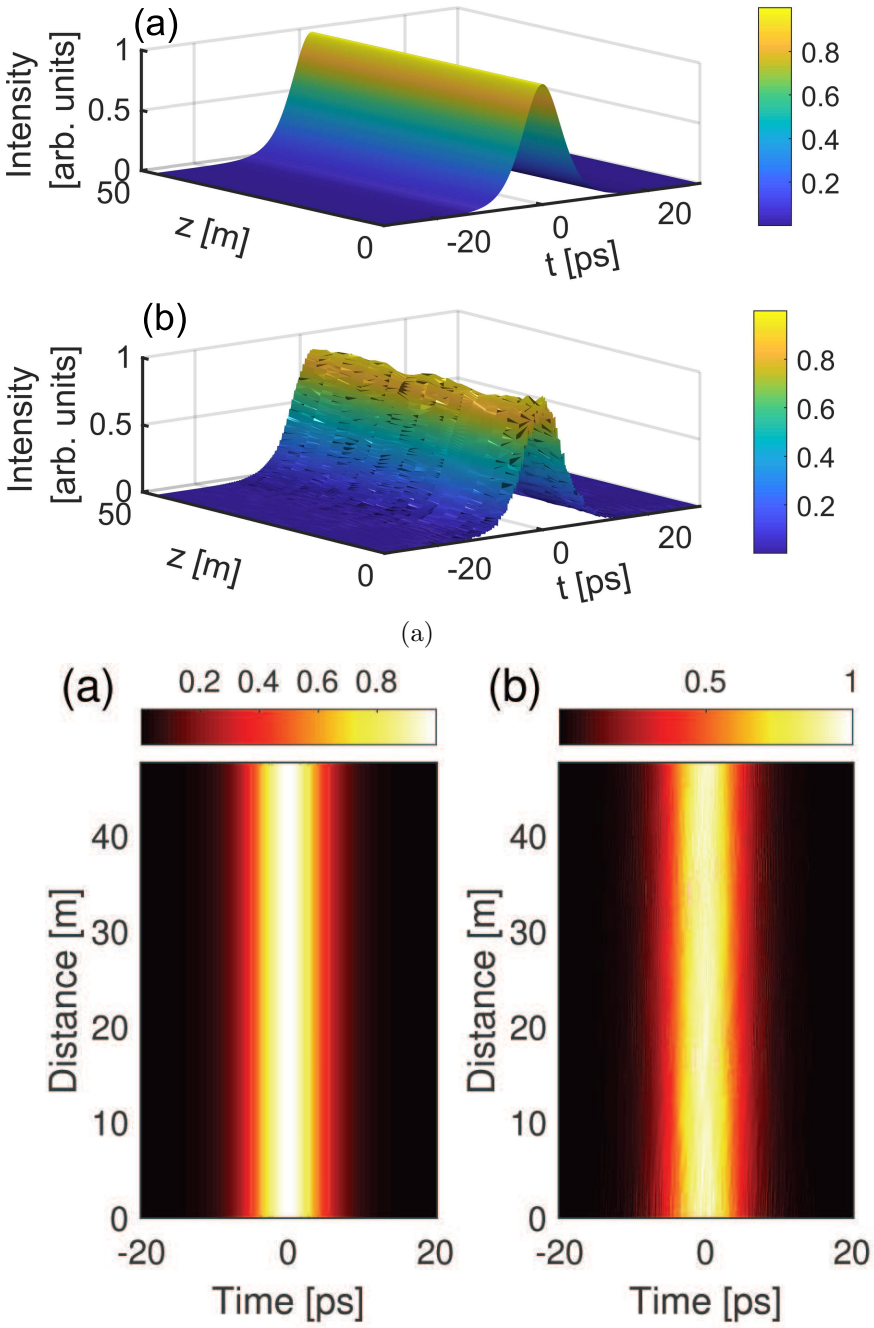

Figure 5.4: The propagation of bright soliton along the fiber. The left panel represents the evolution of the bright soliton pulse and the influence of noise, while the panel right portrays the contour evolution.

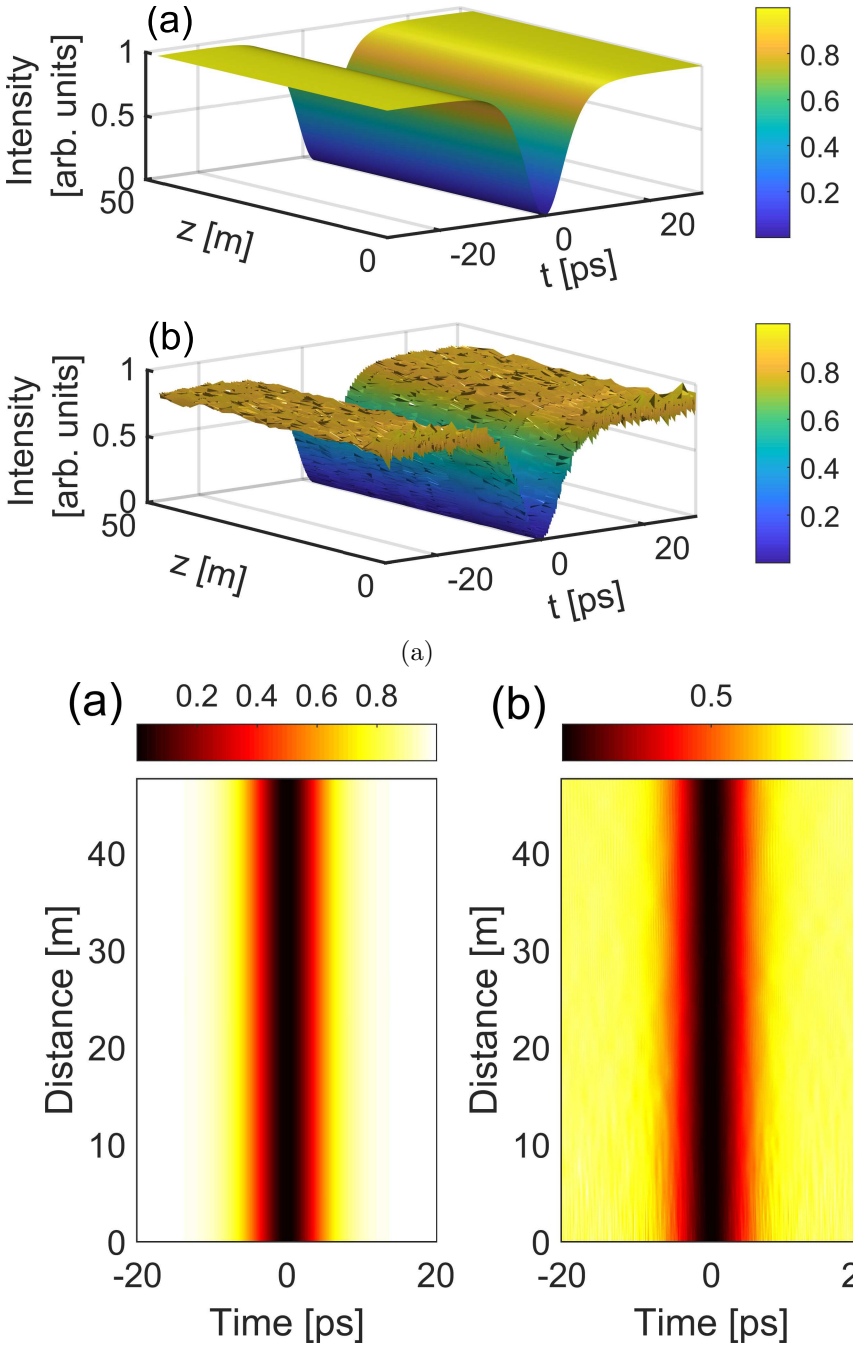

Figure 5.5: The propagation of dark soliton along the fiber. The left panel represents the evolution of the dark soliton pulse and the influence of noise, while the panel right portrays the contour evolution.

5.2.3 Direct Numerical Simulation

The stability of soliton solutions is of paramount importance for its application and physical feasibility. Unlike the conventional pulses of different form, the solitons are relatively stable, even in an environment subjected to external perturbations. Hence, in order to validate the signature of soliton, such as stable propagation over appreciable distance, and the stability against perturbation, we perform numerical simulation using split-step Fourier method. In order to check the solution stability of our dark soliton solutions, as a representative case, we consider the one soliton solution corresponding to both bright and dark soliton given respectively by Eq. (5.4), and Eq. (5.5). The stability analysis is performed in two parts, (i) direct numerical simulation of propagation of soliton using Vc-CNLSE, and (ii) the propagation of soliton subjected to perturbation such as the photon noise. Figs. (5.4) and (5.5) show the numerical simulation of stable propagation of the bright and dark soliton propagation. Figure labeled *'a'* on top corresponds to the propagation without noise, while the figure labeled *'b'* is the propagation under noise perturbation. Figs. 5.4(b) and 5.5(b) are represents the contour plot of Figs. 5.4(a) and 5.5(a) respectively.

In principle, the propagation of soliton pulse in a fiber-like media is typically subjected to environmental fluctuations, and there are numerous effects that can contribute to instability. Therefore, it is very informative to study the stability of the soliton in an environment subject to external noise or perturbations. We numerically generated a photon white noise, which corresponds to 0.035% of the soliton/background intensity. This is indeed an appreciable noise level, which can potentially perturb any propagation. The initial condition for the simulation is the soliton profile given by Eq. 5.4 and 5.5 along with synthesized numerical noise. It is very evident from the figures labeled *'b'* that both bright and dark soliton show remarkable stability against strong perturbation. Thus, one can draw out a conclusion that the soliton solution constructed through the Hirota method shows excellent stability, which has been confirmed through direct numerical simulations.

5.3 Phase dynamics of Manakov soliton

From the exact solutions given by the Eqs. (5.4)and(5.5) for bright and dark soliton respectively, we arrive at a relation between two modes of propagation as $q_1 = \frac{M}{N} q_2$ where M and N replace $\alpha_1(a)$ and $\beta_1(b)$ and the modified Eq. (5.1) can be given as

$$iq_{1z} \pm \frac{1}{2} D(z) q_{1tt} + R(z)(1 + \frac{|N|^2}{|M|^2}) q_1 |q_1|^2 + ip(z) q_1 = 0 \tag{5.7a}$$

$$iq_{2z} \pm \frac{1}{2} D(z) q_{2tt} + R(z)(1 + \frac{|M|^2}{|N|^2}) q_2 |q_2|^2 + ip(z) q_2 = 0 \tag{5.7b}$$

To obtain the phase of Manakov soliton, first we introduce the solution as given below

$$q_1(z,t) = \rho_1(z,t) e^{i\psi_1(z,t)} \tag{5.8a}$$

$$q_2(z,t) = \rho_2(z,t) e^{i\psi_2(z,t)} \tag{5.8b}$$

Substituting this expression into Eq. (5.7) and separating the real and imaginary parts, we obtain

$$\rho_{1z} + p(z)\rho_1 \pm D(z)\rho_{1t}\psi_{1t} + \frac{D(z)}{2}\psi_{1tt} = 0 \tag{5.9a}$$

$$\rho_{2z} + p(z)\rho_2 \pm D(z)\rho_{2t}\psi_{2t} + \frac{D(z)}{2}\psi_{2tt} = 0 \tag{5.9b}$$

$$2R(z)(1 + \frac{|N|^2}{|M|^2})\rho_1^3 \pm D(z)\rho_{1tt} \mp D(z)\rho_1\psi_{1t}^2 - 2\rho_1\psi_{1z} = 0 \tag{5.10a}$$

$$2R(z)(1 + \frac{|M|^2}{|N|^2})\rho_2^3 \pm D(z)\rho_{2tt} \mp D(z)\rho_2\psi_{2t}^2 - 2\rho_1\psi_{2z} = 0 \tag{5.10b}$$

The stationary condition for $|q_j|^2$ gives us an expression $\rho_{jz} + p(z)\rho_j = 0$, from which one can deduce $\rho_j = \rho_{0j}\ e^{-\int p(z)dz}$, where ρ_{0j} represent the amplitude of pulse without gain or loss. Further, by using Eq. (5.9), we obtain a phase

relation $\psi_j = \int \frac{c_j(z)}{\rho_{0j}} dt + A_j(z)$, where $c_j(z)$ and $A_j(z)$ are integration constants. Assuming, $\frac{dA_j}{dz}$ as a constant Ω_j, the expression for phase can be written as

$$\psi_j = \int \frac{c_j(z)}{\rho_{0j}^2} dt + \Omega_j z, \qquad j = 1, 2 \tag{5.11}$$

Substituting the expression of phase (5.11) into (5.10), we obtain the following equation for $I_{0j} = |\rho_{0j}|^2$

$$\left(\frac{dI_{01}}{dt}\right)^2 = \mp 2\delta(1 + \frac{|N|^2}{|M|^2})I_{01}^3 \pm \frac{8\Omega_1}{D(z)} I_{01}^2 + 4K_1 I_{01} - 4c_1^2 \tag{5.12a}$$

$$\left(\frac{dI_{02}}{dt}\right)^2 = \mp 2\delta(1 + \frac{|M|^2}{|N|^2})I_{02}^3 \pm \frac{8\Omega_2}{D(z)} I_{02}^2 + 4K_2 I_{02} - 4c_2^2 \tag{5.12b}$$

where $\delta = \frac{R(z)}{D(z)} e^{-2\int p(z)dz}$ and K_i is an integration constant. For the bright soliton the c_j and K_j can be considered as zero. Hence the above expression can be cast into the form

$$\left(\frac{dI_{01}}{dt}\right)^2 = -2\delta(1 + \frac{|\beta_1|^2}{|\alpha_1|^2})I_{01}^2(I_{01} - \rho_{1s}) \tag{5.13a}$$

$$\left(\frac{dI_{02}}{dt}\right)^2 = -2\delta(1 + \frac{|\alpha_1|^2}{|\beta_1|^2})I_{02}^2(I_{02} - \rho_{2s}) \tag{5.13b}$$

where

$$\rho_{1s} = \frac{4\Omega_1}{\delta D(z)(1 + \frac{|\beta_1|^2}{|\alpha_1|^2})}, \quad \rho_{2s} = \frac{4\Omega_2}{\delta D(z)(1 + \frac{|\alpha_1|^2}{|\beta_1|^2})} \tag{5.14}$$

By integrating Eq.(5.13), we obtain the intensity $I_j = I_{0j} e^{-2\int p(z)dz}$ as

$$I_1 = \rho_{1s} e^{-2\int p(z)dz} Sech^2(\sqrt{\frac{\delta}{2}\rho_{1s}(1 + \frac{|\beta_1|^2}{|\alpha_1|^2})}\ t) \tag{5.15a}$$

$$I_2 = \rho_{2s} e^{-2\int p(z)dz} Sech^2(\sqrt{\frac{\delta}{2}\rho_{2s}(1 + \frac{|\alpha_1|^2}{|\beta_1|^2})}\ t) \tag{5.15b}$$

comparing by these bright soliton intensities with the exact solutions (5.4), we have $\begin{pmatrix}\rho_{1s}\\ \rho_{2s}\end{pmatrix} = \begin{pmatrix}|\alpha_1|^2\\ |\beta_1|^2\end{pmatrix}\frac{1}{4\varrho_1}$. Thus, the phase for bright vector soliton can be written as;

$$\psi_j = \frac{\delta(|\alpha_1|^2 + |\beta_1|^2)D(z)}{16\varrho_1}z \tag{5.16}$$

this shows that the phase of bright vector soliton depends only on the spatial co-ordinate, and the phase remains constant across the entire pulse. But in the variable coefficient model, the GVD parameter $D(z)$ significantly influences the soliton phase.

For the dark vector soliton the Eq.(5.12) can be cast into the form

$$\left(\frac{dI_{01}}{dt}\right)^2 = 2\delta(1+\frac{|b|^2}{|a|^2})(I_{01}-\rho_{1a})^2(I_{01}-\rho_{1b}) \tag{5.17a}$$

$$\left(\frac{dI_{02}}{dt}\right)^2 = 2\delta(1+\frac{|a|^2}{|b|^2})(I_{01}-\rho_{2a})^2(I_{02}-\rho_{2b}) \tag{5.17b}$$

Here, ρ_{ja} and ρ_{jb} correspond to the double root and the single root of (5.12), respectively. By integrating Eq.(5.12), the intensity profile of dark one-soliton solution for Vc-CNLSE can be written as

$$|q_1|^2 = I_1 = \rho_{1a}e^{-2\int p(z)dz}(1-m_1^2 sech^2(\sqrt{\frac{\delta}{2}(1+\frac{|b|^2}{|a|^2})\rho_{1a}}m_1 t)) \tag{5.18a}$$

$$|q_2|^2 = I_2 = \rho_{2a}e^{-2\int p(z)dz}(1-m_2^2 sech^2(\sqrt{\frac{\delta}{2}(1+\frac{|a|^2}{|b|^2})\rho_{2a}}m_2 t)) \tag{5.18b}$$

where $m_j^2 = \frac{\rho_{ja}-\rho_{jb}}{\rho_{ja}}$. By equating (5.17) and (5.12), we get the following set of

relations

$$\Omega_1 = \frac{\delta}{4}(1+\frac{|b|^2}{|a|^2})\rho_{1a}(3-m_1^2)D(z) \tag{5.19}$$

$$\Omega_2 = \frac{\delta}{4}(1+\frac{|a|^2}{|b|^2})\rho_{2a}(3-m_2^2)D(z) \tag{5.20}$$

$$c_1^2 = \frac{\delta}{4}(1+\frac{|b|^2}{|a|^2})\rho_{1a}^3(1-m_1^2) \tag{5.21}$$

$$c_2^2 = \frac{\delta}{4}(1+\frac{|a|^2}{|b|^2})\rho_{2a}^3(1-m_2^2) \tag{5.22}$$

$$K_1 = \frac{\delta}{4}(1+\frac{|b|^2}{|a|^2})(\rho_{1a}^2+2\rho_{1a}\rho_{1b}) \tag{5.23}$$

$$K_2 = \frac{\delta}{4}(1+\frac{|a|^2}{|b|^2})(\rho_{2a}^2+2\rho_{2a}\rho_{2b}) \tag{5.24}$$

with these expressions, the phase of dark soliton via Eq.(5.11) can be written as

$$\psi_1 = \sqrt{\frac{\delta}{2}(1+\frac{|b|^2}{|a|^2})(1-m_1^2)\rho_{1a}}\ t + tan^{-1}[\frac{m_1\ tanh(\sqrt{\frac{\delta}{2}(1+\frac{|b|^2}{|a|^2})\rho_{1a}}\ m_1 t)}{\sqrt{1-m_1^2}}] + \Omega_1 z \tag{5.25}$$

$$\psi_2 = \sqrt{\frac{\delta}{2}(1+\frac{|a|^2}{|b|^2})(1-m_2^2)\rho_{2a}}\ t + tan^{-1}[\frac{m_2\ tanh(\sqrt{\frac{\delta}{2}(1+\frac{|a|^2}{|b|^2})\rho_{2a}}\ m_2 t)}{\sqrt{1-m_2^2}}] + \Omega_2 z \tag{5.26}$$

Its interesting to note that the Eq. (5.18) is almost same with the dark vector one-soliton solution (5.5) that derived by HB method. The intensity of dark soliton via Eq.(5.5) can be written as

$$|q_1|^2 = a^2 e^{-2\int p(z)dz}(1-\frac{B_1^2}{a^2}e^{2\int p(z)dz}\ sech^2(\frac{k_1}{2})) \tag{5.27a}$$

$$|q_2|^2 = b^2 e^{-2\int p(z)dz}(1-\frac{B_2^2}{b^2}e^{2\int p(z)dz}\ sech^2(\frac{k_1}{2})) \tag{5.27b}$$

Here, by equating the parameters $a^2 = \rho_{1a}$, $b^2 = \rho_{2a}$, $\frac{B_1^2}{a^2}e^{2\int p(z)dz} = m_1^2$, $\frac{B_2^2}{b^2}e^{2\int p(z)dz} = m_2^2$, we observed that the given expressions for intensity

(Eqs. (5.18) and (5.27)) of dark solitons are exactly same with conditions $k_1 = \sqrt{2\delta(a^2+b^2)m_j^2}$. It is worth mentioning that, unlike the bright vector soliton, the soliton intensity affects on the time-dependent phase of dark vector soliton. The intensity and corresponding phase profiles for different values of blackness factor m_j are depicted in Fig. 5.3. It is evident that the phase of dark soliton changes across the width, with a total phase shift of $2sin^{-1}(m_j)$. For a black soliton ($m_j = 1$), a phase shift of π occurs exactly at the center of the dip. For the gray solitons ($m_j < 1$), phase varies gradually between $0 - \pi$.

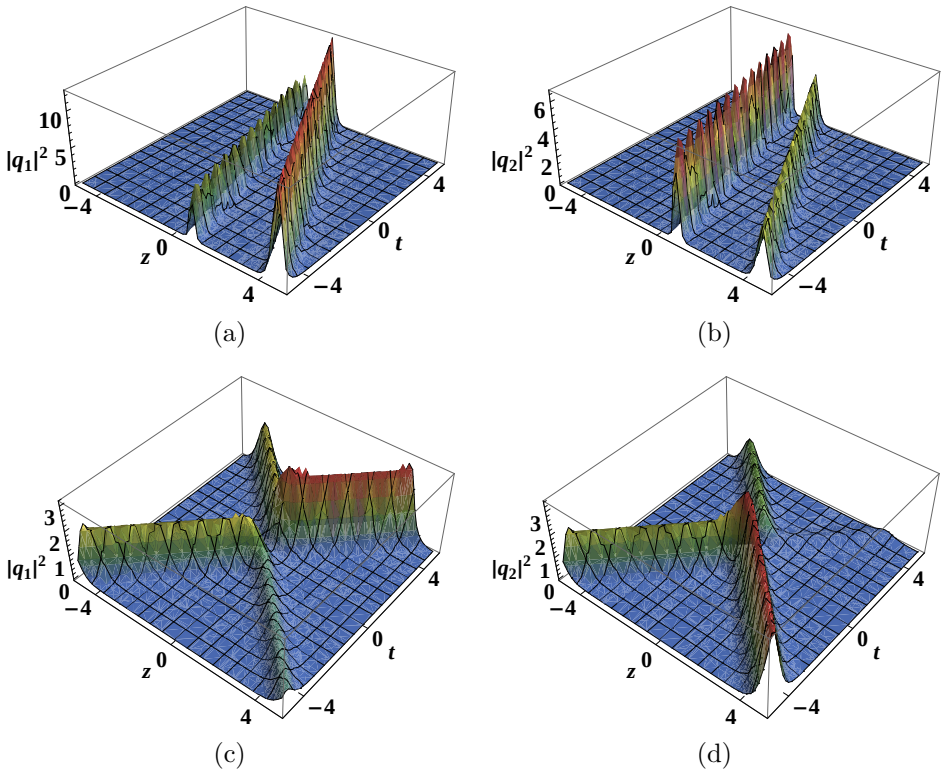

Figure 5.6: The bright two-soliton propagation through homogenous fiber for parameters, (a)$\alpha_1 = 1 + 0.5i$, $\alpha_2 = 1 - 0.5i$ (b) $\beta_1 = 1$, $\beta_2 = 1 + 0.5i$ with $k_1 = 2 - i$, $k_2 = 2 - 2i$, $\phi_1 = -5$ and $\phi_2 = 5$ (c) Energy sharing collision with $\alpha_1 = 1$, $\alpha_2 = 1$(d) $\beta_1 = 1$, $\beta_2 = 2 + i$ with $k_1 = 2 + 0.5i$, $k_2 = 2 - 0.5i$. Other physical quantities are $D(z) = 1$, $R(z) = 0.5$, and $p = 0$.

5.4 Two-soliton solutions

In order to get the bright vector two-soliton solution, the power series expansions for G and F are truncated as follows; $G = g_1 + g_3$,$G = h_1 + h_3$ and

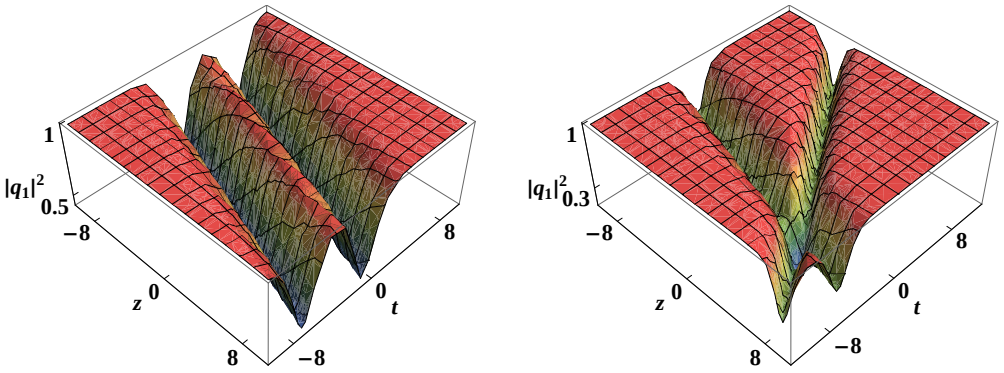

(a) (b)

Figure 5.7: The dark two-soliton propagation through homogenous fiber for parameters , (a)Same direction of propagation with $k_1 = k_2 = 1.5$, $\phi_1 = -5$ and $\phi_2 = 5$ (b)soliton interaction with $k_1 = -1.5$, $k_2 = 1.5$. Other physical quantities are $a = b = k = D(z) = \delta = 1$, and $p = 0$

$F = 1 + f_2 + f_4$. Then, back to bilinear equations (5.3), we obtain;

$$g(z) = e^{-\int p(z)dz}$$

$$g_1 = \alpha_1 e^{\theta_1} + \alpha_2 e^{\theta_2}$$

$$g_3 = \sigma_1 e^{\theta_1+\theta_1^*+\theta_2} + \sigma_2 e^{\theta_2+\theta_2^*+\theta_1}$$

$$h_1 = \beta_1 e^{\theta_1} + \beta_2 e^{\theta_2}$$

$$h_3 = \varsigma_1 e^{\theta_1+\theta_1^*+\theta_2} + \varsigma_2 e^{\theta_2+\theta_2^*+\theta_1}$$

$$f_2 = \varrho_1 e^{\theta_1+\theta_1^*} + \varrho_2 e^{\theta_1+\theta_2^*} + \varrho_3 e^{\theta_2+\theta_1^*} + \varrho_4 e^{\theta_2+\theta_2^*}$$

$$f_4 = \varrho_5 e^{\theta_1+\theta_1^*+\theta_2+\theta_2^*}$$

$$\theta_1 = k_1 t - \omega_1 \int D(z)dz + \phi_1$$

$$\theta_2 = k_2 t - \omega_2 \int D(z)dz + \phi_2$$

$$\varrho_1 = \frac{\delta(\alpha_1\alpha_1^* + \beta_1\beta_1^*)}{2(k_1 + k_1^*)^2}$$
$$\varrho_2 = \frac{\delta(\alpha_1\alpha_2^* + \beta_1\beta_2^*)}{2(k_1 + k_2^*)^2}$$
$$\varrho_3 = \frac{\delta(\alpha_1^*\alpha_2 + \beta_1^*\beta_2)}{2(k_1^* + k_2)^2}$$
$$\varrho_4 = \frac{\delta(\alpha_2\alpha_2^* + \beta_2\beta_2^*)}{2(k_2 + k_2^*)^2}$$
$$\sigma_1 = (k_1 - k_2)(\frac{\alpha_1\rho_3}{k_1 + k_1^*} - \frac{\alpha_2\rho_1}{k_2 + k_1^*})$$
$$\sigma_2 = (k_1 - k_2)(\frac{\alpha_1\rho_4}{k_1 + k_2^*} - \frac{\alpha_2\rho_2}{k_2 + k_2^*})$$
$$\varsigma_1 = (k_1 - k_2)(\frac{\beta_1\rho_3}{k_1 + k_1^*} - \frac{\beta_2\rho_1}{k_2 + k_1^*})$$
$$\varsigma_2 = (k_1 - k_2)(\frac{\beta_1\rho_4}{k_1 + k_2^*} - \frac{\beta_2\rho_2}{k_2 + k_2^*})$$
$$\varrho_5 = \frac{\delta(|\alpha_1|^2|\alpha_2|^2 + |\beta_1|^2|\beta_2|^2)|k_1 - k_2|^4}{4(k_1 + k_1^*)(k_2 + k_2^*)|k_1 + k_2|^4}$$

The final form of bright two-soliton solutions can be written as,

$$q_1(z,t) = e^{-\int p(z)dz}\frac{(g_1 + g_3)}{(1 + f_2 + f_4)} \tag{5.28a}$$

$$q_2(z,t) = e^{-\int p(z)dz}\frac{(h_1 + h_3)}{(1 + f_2 + f_4)} \tag{5.28b}$$

To construct the pair of dark two-soliton solutions, the power series expansions for G, H and F are truncated as follows, $G = g_0(1+g_1+g_2)$, $H = h_0(1+h_1+h_2)$ and $F = 1 + f_1 + f_2$. Then, from bilinear equations Eq. (5.3), we obtain

$$g_0 = ae^{i\phi} \qquad h_0 = be^{i\phi}$$
$$g_1 = \mu_1\, e^{\theta_1} + \mu_2 e^{\theta_2}, \qquad h_1 = \nu_1\, e^{\theta_1} + \nu_2 e^{\theta_2}$$
$$g_2 = A_{12}\mu_1\mu_2\, e^{\theta_1+\theta_2}, \qquad h_2 = A_{12}\nu_1\nu_2\, e^{\theta_1+\theta_2}$$
$$f_1 = e^{\theta_1} + e^{\theta_2} \qquad f_2 = A_{12}e^{\theta_1+\theta_2}$$

$$\phi = k_0 t - \omega_0 \int D(z)dz, \qquad g(z) = e^{-\int p(z)dz}$$

$$\lambda = \frac{1}{2}\delta(a^2+b^2)D(z), \qquad \omega_0 = -\frac{\lambda}{D(z)} - \frac{k_0^2}{2}$$

$$\alpha_1 = \frac{2\omega_1 + 2kk_1 + ik_1^2}{2\omega_1 + 2kk_1 - ik_1^2}, \qquad \beta_1 = \alpha_1$$

$$\alpha_2 = \frac{2\omega_2 + 2kk_2 + ik_2^2}{2\omega_2 + 2kk_2 - ik_2^2}, \qquad \beta_2 = \alpha_2$$

$$\theta_1 = k_1 t - \omega_1 \int D(z)dz + \phi_1$$

$$\theta_2 = k_2 t - \omega_2 \int D(z)dz + \phi_2$$

$$\omega_1 = \frac{k_1}{2}(-2k \pm \sqrt{2\delta(a^2+b^2) - k_1^2})$$

$$\omega_2 = \frac{k_2}{2}(-2k \pm \sqrt{2\delta(a^2+b^2) - k_2^2})$$

$$A_{12} = -\frac{2i(\alpha_1-\alpha_2)(\omega_2-\omega_1-kk_1+kk_2) - (\alpha_1+\alpha_2)(k_1-k_2)^2}{2i(1-\alpha_1\alpha_2)(\omega_1+\omega_2+kk_1+kk_2) - (\alpha_1\alpha_2+1)(k_1+k_2)^2}$$

Then, the final form of dark vector two-soliton solutions can be written as,

$$q_1(z,t) = e^{-\int p(z)dz}\frac{g_0(1+g_1+g_2)}{(1+f_1+f_2)} \tag{5.29a}$$

$$q_2(z,t) = e^{-\int p(z)dz}\frac{h_0(1+h_1+h_2)}{(1+f_1+f_2)} \tag{5.29b}$$

By using Eqs. (5.28) and (5.29), we can investigate the same direction of propagation or oppositely moving vector solitons in homogeneous or inhomogeneous fiber system. Figs. 5.6 and 5.7 represent two-soliton solution in homogeneous systems. Comparing with the dark pulse, Manakov bright solitons have an additional feature, which exhibit the well-known energy exchange collision [20]. The energy sharing collision of bright soliton are depicted in Figs. 5.6(c) and 5.6(d).

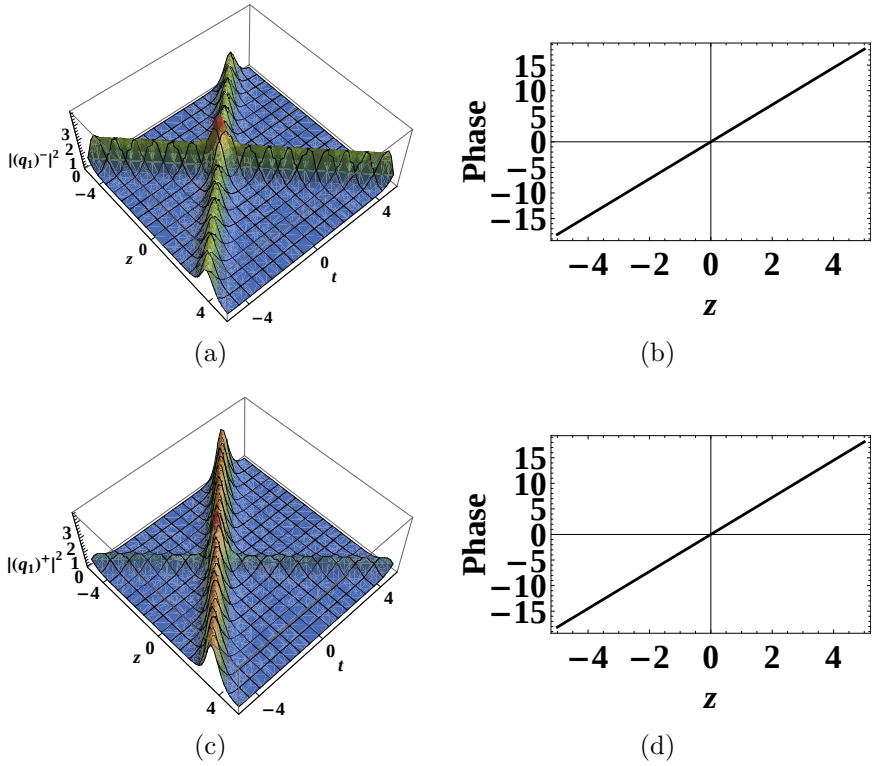

Figure 5.8: The bright two-soliton energy sharing collision via the asymptotic expression. (a)Before collision $S_1^{1-}+S_1^{2-}$ (b) Corresponding phase with $\psi_1^{1-}+\psi_1^{2-}$ (c) after collision $S_1^{1+}+S_1^{2+}$ (d) Corresponding phase with $\psi_1^{1+}+\psi_1^{2+}$. Other physical quantities are $\alpha_1 = 1$, $\alpha_2 = 1$, $k_1 = 2 + 0.5i$, $k_2 = 2 - 0.5i$, $D(z) = 1$, $R(z) = 0.5$, and $p = 0$.

5.4.1 Asymptotic analysis and two-soliton phase

The behavior of head-on collision between the two-vector solitons in fibers can be analyzed by the asymptotic states of soliton solution. Based on the two-soliton solution, we can observe the elastic collision between bright and dark vector solitons. The asymptotic states of bright vector two- soliton solution Eq. (5.28) are introduced as follows.

1) Before collision

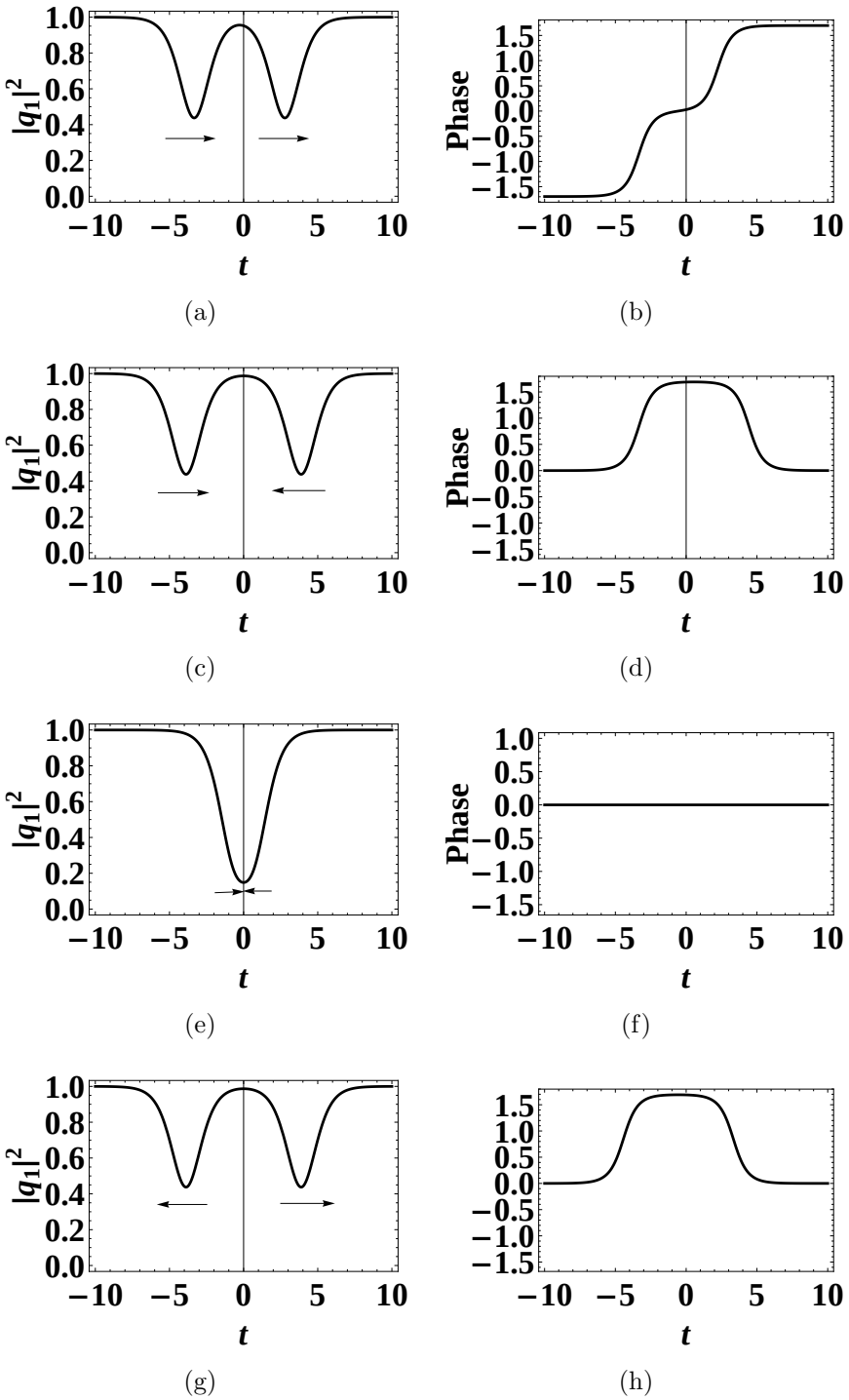

Figure 5.9: The resultant intensity and phase of two dark soliton via the asymptotic expressions for before and after collision (a) same direction of propagation with $k_1 = 1.5$ and $k_2 = 1.5$, $\phi_1 = 5$ and $\phi_2 = -5$.(b) Corresponding phase (c) before collision with $k_1 = -1.5$ and $k_2 = 1.5$, $\phi_1 = 5$ and $\phi_2 = 5$. (d) Corresponding phase (e)at collision with $k_1 = -1.5$ and $k_2 = 1.5$, $\phi_1 = \phi_2 = 0$.(f)Corresponding phase. (g) after collision with $k_1 = 1.5$ and $k_2 = -1.5$, $\phi_1 = 5$ and $\phi_2 = 5$. (h)Corresponding phase. Other relevant physical parameters are $k_0 = a = D(z) = 1$, $p = 0$ and $R = 0.5$

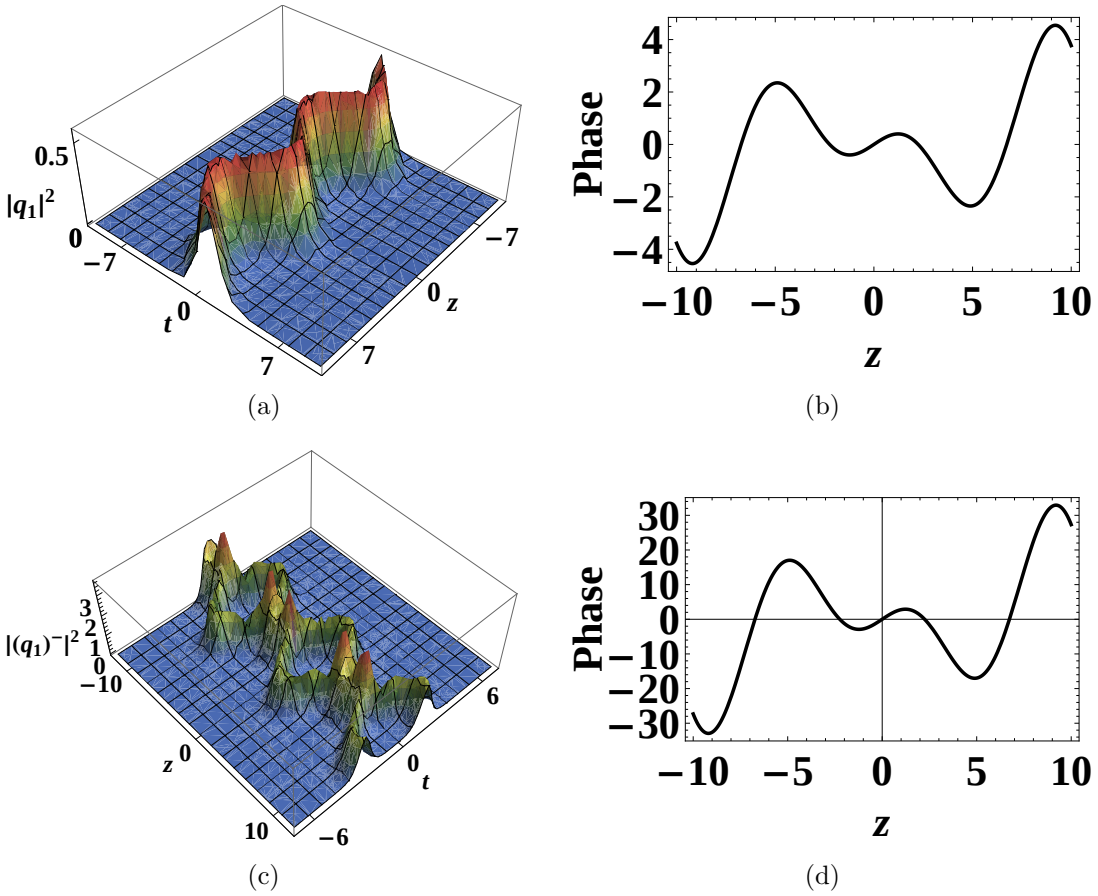

Figure 5.10: The bright soliton propagation with varying GVD parameter, where $D(z) = Cos(0.7z)$. (a)One soliton with $k_1 = 1 + i$, $\alpha_1 = 1 + i$, $\beta_1 = 2 - i$, $R(z) = 0.5$ and $p = 0$. (b)Corresponding phase. (c) Two-soliton with $\alpha_1 = 1$, $\alpha_2 = 1$, $k_1 = 2 + 0.5i$, $k_2 = 2 - 0.5i$, $R(z) = 0.5$, and $p = 0$. (d)Corresponding phase.

(a)$S^{1-}(\theta_1 + \theta_1^* \sim 0, \theta_2 + \theta_2^* \to -\infty)$

$$\begin{pmatrix} q_1 \\ \\ q_2 \end{pmatrix} \to \begin{pmatrix} S_1^{1-} \\ \\ S_2^{1-} \end{pmatrix} = \begin{pmatrix} \alpha_1 \\ \\ \beta_1 \end{pmatrix} \frac{e^{-\int p(z)dz}}{2\sqrt{\varrho_1}} e^{-i\theta_{1I}} sech(\theta_{1R} + \frac{\ln \varrho_1}{2}) \quad (5.30)$$

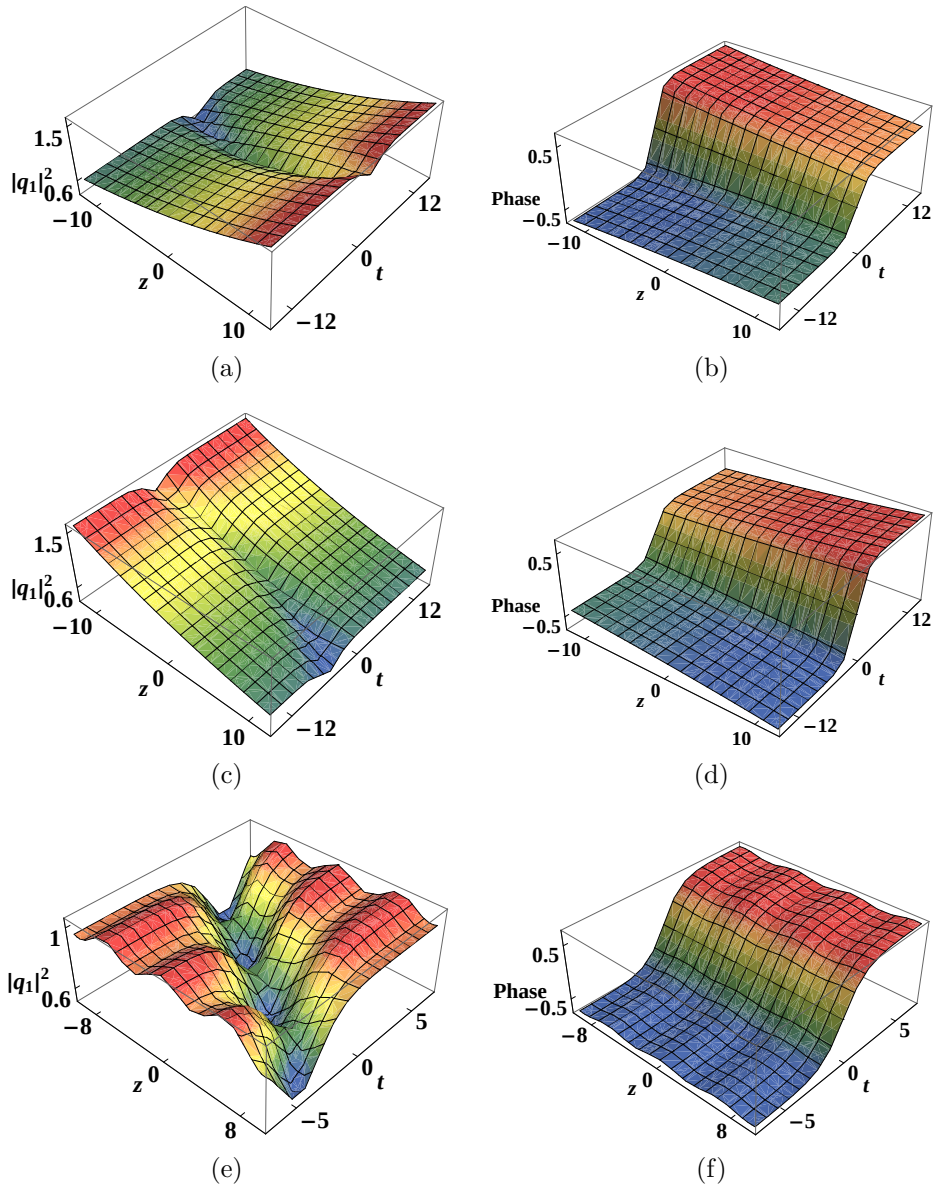

Figure 5.11: The dark vector soliton propagation through inhomogeneous fiber for parameters, (a)pulse amplification (gain) with $p = -0.02$ (b)Corresponding phase. (c)Pulse absorption (loss) with $p = 0.02$. (d)Corresponding phase. (e) periodic background as $p = 0.05sin(z)$. (f)Corresponding phase.Other physical quantities are $k = D(z) = 1$, $R = 0.5$

(b)$S^{2-}(\theta_2+\theta_2^*\sim 0, \theta_1+\theta_1^*\to\infty)$

$$\begin{pmatrix} q_1 \\ \\ q_2 \end{pmatrix} \to \begin{pmatrix} S_1^{2-} \\ \\ S_2^{2-} \end{pmatrix} = \begin{pmatrix} \sigma_1 \\ \\ \varsigma_1 \end{pmatrix} \frac{e^{-\int p(z)dz}}{2\sqrt{\varrho_1\varrho_5}} e^{-i\theta_{2I}} sech(\theta_{2R}+\frac{1}{2}\ln(\varrho_5/\varrho_1)) \quad (5.31)$$

2)After collision

(a)$S^{1+}(\theta_1+\theta_1^*\sim 0, \theta_2+\theta_2^*\to\infty)$

$$\begin{pmatrix} q_1 \\ \\ q_2 \end{pmatrix} \to \begin{pmatrix} S_1^{1+} \\ \\ S_2^{1+} \end{pmatrix} = \begin{pmatrix} \sigma_2 \\ \\ \varsigma_2 \end{pmatrix} \frac{e^{-\int p(z)dz}}{2\sqrt{\varrho_4\varrho_5}} e^{-i\theta_{1I}} sech(\theta_{1R}+\frac{1}{2}\ln(\varrho_5/\varrho_4)) \quad (5.32)$$

(b)$S^{2+}(\theta_2+\theta_2^*\sim 0, \theta_1+\theta_1^*\to-\infty)$

$$\begin{pmatrix} q_1 \\ \\ q_2 \end{pmatrix} \to \begin{pmatrix} S_1^{2+} \\ \\ S_2^{2+} \end{pmatrix} = \begin{pmatrix} \alpha_2 \\ \\ \beta_2 \end{pmatrix} \frac{e^{-\int p(z)dz}}{2\sqrt{\varrho_4}} e^{-i\theta_{2I}} sech(\theta_{2R}+\frac{\ln\varrho_4}{2}) \quad (5.33)$$

Corresponding phase can be written as

$$\psi_j^{1-} = \frac{\delta(|\alpha_1|^2+|\beta_1|^2)D(z)}{16\varrho_1} z \quad (5.34)$$

$$\psi_j^{2-} = \frac{\delta(|\sigma_1|^2+|\varsigma_1|^2)D(z)}{16\varrho_1\varrho_5} z \quad (5.35)$$

$$\psi_j^{1+} = \frac{\delta(|\sigma_2|^2+|\varsigma_2|^2)D(z)}{16\varrho_4\varrho_5} z \quad (5.36)$$

$$\psi_j^{1-} = \frac{\delta(|\alpha_2|^2+|\beta_2|^2)D(z)}{16\varrho_4} z \quad (5.37)$$

The asymptotic analysis of dark vector two-soliton solutions given by Eq. (5.29) are conducted as follows.

1) Before collision

(a)$S^{1-}(\theta_1 \sim 0, \theta_2 \to -\infty)$

$$\begin{pmatrix} q_1 \\ \\ q_2 \end{pmatrix} \to \begin{pmatrix} S_1^{1-} \\ \\ S_2^{1-} \end{pmatrix} = \begin{pmatrix} a \\ \\ b \end{pmatrix} \frac{e^{i\psi}}{2e^{\int p(z)dz}} \times [(1+\mu_1) + (\mu_1 - 1)tanh(\frac{\theta_1}{2})] \quad (5.38)$$

(b)$S^{2-}(\theta_2 \sim 0, \theta_1 \to \infty)$

$$\begin{pmatrix} q_1 \\ \\ q_2 \end{pmatrix} \to \begin{pmatrix} S_1^{2-} \\ \\ S_2^{2-} \end{pmatrix} = \begin{pmatrix} a \\ \\ b \end{pmatrix} \frac{\mu_1 e^{i\psi}}{2e^{\int p(z)dz}} \times [(1+\mu_2) + (\mu_2 - 1)tanh(\frac{\theta_2}{2} + ln\sqrt{A_{12}})] \quad (5.39)$$

2)After collision

(a)$S^{1+}(\theta_1 \sim 0, \theta_2 \to \infty)$

$$\begin{pmatrix} q_1 \\ \\ q_2 \end{pmatrix} \to \begin{pmatrix} S_1^{1+} \\ \\ S_2^{1+} \end{pmatrix} = \begin{pmatrix} a \\ \\ b \end{pmatrix} \frac{\mu_2 e^{i\psi}}{2e^{\int p(z)dz}} \times [(1+\mu_1) + (\mu_1 - 1)tanh(\frac{\theta_1}{2} + ln\sqrt{A_{12}})] \quad (5.40)$$

(b)$S^{2+}(\theta_2 \sim 0, \theta_1 \to -\infty)$

$$\begin{pmatrix} q_1 \\ \\ q_2 \end{pmatrix} \to \begin{pmatrix} S_1^{2+} \\ \\ S_2^{2+} \end{pmatrix} = \begin{pmatrix} a \\ \\ b \end{pmatrix} \frac{e^{i\psi}}{2e^{\int p(z)dz}} \times [(1+\mu_2) + (\mu_2 - 1)tanh(\frac{\theta_2}{2})] \quad (5.41)$$

with the condition $k_j = \sqrt{2\delta(a^2+b^2)m_j^2}$, corresponding phase can be written as

$$\psi_j^{1-} = \sqrt{\frac{\delta}{2}(a^2+b^2)(1-(m_j^{1-})^2)}\ t + tan^{-1}[\frac{m_j^{1-}\ tanh(\sqrt{\frac{\delta}{2}(a^2+b^2)}\ m_j^{1-}t + \frac{\phi_1}{2})}{\sqrt{1-(m_j^{1-})^2}}] + \frac{\sqrt{1-(m_j^{1-})^2}}{2m_j^{1-}}\phi_1 + \Omega_j^{1-}z \quad (5.42)$$

$$\psi_j^{2-} = \sqrt{\frac{\delta}{2}(a^2+b^2)(1-(m_j^{2-})^2)}\ t + tan^{-1}[\frac{m_j^{2-}\ tanh(\sqrt{\frac{\delta}{2}(a^2+b^2)}\ m_j^{2-}t + \frac{\phi_2}{2} + ln\sqrt{A_{12}})}{\sqrt{1-(m_j^{2-})^2}}] + \frac{\sqrt{1-(m_j^{2-})^2}}{2m_j^{2-}}(\phi_2 + ln[A_{12}]) + \Omega_j^{2-}z \quad (5.43)$$

$$\psi_j^{1+} = \sqrt{\frac{\delta}{2}(a^2+b^2)(1-(m_j^{1+})^2)}\ t + tan^{-1}[\frac{m_j^{1+}\ tanh(\sqrt{\frac{\delta}{2}(a^2+b^2)}\ m_j^{1+}t + \frac{\phi_1}{2} + ln\sqrt{A_{12}})}{\sqrt{1-(m_j^{1+})^2}}] + \frac{\sqrt{1-(m_j^{1+})^2}}{2m_j^{1+}}(\phi_1 + ln[A_{12}]) + \Omega_j^{1+}z \quad (5.44)$$

$$\psi_j^{2+} = \sqrt{\frac{\delta}{2}(a^2+b^2)(1-(m_j^{2+})^2)}\ t + tan^{-1}[\frac{m_j^{2+}\ tanh(\sqrt{\frac{\delta}{2}(a^2+b^2)}\ m_j^{2+}t + \frac{\phi_2}{2})}{\sqrt{1-(m_j^{2+})^2)}}] + \frac{\sqrt{1-(m_j^{2+})^2)}}{2m_j^{2+}}\phi_2 + \Omega_j^{2+}z \quad (5.45)$$

where

$$(m_1^{j-})^2 = \frac{(B_1^{j-})^2}{a^2} e^{2\int p(z)dz}, \qquad (m_2^{j-})^2 = \frac{(B_2^{j-})^2}{b^2} e^{2\int p(z)dz}$$
$$(m_1^{j+})^2 = \frac{(B_1^{j+})^2}{a^2} e^{2\int p(z)dz}, \qquad (m_2^{j+})^2 = \frac{(B_2^{j+})^2}{b^2} e^{2\int p(z)dz}$$

$$\begin{pmatrix} B_1^{1-} \\ B_2^{1-} \end{pmatrix} = \begin{pmatrix} a \\ b \end{pmatrix} |\frac{(\mu_1 - 1)}{2e^{\int p(z)dz}}|, \qquad \begin{pmatrix} B_1^{2-} \\ B_2^{2-} \end{pmatrix} = \begin{pmatrix} a \\ b \end{pmatrix} |\frac{\mu_1(\mu_2 - 1)}{2e^{\int p(z)dz}}|$$
$$\begin{pmatrix} B_1^{1+} \\ B_2^{1+} \end{pmatrix} = \begin{pmatrix} a \\ b \end{pmatrix} |\frac{\mu_2(\mu_1 - 1)}{2e^{\int p(z)dz}}|, \qquad \begin{pmatrix} B_1^{2+} \\ B_2^{2+} \end{pmatrix} = \begin{pmatrix} a \\ b \end{pmatrix} |\frac{(\mu_2 - 1)}{2e^{\int p(z)dz}}|$$

From the above asymptotic expressions of before and after collision, we can identify that total energy of each of the solitons is conserved during the interaction process. The resultant intensity of bright vector soliton due to energy sharing collisions and corresponding phase are depicted in Fig. 5.8. It is obvious that the resultant phase of bright solitons remains unchanged during collision. But in the case of dark soliton, the phase behaves markedly different from the bright soliton case. Here, we have studied the phase profile of two gray vector solitons as shown in the Fig. 5.9. When both soliton travel in same direction, the resultant phase produce a net phase shift equal to the sum of individual phase shift as shown in Fig. 5.9(b). Fig. 5.9(d) represents the phase profile of two oppositely moving gray soliton before the collision while, Fig. 5.9(h) depicts the recovered phase after collision. It is evident that the solitons recover the phase after collision and maintains its phase shift [4]. At the collision point the phase profiles of the two solitons cancel each other as shown in the Fig. 5.9(f).

5.5 Results and discussions

In previous sections, the Manakov model and its pair of vector soliton with constant mode of propagation has been discussed in detail. Especially, the corresponding phase profile of vector solitons have been emphasized explicitly for the first time to best of our knowledge. Recently, the intensity of Manakov vector

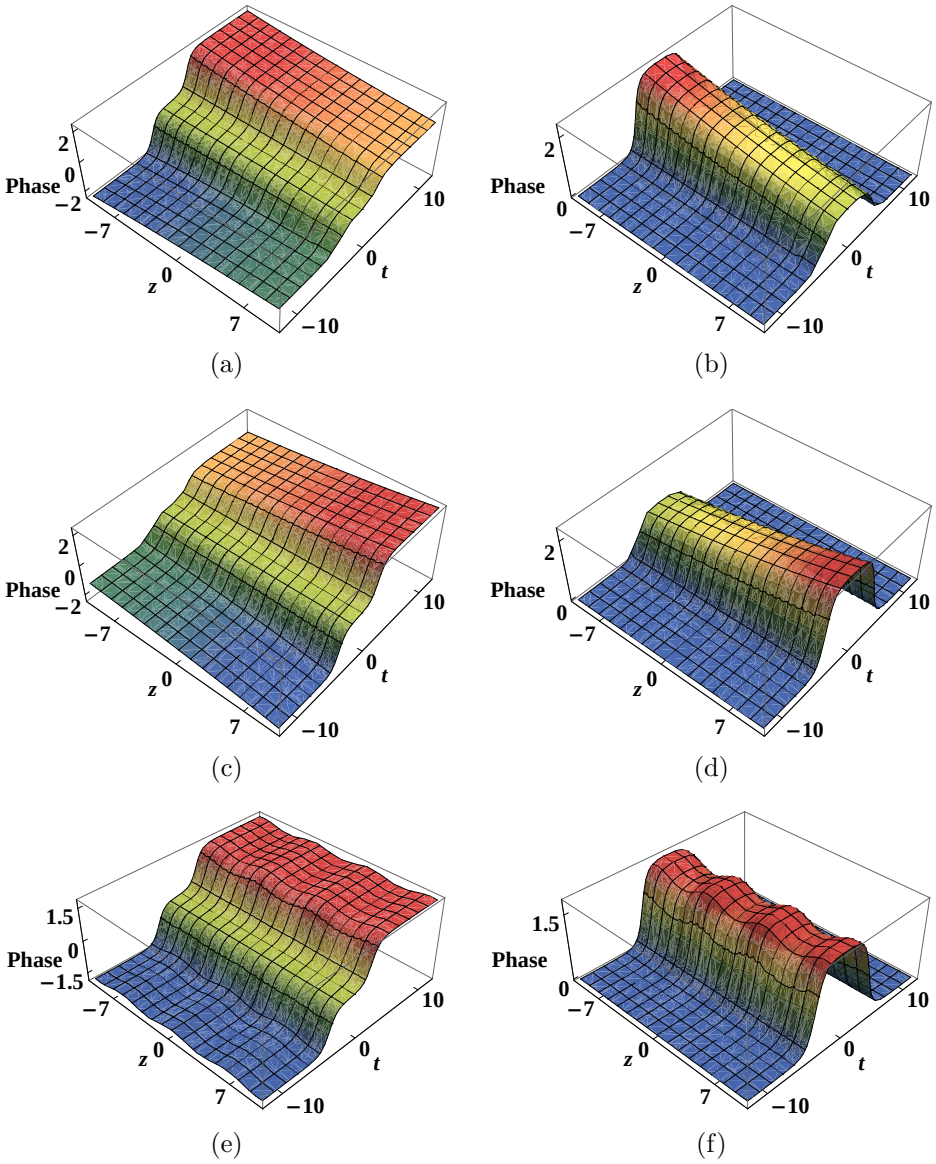

Figure 5.12: The dark two-soliton phase via the asymptotic expressions (a) gain of two-soliton with same direction of propagation. (b) gain of two-soliton with opposite direction of propagation. (c) Loss of two-soliton with same direction of propagation. (d) Loss of two-soliton with opposite direction of propagation. (e) Periodic background in two-solitons for the same direction of propagation. (f)Periodic background in two-solitons for the opposite direction of propagation. Where same direction of propagation studied with parameter $k_1 = 1.5$ and $k_2 = 1.5$, for the interactive mode $k_1 = -1.5$ and $k_2 = 1.5$. Other relevant physical quantities are $k_0 = a = D(z) = 1$ and $R = 0.5$

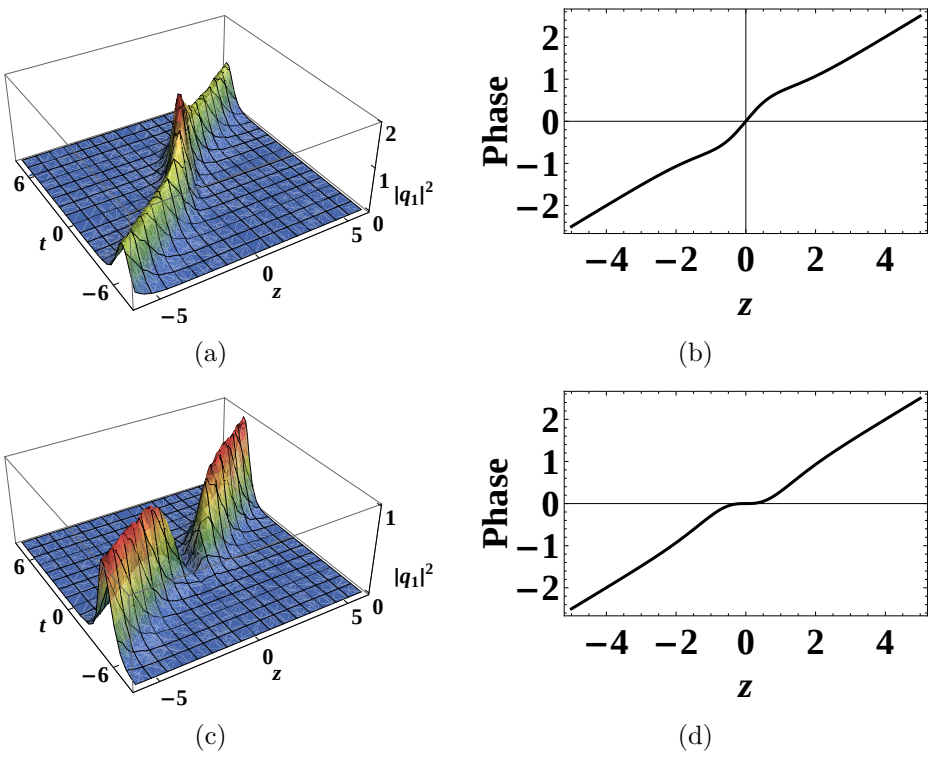

Figure 5.13: The bright vector soliton tunneling for parameters, (a)Dispersion barrier with $D(z) = 1 + hsech[z - z_0]^2$ and $h = 1$. (b)Corresponding phase.(c) Dispersion well with $h = -1$. (d)Corresponding phase. Other relevant physical quantities are $k_1 = 1 + i$, $\alpha_1 = 1 + i$, $\beta_1 = 2 - i$, $R(z) = 0.5$, $z_0 = 0$ and $p = 0$.

soliton with varying coefficients is studied [21, 26]. But the actual phase profile of bright and dark vector solitons in the CNLSE or Vc-CNLSE models are not addressed yet. Here, we report the inhomogeneous effects on soliton intensity and corresponding phase of Manakov bright and dark vector solitons.

When considering a periodically varying GVD parameter [35, 36], solitons exhibit oscillating phase variation along the spatial axis, while the amplitude and width of vector solitons remain constants. The effect of GVD parameter ($D(z) = Cos(0.7z)$) in one and two bright solitons dynamics are depicted in Fig. 5.10. In contrast to the concept of constant phase of bright soliton in NLSE [1], the $D(z)$ plays a significant role on the evolution dynamics of soliton phase in varying coefficients models.

In the presence of medium gain or loss, soliton intensity undergoes amplifi-

cation or absorption. When $p(z)$ is a constant value as $p = -0.02$ ($p = 0.02$), medium exhibit constant gain(loss). The effect of gain(loss) on dark solitons phase are depicted in Fig. 5.11. It is quite evident that dark soliton phase gradually decreases(increases) with respect to the medium gain(loss). This is attributed to the fact that the soliton intensity varies inversely with the actual phase of dark soliton. During the time of amplification(absorption), soliton intensity increases(decreases) correspondingly, which reduces(raises) the total phase shift of dark soliton spatially as shown in Figs. 5.11(b) and 5.11(d). The phase evolution due to influence of background oscillation ($p = 0.05sin(z)$) is depicted in Fig. 5.11(f).

In similar lines with the dark one-soliton situations, we extended the phase dynamics of the two-soliton solutions as shown in Fig. 5.12. Unlike the bright two-soliton which has same resultant phase before and after collision, dark soliton exhibit different form of resultant phase shift due to the mode of two-soliton propagation. The medium inhomogeneity and corresponding phase change on the same direction of propagation is depicted in Figs. 5.12(a), 5.12(c) and 5.12(e). The phase variation of dark soliton due to the interactions between two-solitons are depicted (with same inhomogeneity) in Figs. 5.12(b), 5.12(d) and 5.12(f).

5.5.1 Nonlinear tunneling and soliton phase

In recent past, the nonlinear tunneling phenomenon of solitons have been explored in many leading research works [21, 37–40]. The first experimental achievement of tunneling phenomena through a potential barrier was reported in Ref. [41]. To investigate nonlinear tunneling effect of Manakov vector soliton through the dispersion barrier or well, we choose the parameter as follows [31, 37]:

$$D(z) = r_0 \pm h\, sech^2(c(z - z_0))$$
$$R(z) = R_0$$

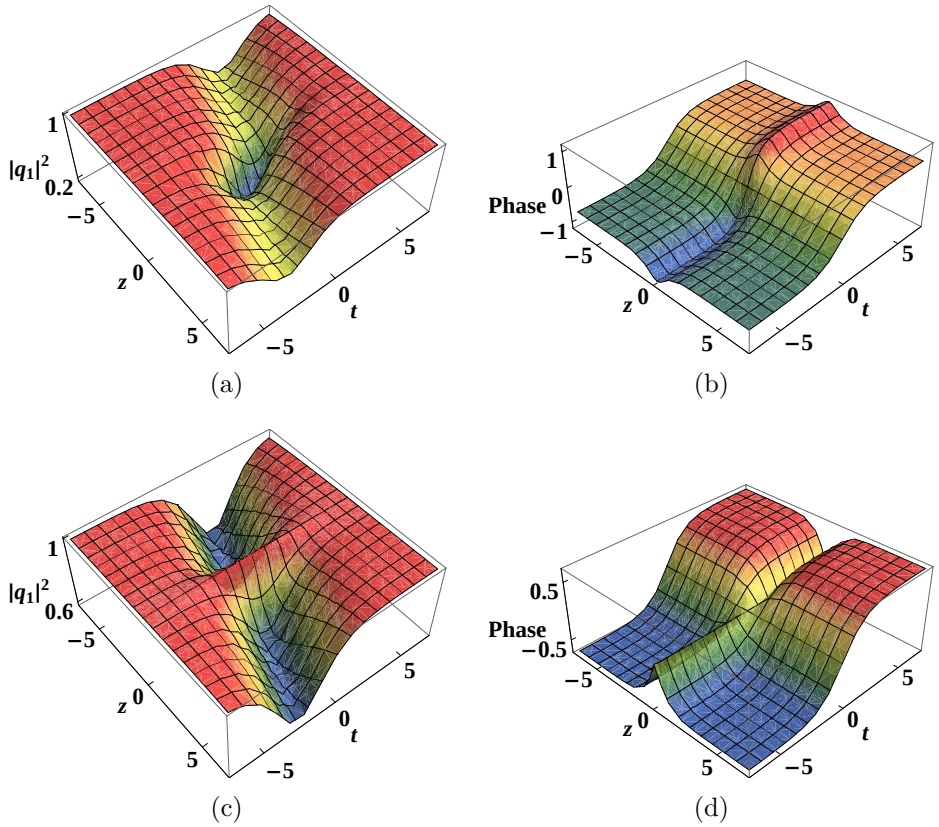

Figure 5.14: The dark vector soliton tunneling for parameters, (a)Dispersion barrier with $D(z) = 1 + hsech[z - z_0]^2$, and $h = 1$.(b) Dispersion well with $h = -1$. Other physical quantities are $k_0 = k_1 = a = 1$, $R(z) = 0.5$ and $z_0 = 0$.

where $\pm h$ indicates the height of the barrier/well. The parameter c is related to its width and z_0 indicates the location of the dispersion barrier/well and R_0 is a constant parameter. When bright (dark) soliton propagate through the dispersion barrier, the intensity (blackness) of the pulse grows and forms a peak at the barrier location and retains its shape after crossing the barrier. Similarly, when bright (dark) soliton propagate through the dispersion well the intensity (blackness) of pulse diminishes and a valley is formed at $z = z_0$ and restore its shape after crossing the well. In this work, apart from the intensity or blackness of tunneling soliton, we exclusively studied the corresponding phase change of vector soliton when it pass through the dispersion barrier and well.

The Manakov bright soliton propagation through dispersion barrier and corresponding phase change are illustrated in Figs.5.13(a) and 5.13(b) respectively.

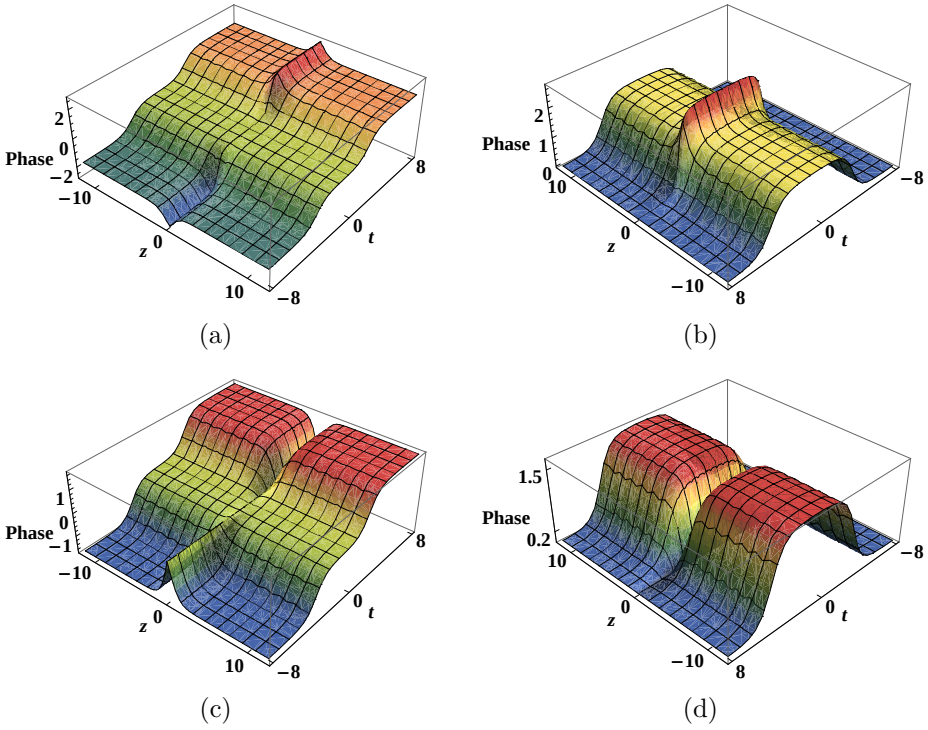

Figure 5.15: The phase change of dark two-soliton and tunneling effect for parameter $D(z) = 1 + hsech[z - z_0]^2$ (a) Dispersion barrier in same direction mode with $h = 0.7$.(a) Dispersion barrier in opposite direction mode with $h = 0.7$.(c) Dispersion well in same direction mode with $h = -1$.(d) Dispersion well in opposite direction mode with $h = -1$. Where same direction of propagation studied with parameter $k_1 = 1.5$ and $k_2 = 1.5$, for the opposite mode $k_1 = -1.5$ and $k_2 = 1.5$. Other physical quantities are $k_0 = a = 1$, $R(z) = 0.5$ and $z_0 = 0$.

Similarly, the soliton passing through dispersion well and corresponding phase change are respectively depicted in Figs.5.13(c) and 5.13(d). It is evident that, at the region of barrier, the phase becomes more steeper and maintains its original phase. But in the case of dispersion well, the phase vanishes at well and retains its actual phase after crossing the given well.

The dark soliton propagation through dispersion barrier and corresponding phase change are portrayed in Figs. 5.14(a) and 5.14(b), respectively. When dark soliton pass through the dispersion barrier, the maximum phase shift takes place at the region of barrier then it retains original form. Similarly, dark soliton propagation through dispersion well and corresponding phase change are respectively depicted in Figs.5.14(c) and 5.14(d). In the case of well, phase van-

ish at the region of well and retains its original shape after passing through it. For better insight, nonlinear tunneling effect on Manakov dark two-solitons is shown in Fig.5.15, where same direction and interactive mode of propagation of two-soliton are considered.

5.6 Conclusion

In this chapter, we have investigated the phase dynamics of Manakov bright and dark vector solitons in inhomogeneous fibers by employing two component Vc-CNLS model. The exact one and two soliton solutions have been derived by Hirota's bilinear method. To study the phase dynamics of the system, we have applied a general ansatz method which enabled explicit analytical expressions for intensity as well as phase of the soliton. By equating the unknown parameters of this ansatz with the exact solutions of well-known HB method, we have obtained exact phase of Manakov soliton. By using the asymptotic analysis of two-soliton solutions, the phase of the individual solitons have been explored. Unlike the bright vector soliton which has constant phase in homogeneous medium, the time dependent phase of dark soliton exhibits a gradual phase change. The influence of varying coefficients such as periodically varying GVD, medium gain/loss and background oscillations on the dynamics of phase evolution have also been discussed in detail, up to the two-soliton level. Moreover, we have studied nonlinear tunneling effect of Manakov soliton in the context of dispersion barrier/well. When solitons pass through the dispersion barrier(well), the maximum(minimum) phase change takes place at the region of barrier(well) and the phase retains its original form after crossing the given barrier(well).

In contrast to conventional way of intensity based soliton description, we have presented a comprehensive analysis on the phase dynamics of the soliton in a self-explanatory way. Unlike the common usage of HB method for soliton intensity, we have extended the capability of HB method in understanding the phase profile of the multi-soliton solutions. As it is known, the phase profile has significant role in multi-soliton solutions, especially in the bound state soliton system, where the

relative phase plays a significant role in explaining the nature of vector soliton interaction, such as attractive or repulsive. We believe the aforementioned results in this chapter can serve as a potential reference for many future studies related to the phase dynamics of much complex systems.

Bibliography

[1] G.P. Agrawal, Nonlinear Fiber Optics (Academic, New York, 2013)

[2] C. R. Menyuk, Opt. Lett. **12**, 614 (1987).

[3] A. Hasegawa, Y. Kodama, Solitons in Optical Communications (Oxford University Press, Oxford, 1995)

[4] Y.S. Kivshar, G.P. Agrawal, Optical Solitons from Fibers to Photonic Crystals, Academic, New York, 2003.

[5] A. Hasegawa, F.D. Tappert, Appl. Phys. Lett. **23**, 142 (1973)

[6] L. F. Mollenauer, R. H. Stolen, and J. P. Gordon, Phys. Rev. Lett. **45**, 1095 (1980)

[7] Yuri S. Kivshar, Barry Luther-Davies, Physics Reports **298**, 81 (1998)

[8] P. Emplit, J. P. Hamaide, F. Reynaud, and A. Barthelemy, Opt. Commun. **62**, 374 (1987).

[9] A. M. Weiner, J. P. Heritage, R. J. Hawkins, R. N. Thurston, E. M. Kirschner, D. E. Leaird, and W. J. Tomlinson, Phys.Rev. Lett. **61**, 2445(1988)

[10] Yuri S. Kivshar et al Chaos, Solitons and Fractals Vol. **4**, 1745 (1994)

[11] S.V. Manakov, Sov. Phys. JETP **38**, 248 (1974).

[12] C. R. Menyuk, IEEE J. Quantum Electron, **QE-25**, 2674(1989).

[13] D. J. Kaup and B.A. Malomed, Phys. Rev. A **48**, 599 (1993).

[14] J. U. Kang, G. I. Stegeman, J. S. Aitchison, and N. Akhmediev, Phys. Rev. Lett. **76**, 3699 (1996).

[15] B. Frisquet, B. Kibler, J. Fatome, P. Morin, F. Baronio, M. Conforti, G. Millot, and S. Wabnitz , Phys. Rev. A **92**, 053854(2015).

[16] R. Radhakrishnan, M. Lakshmanan, J. Hietarinta, Phys. Rev. E **56**, 2213 (1997).

[17] M. N. Islam, Ultrafast Fiber Switching Devices and Systems (Cambridge University Press, New York, 1992).

[18] R.Radhakrishnan and M.Lakshmanan J.Phys.A:Math.Gen.**28**, 2683(1995).

[19] T. Kanna and M. Lakshmanan, Phys. Rev. Lett. **86**, 5043 (2001).

[20] T. Kanna and M. Lakshmanan, Phys. Rev. E. **67**, 046617 (2003).

[21] N.M. Musammil, K. Porsezian, P.A. Subha, and K. Nithyanandan, Chaos **27**, 023113(2017)

[22] S Rajendran, P Muruganandam and M Lakshmanan, J. Phys. B: At.Mol. Phys **42**(14), 145307, (2009)

[23] S Rajendran, P Muruganandam and M Lakshmanan, Journal of Mathematical Physics **52**(2), 023515,(2011)

[24] S Rajendran, P Muruganandam and M Lakshmanan, Physica D: Nonlinear Phenomena **239**(7), 366,(2010)

[25] C.G. Latchio Tiofacka, Alidou Mohamadoub, Timoleon C. Kofane, and K. Porsezian, J. Mod. Opt.**57**, 261(2010)

[26] Sushmita Chakraborty, Sudipta Nandy, and Abhijit Barthakur, Phys. Rev. E **91**, 023210 (2015)

[27] Yunqing Yang, Zhenya Yan, and Dumitru Mihalache, J. Math. Phys. **56**, 053508 (2015)

[28] R. Hirota, The Direct Method in Soliton Theory (Cambridge University Press, Cambridge, 2004)

[29] K. Porsezian and K. Nakkeeran, Phys. Rev. Lett. **76**,3955 (1996).

[30] Liu W J, B Tian, H Q Zhang, T Xu, and H Li, Phys. Rev. A **79**, 063810(2009)

[31] N.M. Musammil, K. Porsezian, K. Nithyanandan, P.A. Subha, and P. Tchofo Dinda, Optical Fiber Technology **37**, 11(2017)

[32] R. N. Thurston and Andrew M. Weiner. Collisions of dark solitons in optical fibers. J. Opt. Soc. Am. B **8**, 471(1991)

[33] Dmitri Foursa and Philippe Emplit. Investigation of black-gray soliton interaction. Phys. Rev. Lett.**77**, 4011 (1996)

[34] N.M. Musammil, P.A. Subhab, and K. Nithyanandan, Optik **159**, 176(2018)

[35] Malomed B A 2006 Soliton Management in Periodic Systems (Berlin: Springer)

[36] K.Porsezian, A.Hasegawa, V.N.Serkin, T.L. Belyaeva, and R.Ganapathy, Phys. Lett. A., **361**, 504 (2007)

[37] A.C. Newell, J. Math. Phys. **19**, 1126(1978)

[38] V.N. Serkin and T.L. Belyaeva, J. Exp. Theor. Phys. Lett. **74**, 573 (2001)

[39] V.N. Serkin, V.M. Chapela, J. Percino, and T.L. Belyaeva, Opt. Commun. **192**, 237 (2001)

[40] T.L. Belyaeva and V.N. Serkin, Eur. Phys. J. D **66**, 153 (2012)

[41] Assaf Barak, Or Peleg, Chris Stucchio, Avy Soffer, and Mordechai Segev, Phys. Rev. Lett. **100**, 153901(2008)

Chapter 6

Ultrashort dark solitons interactions and nonlinear tunneling in the Vc-MNLS equation

6.1 Introduction

In several experiments on optical soliton propagation in fibers, the output pulse has been found to be asymmetric due to the self-steepening (SS) effect. SS is found to be crucial in optical communication system, especially in the ultrashort pulse propagation in long distance optical fibers system. The modified nonlinear Schrödinger equation (MNLSE) describing the soliton propagation with SS effect has been under considerable interest over a long time [1–7]. To study the MNLSE, many mathematical techniques have been demonstrated and a large class of analytical solutions have been discussed in literature[8]. All those investigations focused on the MNLSE model with constant coefficient, considering an ideal optical fiber transmission system. However, as a result of non-uniformities, influenced by the spatial variations of the fiber parameters, the realistic optical

fiber medium exhibits inhomogeneous behavior. In this chapter, we consider the following variable coefficient MNLS equation (Vc-MNLSE), which governs the ultrashort dark soliton propagation in an inhomogeneous fiber with the distributed dispersion, nonlinearity, SS and linear gain/loss [9, 10];

$$iq_\xi - \frac{1}{2}D(\xi)q_{\tau\tau} + R(\xi)(q|q|^2) + iS(\xi)(q|q|^2)_\tau + ip(\xi)q = 0 \tag{6.1}$$

where, $q(\xi, \tau)$ is the complex amplitude of the pulse envelope, the variables ξ and τ represent the normalized spatial and temporal coordinates. The GVD, Kerr nonlinearity, SS and amplification/absorption effects are related to the coefficients $D(\xi)$, $R(\xi)$, $S(\xi)$ and $p(\xi)$, respectively.

The bright-soliton propagation and the variation of bright soliton energy due to self phase modulation (SPM) and SS in Vc-MNLSE has been studied in [9]. The dark and anti-dark solitons propagation have been discussed in [10]. In this chapter, we report a more general form of dark soliton solutions for Vc-MNLSE with the conventional form of bilinear transformation as in Refs. [11–15]. Such study has not been discussed in the context of Vc-MNLSE. By using this approach, we exclusively studied the ultrashort dark soliton dynamics with various inhomogeneous effects, such as pulse amplification/absorption, compression, boomerang soliton, dispersion-managed transmission systems and nonlinear tunneling. In addition to that, we have studied the impact of SPM and SS effect on the pulse energy, and by using asymptotic analysis we observed the energy conservation of dark soliton during an elastic collision. Moreover, by the direct numerical simulation, we studied the shock formation of pulse under the influence of SS effect.

Here, we have also paved much attention on nonlinear (NL) tunneling effect. We study the NL tunneling of ultrashort dark soliton for the first time to be best of our knowledge.

The remaining of the chapter is organized as follows. Sec.2 presents the exact dark soliton solutions by the Hirota's bilinear method. In Sec. 3, the one soliton solution and the influence of SS in the soliton dynamics have been presented. Sec.4 presents the two solitons solution and asymptotic analysis to study the collision behavior. A brief discussion about the various physical effects involved in the dynamics of dark soliton propagation through inhomogenous fiber is presented in Sec. 5. The tunneling of dark soliton through barrier/well is discussed in Sec.6, followed by a brief summary and conclusion in Sec.7.

6.2 Exact dark soliton solutions by Hirota method

In this section, we use Hirota's bilinear method to investigate the analytical dark soliton solutions of Eq. (6.1). Here, we use the transformation as followed in Refs. [11–15], which is expected to give an exact form of dark soliton solutions. By using this transformation, the nonlinear differential equations can be transformed into bilinear differential equations. Then, with the different levels of perturbation expansion, the exact form of dark soliton solutions can be derived.

In order to construct the dark soliton solutions, we apply the following form of Hirota bilinear transformation;

$$q(\xi,\tau) = g(\xi)\frac{G}{F} \tag{6.2}$$

where, G is a complex function and F is a real function. By substituting this transformation into Eq. (6.1), the following bilinear equations can be obtained,

$$[iD_\xi - \frac{1}{2}D(\xi)D_\tau^2 + \lambda(\xi)](G.F) = 0 \tag{6.3}$$

$$\delta|G|^2 + D_\tau^2(F.F) + i\gamma(D_\tau(G^*.G) + 3\frac{G^*}{F}D_\tau(G.F)) = \frac{2\lambda(\xi)}{D(\xi)}F^2 \tag{6.4}$$

with the condition $g_\xi(\xi) + g(\xi)p(\xi) = 0$. Here, $\lambda(\xi)$ is an analytic function to be determined, δ and γ can be introduced as, $\delta = \frac{2R(\xi)}{D(\xi)}g(\xi)^2$, $\gamma = \frac{2S(\xi)}{D(\xi)}g(\xi)^2$. D_ξ and D_τ are the bilinear differential operators [11] defined by

$$D_z^m D_t^n(g.f) = (\frac{\partial}{\partial z} - \frac{\partial}{\partial z'})^m(\frac{\partial}{\partial t} - \frac{\partial}{\partial t'})^n g(z,t)f(z,t)|_{z'=z,t'=t}$$

By solving the above set of equations (6.3)-(6.4), we consider the power series expansion of G and F as,

$$G = g_0[1 + \sum_{n=1}^{\infty}\varepsilon^n g_n(\xi,\tau)] \tag{6.5}$$

$$F = 1 + \sum_{n=1}^{\infty}\varepsilon^n f_n(\xi,\tau) \tag{6.6}$$

with ε as the formal expansion parameter. While applying Hirota Direct method, we assume g_0, g_n and f as polynomials of exponential functions.

6.3 One-soliton solutions

In order to get the dark one-soliton solution, the power series expansions for G and F are truncated corresponding to the lowest order in ϵ as follows; $G = g_0(1+g_1)$ and $F = 1+f_1$. Then, back to bilinear equations (6.3)-(6.4), we obtain

$$\begin{aligned}
g_0 &= a_0 e^{i\psi}, & g_1 &= \alpha_1 e^{\theta_1}, & f_1 &= e^{\theta_1} \\
g(\xi) &= e^{-\int p(\xi)d\xi}, & \psi &= k\tau - \omega\int D(\xi)d\xi, & \theta_1 &= k_1\tau - \omega_1\int D(\xi)d\xi \\
\lambda &= \frac{a_0^2}{2}[\delta - \gamma k]D(\xi), & \omega &= -\frac{\lambda}{D(\xi)} - \frac{k^2}{2}, & \alpha_1 &= \frac{2\omega_1 + 2kk_1 + ik_1^2}{2\omega_1 + 2kk_1 - ik_1^2}
\end{aligned}$$

$$\omega_1 = \frac{1}{12k\gamma a_0^2 - 4k_1^2}(4kk_1^3 + \gamma a_0^2 k_1(-12k^2 - 3ikk_1 + k_1^2)$$
$$-\sqrt{(-k_1^2(4k_1^4 + 4a_0^2k_1^2(k\gamma - 2\delta + 3i\gamma k_1) - \gamma a_0^2(39k^2\gamma - 24k\delta + 30ik\gamma k_1 + \gamma k_1^2))))}$$

The one-soliton solution can be written as,

$$q(\xi,\tau) = \frac{a_0[(1+\alpha_1)+(\alpha_1-1)tanh(\frac{\theta_1}{2})]}{2e^{\int p(\xi)d\xi}e^{-i\psi}} \tag{6.7}$$

Here, $a_0e^{i\psi}$ represents the background wave solution. a_0 and ψ are real functions denoting the amplitude and phase of the background wave. Using Eq. (6.7) with $Re[\omega_1]$, the propagation of dark one-soliton through homogenous fiber is depicted in the Fig.6.1(a). From the Eq. (6.7), we can analyze the dynamics of dark soliton pulse in inhomogeneous fibers. The variation of pulse intensity due to SS effect is depicted in the Fig.6.1(b).

In order to study the dynamics of dark soliton and to characterize the inhomogeneous features of propagating optical dark soliton, some of the physical quantities such as velocity, width, amplitude and energy are important. Such quantities can be defined as follows,

$$V = \frac{\omega_1}{\kappa_1}D(\xi), \quad W = \frac{1}{\kappa_1}, \quad A = |\frac{a_0(1+\alpha_1)}{2e^{\int p(\xi)d\xi}}|$$

The energy E and power P, in terms of the background amplitude a_0 can be expressed as $E = \int_{-\infty}^{\infty} Pd\tau$ and $P(\xi,\tau) = a_0^2 - |q|^2$, respectively. Here, the instantaneous power is obtained as a difference between the total power and the corresponding value for the background [16]. The energy, corresponding to the one-soliton solution as given by the Eq. (6.7), can be written as

$$E = \int_{-\infty}^{\infty}(a_0^2 - \mid q \mid^2)d\tau = \frac{2-\alpha_1-\alpha_1^*}{a_0^{-2}e^{2\int p(\xi)d\xi}k_1} \tag{6.8}$$

From the above set of equations, we can analyze the effect of inhomogeneity on the physical quantities of dark soliton. It is interesting to note that, $p(\xi)$ affects the soliton amplitude and energy, $D(\xi)$ affects the soliton velocity. The soliton width is related to the wave number k_1. The Fig.6.2(a) shows the variation

of energy as a function of R for some representative values of S. On contrast, Fig.6.2(b) portrays the energy for different values of R as a function of S. As seen there, the energies of dark soliton decay with the increasing of the value of SS parameter(S) or SPM parameter(R).

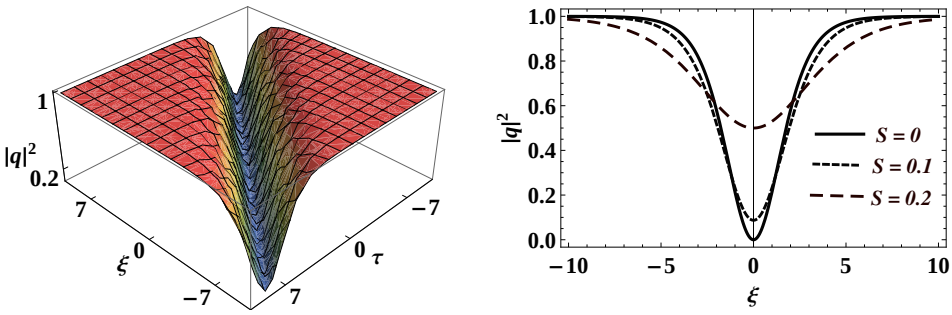

(a) (b)

Figure 6.1: The dark one-soliton propagation through homogenous fiber for parameters $k_1 = 1.5$, $k = a_0 = D(\xi) = 1$, $p = 0$,$R = 0.25$ (a)with $S = 0.1$ (b)with different values of S as $0, 0.1 and 0.2$

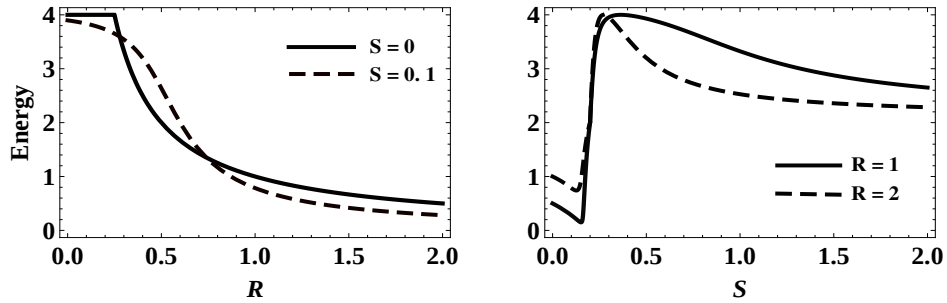

(a) (b)

Figure 6.2: The dark soliton energy (a) as a function of R and (b) as a function of S using Eq.(6.8). The parameters of other relevant physical quantities are $k_1 = 1.5$, $k = a_0 = D(\xi) = 1$ and $p = 0$

6.3.1 Direct numerical simulation

One of the essential aspect of a solitary wave is its stability on propagation. Unlike the conventional pulses of different form, the solitons are relatively stable, even in an environment subjected to external perturbations. Hence, in order to validate the signature of soliton, such as stable propagation over appreciable distance, and the stability against perturbation, we perform numerical simula-

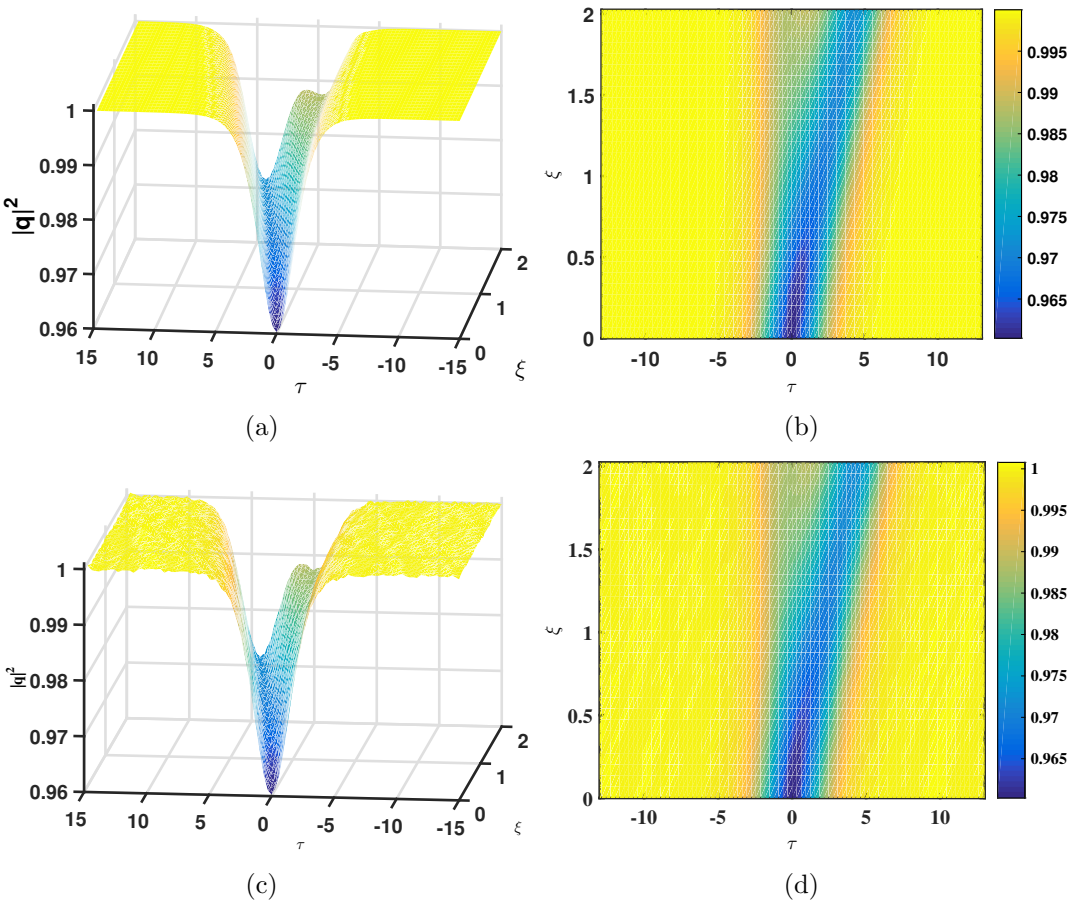

Figure 6.3: Figs (a) and (b) show the dark soliton evolution and the formation of shcok wave. Figs (c) and (d) shows the stable propagation of the soliton and the shock wave formation in the presence of strong photon noise. The parameters of relevant physical quantities are $k_1 = k = a_0 = 1$ $\delta = 2$, $\gamma = 1$and $p(\xi) = 0$.

tion using split-step Fourier method. In order to check the solution stability of our dark soliton solutions, as a representative case, we consider the one soliton solution given by Eq. (6.7), and perform the stability analysis in two parts, (i) direct numerical simulation of propagation of soliton using Vc-MNLSE, and (ii) the propagation of soliton subject to perturbation such as the photon noise. Fig.6.3 shows the numerical simulation of stable propagation of the dark soliton in the continuous back ground. Fig.6.3(a) shows the stable propagation of soliton pulse, and followed the shock wave formation as a consequence of SS due to the intensity dependent group velocity [6]. As of now, the propagation of soliton pulses have been considered in an ideal environment. However, there are numer-

ous effects can contribute to instability in the soliton propagation. Therefore, it is very informative to study the stability of the soliton in an environment subject to external noise or perturbations. To this end, we generated a photon noise, which corresponds to 0.35% of the continuous background. This is indeed an appreciable noise level, which can potentially perturb any propagation, as evident from the smooth pulse shown in Fig. 6.3(a) and the noisy pulse depicted in Fig. 6.3(c). So, the initial condition for the simulation is the soliton profile with strong perturbation. Fig. 6.3(c) shows the simulation results for the same parameters as chosen earlier. It is very evident that the dark soliton show remarkable stability against strong perturbation. The formation of the shock wave can also be clearly observed in the simulation. Thus, one can draw out a conclusion that the dark soliton solution constructed through the Hirota method shows excellent stability, which has been confirmed through direct numerical simulations.

6.4 Two-soliton solutions

To get the dark two-soliton solution, the power series expansions for G and F are truncated as follows, $G = G_0(1 + g_1 + g_2)$ and $F = 1 + f_1 + f_2$. Then, back to bilinear Eqs. (6.3)-(6.4), we obtain

$$g_0 = a_0 e^{ik\tau - i\omega \int D(\xi)d\xi}, \qquad \lambda = \frac{a_0^2}{2}[\delta - \gamma k]D(\xi), \qquad \omega = -\frac{\lambda}{D(\xi)} - \frac{k^2}{2}$$

$$g_1 = \alpha_1\, e^{\theta_1} + \alpha_2 e^{\theta_2}, \quad f_1 = e^{\theta_1} + e^{\theta_2}, \quad g_2 = A_{12}\alpha_1\alpha_2\, e^{\theta_1+\theta_2}, \quad f_2 = A_{12}e^{\theta_1+\theta_2}$$

$$\theta_i = k_i\tau - \omega_i \int D(\xi)d\xi, \qquad \alpha_i = \frac{2\omega_i + 2kk_i + ik_i^2}{2\omega_i + 2kk_i - ik_i^2}$$

where $i = 1, 2$.

$$\omega_1 = \frac{1}{12k\gamma a_0^2 - 4k_1^2}(4kk_1^3 + \gamma a_0^2 k_1(-12k^2 - 3ikk_1 + k_1^2)$$
$$-\sqrt{(-k_1^2(4k_1^4 + 4a_0^2k_1^2(k\gamma - 2\delta + 3i\gamma k_1) - \gamma a_0^2(39k^2\gamma - 24k\delta + 30ik\gamma k_1 + \gamma k_1^2))))}$$

$$\omega_2 = \frac{1}{12k\gamma a_0^2 - 4k_1^2}(4kk_1^3 + \gamma a_0^2 k_1(-12k^2 - 3ikk_1 + k_1^2)$$
$$-\sqrt{(-k_1^2(4k_1^4 + 4a_0^2k_1^2(k\gamma - 2\delta + 3i\gamma k_1) - \gamma a_0^2(39k^2\gamma - 24k\delta + 30ik\gamma k_1 + \gamma k_1^2))))}$$

$$A_{12} = -\frac{2i(\alpha_1 - \alpha_2)(\omega_2 - \omega_1 - kk_1 + kk_2) - (\alpha_1 + \alpha_2)(k_1 - k_2)^2}{2i(1 - \alpha_1\alpha_2)(\omega_1 + \omega_2 + kk_1 + kk_2) - (\alpha_1\alpha_2 + 1)(k_1 + k_2)^2}$$

The two-soliton solution can be written as,

$$q(\xi, \tau) = e^{-\int p(\xi)d\xi}\frac{g_0(1 + g_1 + g_2)}{(1 + f_1 + f_2)} \tag{6.9}$$

Using Eq. (6.9), the propagation of dark two-soliton through homogenous fiber is depicted in the Fig. 6.4.

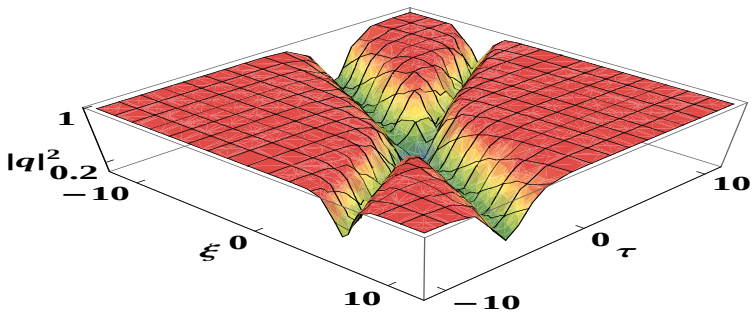

Figure 6.4: The dark two-soliton propagation through homogenous fiber for parameters $k_1 = -1.5$, $k_2 = 1.5$, $k = a_0 = D(\xi) = 1$, $p = 0$, $\delta = 1$ and $\gamma = 0.2$.

6.4.1 Two-soliton interactions

The interaction behaviors between two solitons in fibers can be revealed by the asymptotic states of soliton solution. Based on the two-soliton solution, we dis-

cuss the collision between dark solitons in inhomogeneous fibers. The asymptotic analysis of two soliton solutions are constructed as follows:

1) Before collision

(a)$S_1^-(\theta_1 \sim 0, \theta_2 \to -\infty)$

$$q(\xi,\tau) \to S_1^- = \frac{a_0 e^{i\psi}}{2e^{\int p(\xi)d\xi}}[(1+\alpha_1) + (\alpha_1 - 1)tanh(\frac{\theta_1}{2})] \tag{6.10}$$

(b)$S_2^-(\theta_2 \sim 0, \theta_1 \to \infty)$

$$q(\xi,\tau) \to S_2^- = \frac{a_0\alpha_1 e^{i\psi}}{2e^{\int p(\xi)d\xi}}[(1+\alpha_2) + (\alpha_2 - 1)tanh(\frac{\theta_2}{2} + \ln(\sqrt{A_{12}}))] \tag{6.11}$$

2)After collision

(a)$S_1^+(\theta_1 \sim 0, \theta_2 \to \infty)$

$$q(\xi,\tau) \to S_1^+ = \frac{a_0\alpha_2 e^{i\psi}}{2e^{\int p(\xi)d\xi}}[(1+\alpha_1) + (\alpha_1 - 1)tanh(\frac{\theta_1}{2} + \ln(\sqrt{A_{12}}))] \tag{6.12}$$

(b)$S_2^+(\theta_2 \sim 0, \theta_1 \to -\infty)$

$$q(\xi,\tau) \to S_2^+ = \frac{a_0 e^{i\psi}}{2e^{\int p(\xi)d\xi}}[(1+\alpha_2) + (\alpha_2 - 1)tanh(\frac{\theta_2}{2})] \tag{6.13}$$

From the asymptotic expressions before collision (6.10)- (6.11) and after collision (6.12)- (6.13), one can infer the elastic interaction and particle like behavior of solitons during the time of collisions between S_1 and S_2. The relevant physical quantities of solitons S_1 and S_2 before and after collisions are mentioned in Table 1.

6.5 Results and discussions

In the presented analytical work, we first investigated the constant propagation of dark soliton pulse in the homogeneous medium. In such system, the coefficient corresponding to dispersion and nonlinearity remains constant. Using Hirota Bilinear method, the analytical dark soliton solution corresponding to one and two

Table 6.1: Physical quantities of solitons S_1 and S_2 before and after the collision.

Solitons	Velocities	Widths	Amplitudes	Energies
s_1^-	$\frac{\omega_1}{k_1}D(\xi)$	$\frac{1}{k_1}$	$\lvert\frac{a_0(1+\alpha_1)}{2e^{\int p(\xi)d\xi}}\rvert$	$\frac{a_0^2(2-\alpha_1-\alpha_1^*)}{k_1 e^{2\int p(\xi)d\xi}}$
s_2^-	$\frac{\omega_2}{k_2}D(\xi)$	$\frac{1}{k_2}$	$\lvert\frac{a_0\alpha_1(1+A_{12}\alpha_2)}{e^{\int p(\xi)d\xi}(1+A_{12})}\rvert$	$\frac{a_0^2(2-\alpha_2-\alpha_2^*)}{k_2 e^{2\int p(\xi)d\xi}}$
s_1^+	$\frac{\omega_1}{k_1}D(\xi)$	$\frac{1}{k_1}$	$\lvert\frac{a_0\alpha_2(1+A_{12}\alpha_1)}{e^{\int p(\xi)d\xi}(1+A_{12})}\rvert$	$\frac{a_0^2(2-\alpha_1-\alpha_1^*)}{k_1 e^{2\int p(\xi)d\xi}}$
s_2^+	$\frac{\omega_2}{k_2}D(\xi)$	$\frac{1}{k_2}$	$\lvert\frac{a_0(1+\alpha_2)}{2e^{\int p(\xi)d\xi}}\rvert$	$\frac{a_0^2(2-\alpha_2-\alpha_2^*)}{k_2 e^{2\int p(\xi)d\xi}}$

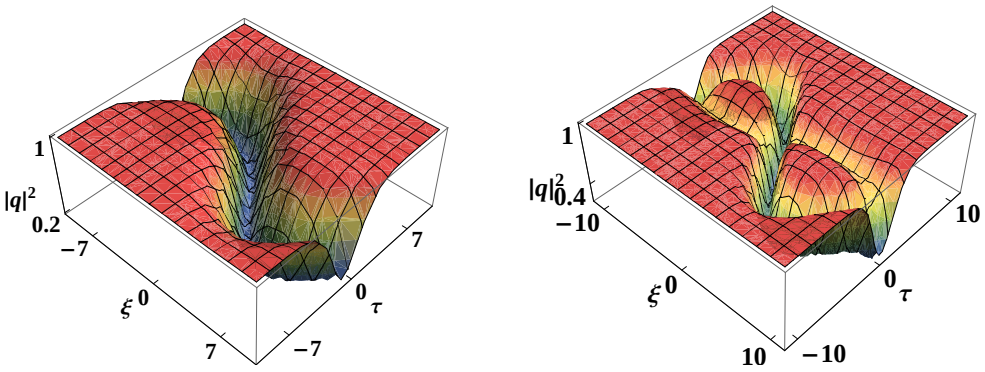

(a) (b)

Figure 6.5: The dispersion and nonlinearity managed dark solitons, (a) One-soliton (b) Two-soliton. Other physical quantities are $k = a_0 = 1, D(\xi) = Cos(0.3\xi)$, $p = 0$, $\delta = 2$ and $\gamma = 1$.

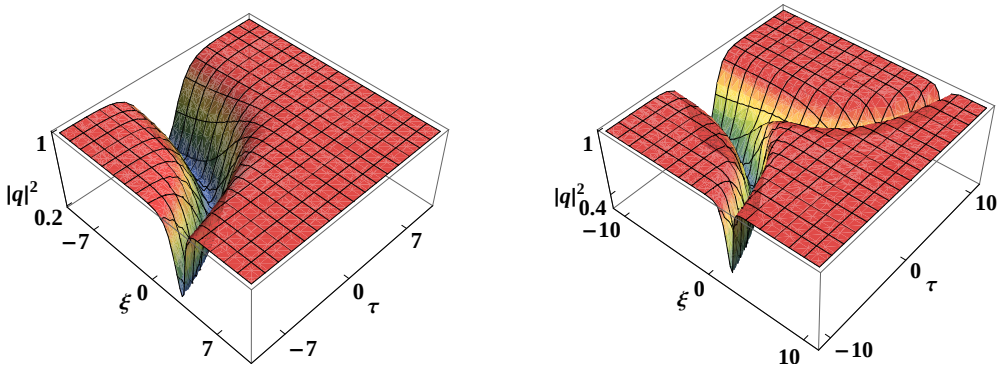

(a) (b)

Figure 6.6: The pulse compression of dark solitons, (a) One-soliton (b) Two-soliton. Other physical quantities are $k = a_0 = 1, D(\xi) = Exp(0.3\xi), p = 0$, $\delta = 2$ and $\gamma = 1$.

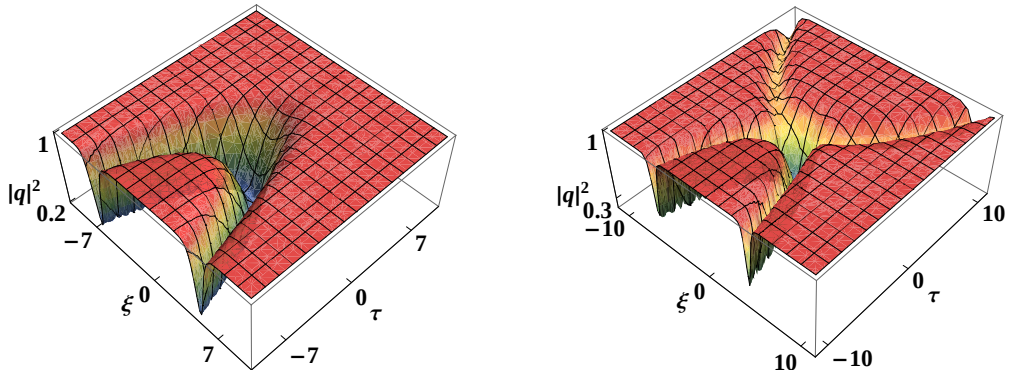

Figure 6.7: The boomerang like dark solitons, (a) One-soliton, (b) Two-soliton. Other physical quantities are $k = a_0 = 1, D(\xi) = 0.3 + 0.5\xi$, $p = 0$,$\delta = 2$ and $\gamma = 1$.

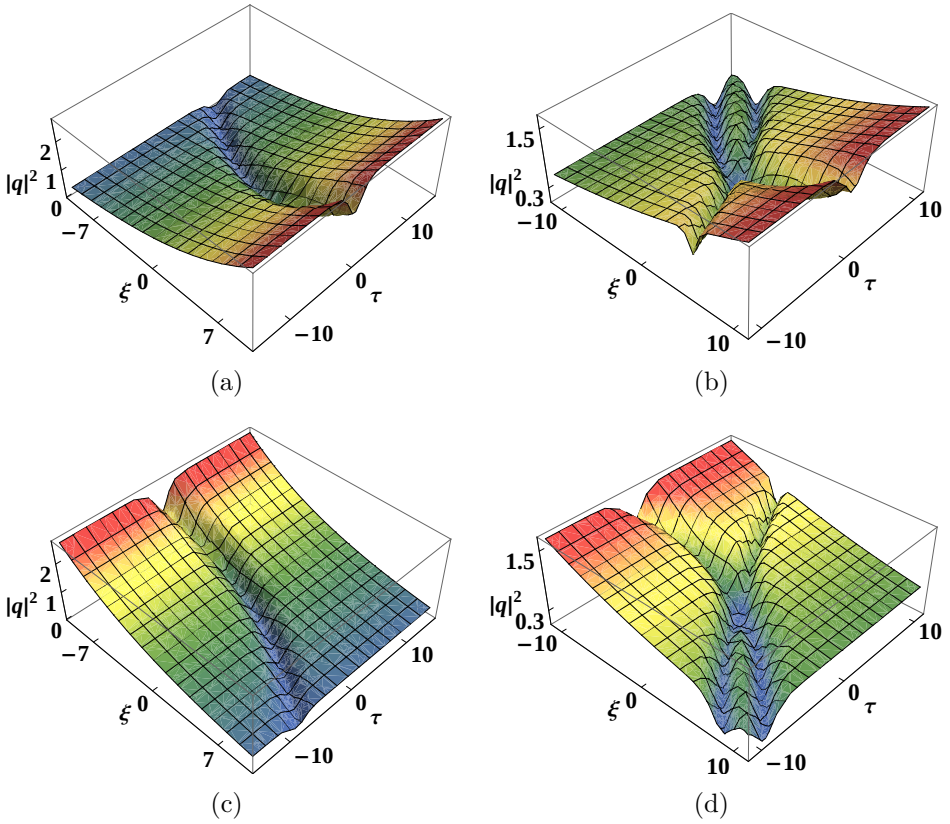

Figure 6.8: The dark solitons propagation with gain, (a) One-soliton, (b) Two-soliton. The other parameters are $k = a_0 = D(\xi) = 1$, $p = -0.05$, $\delta = 2$ and $\gamma = 0.2$. The dark solitons propagation with loss, (c) One-soliton (d) Two-soliton with $p = +0.05$.

are presented graphically in Figs. 6.1 and 6.4 via Eqs. (6.7)and (6.9) respectively. It is found that the dark soliton propagates without deformation in such homogeneous system, and its amplitude and velocity remains constant. In the following section, we examine the dynamical evolution of dark soliton for different physical effects in inhomogenous fibers with variable coefficients, dispersion and nonlinearity.

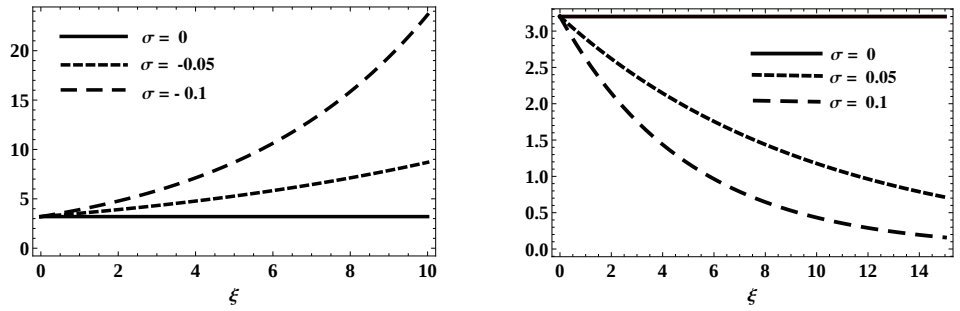

(a) (b)

Figure 6.9: Energy variation with gain/loss via the solution (6.2). (a) Gain with $p = -\sigma$, (b) Loss with $p = +\sigma$. The other relevant physical quantities are $k = a_0 = \delta = D(\xi) = 1$,$k_1 = 1.5$ and $\gamma = 0.1$.

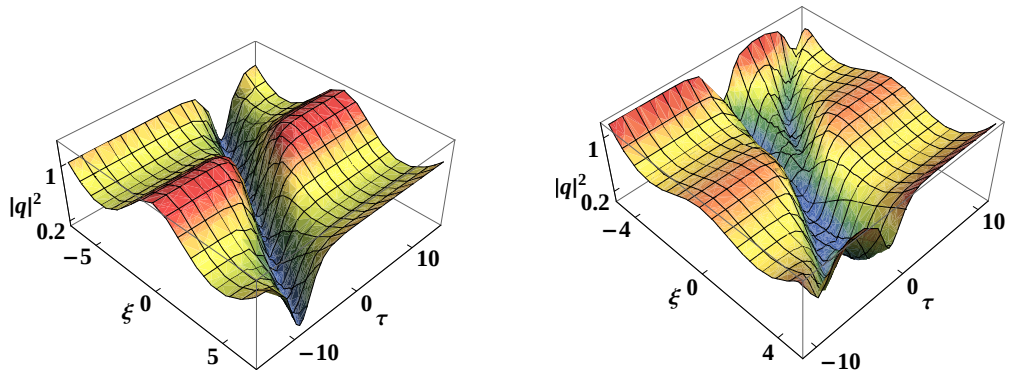

(a) (b)

Figure 6.10: The dark solitons propagation with periodic background, (a) One-soliton, (b) Two-soliton. The other physical quantities are $k = a_0 = D(\xi) = 1$, $p = 0.1sin(0.7\xi)$, $R(\xi) = 1$ and $S(\xi) = 0.5$.

6.5.1 Periodically varying dispersion and nonlinearity

Here, the dispersion-managed dark solitons are investigated by periodic perturbations. Since the GVD parameter $D(\xi)$ and nonlinearity parameters $R(\xi)$ and

$S(\xi)$ are taken in the form of trigonometric periodic function as $a\cos(b\xi)$, where a and b are integers. In this case, the solitons are exhibiting oscillating behavior and the pulse peak position and velocity vary periodically during the time of propagation. The amplitude, energy and width of pulse remains constants [17–20]. Fig. 6.5 represents the one and two soliton pulse propagation with periodically varying effects.

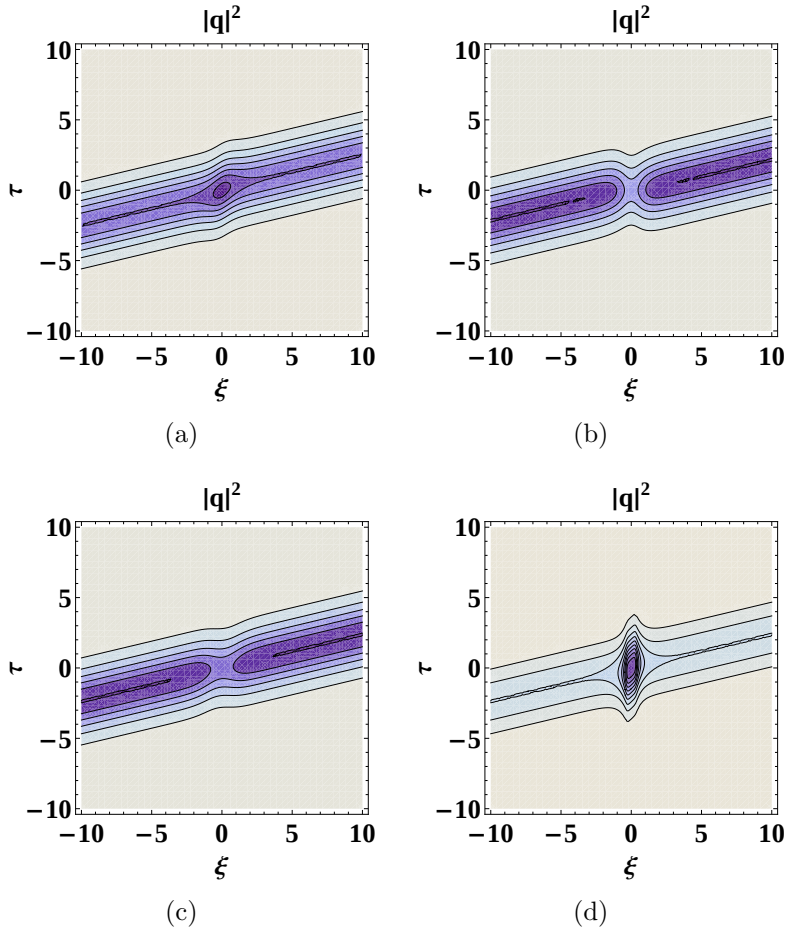

Figure 6.11: Contour plot of nonlinear tunneling of dark one-soliton. (a) Dispersion barrier with $D(\xi) = 1 + hsech[\xi - \xi_0]^2$, $R = 1$, $S = 0.2$ and $h = 0.5$.(b) Dispersion well with $h = -0.9$.(c) Nonlinear barrier with $D(\xi) = 1$,$R = 1 + hsech[\xi - \xi_0]^2$,$S = 0.2(1 + hsech[\xi - \xi_0]^2)$ and $h = 1$.(d) Nonlinear well with $h = -0.5$. Other physical quantities are $k_1 = a_0 = 1$ and $\xi_0 = 0$.

6.5.2 Pulse Compression

Pulse compression (PC) is an widely used technique to shortening the duration of the pulse in nonlinear fiber. Generally, exponential dispersion and nonlinearity is preferred, as it found to compress soliton with a better a compression factor [21, 22]. In this case, the dispersion and nonlinearity parameters are taken in the form of $c\exp(d\xi)$, where c is the initial peak power and d is an integer. The PC occurs, when the leading edge of the pulse is delayed by just the right amount to arrive nearly with the trailing edge. The PC of one and two solitons are depicted in the Fig. 6.6. It is observed that the soliton gets compressed during the propagation of the pulse down the fiber.

6.5.3 Boomerang Soliton

To study the parabolic profile of dark soliton, we choose the dispersion and nonlinearity parameters as $e + f\xi$, where e and f are integers. During the propagation, the soliton exhibits parabolic bending, and after the bending, the width of the soliton decreases gradually. Such type of soliton is commonly known as Boomerang soliton [18, 19]. For the above choices the one and two-soliton solutions are shown in the Fig. 6.7.

6.5.4 Gain/Loss

In the long distance optical fiber transmission system, the optical soliton will deform progressively as a result of fiber loss. In Eq. (6.1) coefficient $p(\xi)$ plays an important role in determining the amplification or absorption of the soliton pulse. The coefficient $p(\xi) = 0$ corresponds to the case of fibers without any loss or gain. When $p(\xi)$ is a constant value, say σ, the solution represents the propagation of soliton pulse in a medium with constant gain or loss.

Fig. 6.8 illustrate the propagation of one and two solitons in a medium with gain/loss. When $\sigma < 0 (\sigma > 0)$, the pulse undergoes the amplification (absorption), and their amplitude of the pulse increases (decreases) as it propagates down

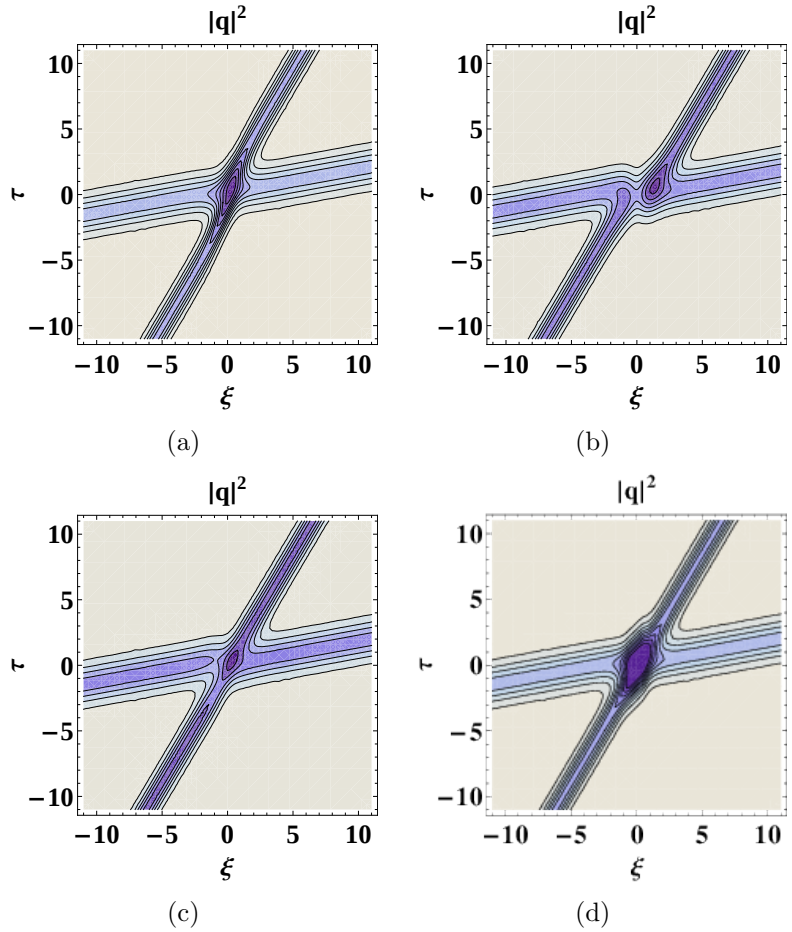

Figure 6.12: Contour plot of nonlinear tunneling of dark two-soliton. (a) Dispersion barrier with $D(\xi) = 1 + hsech[\xi - \xi_0]^2$, $R = 1$,$S = 0.2$ and $h = 0.7$.(b) Dispersion well with $h = -0.9$.(c) Nonlinear barrier with $D(\xi) = 1$,$R = 1 + hsech[\xi - \xi_0]^2$,$S = 0.2(1 + hsech[\xi - \xi_0]^2)$ and $h = 1$.(d) Nonlinear well with $h = -0.5$. Other physical quantities are $k_1 = -1.5$, $k_2 = 1.5$, $a_0 = 1$ and $\xi_0 = 0$.

the fiber. By varying the coefficient $p(\xi)$, the soliton amplification or absorption can be controlled. Fig.6.9, represents the variation of dark soliton energy for some representative values of gain (Fig. 6.9(a)) and loss (Fig. 6.9(b)). It is quite evident that the energy exponentially increases (decreases) with gain (loss).

The gain/loss coefficient $p(\xi)$ can significantly influences the shape of the pulse background, in many recent works, different type of background profiles were considered [23]. Here, we have demonstrated that the background undergoes a periodic oscillation. Fig. 6.10 shows the evolution of one- and two- solitons in

a periodic background with $p(\xi) = g\sin(h\xi)$, where g and h are integers.

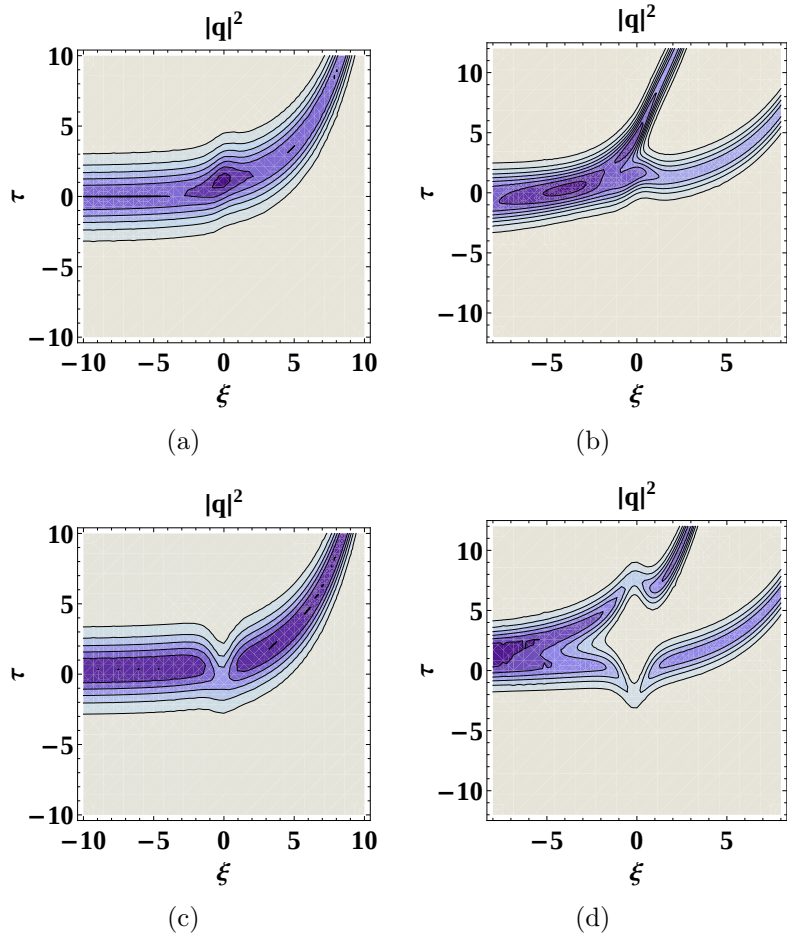

Figure 6.13: Contour plot of nonlinear tunneling with exponential background. Dispersion barrier of (a) One soliton, (b) Two soliton, with $D(\xi) = d_0 e^{-r\xi} + hsech[\xi - \xi_0]^2$,$R = R_0 e^{-r\xi}$,$S = S_0 e^{-r\xi}$ and $h = 0.7$. Dispersion well of (c) One soliton, (d) Two soliton, with the same as for (a-b) except that $h = -0.9$. Other physical quantities are $d_0 = R_0 = 1$ $S_0 = 0.2$,$r = -0.3$ $k_1 = -1.5$, $k_2 = 1.5$ and $\xi_0 = 0$.

6.6 Nonlinear tunneling effect

In the previous sections, we have discussed about the impact of various physical effects and inhomogenous parameters. Now, we intent to investigate the nonlinear tunneling (NL)effect in the one and two dark solitons. It may create a new field of interest and feature wide applications in all-optical switches and logic circuits. Recently, tunneling effect has been investigated in many pioneering works as in Refs.[24, 25]. All research works have shown that the soliton can

pass through the barrier/well without considerable attenuation under a certain conditions, which depends on the ratio between the height of the barrier and the amplitude of the soliton.

Nonlinear tunneling without exponential background

To study the tunneling effect of Vc-MNLS dark soliton through the dispersion barrier or well, we choose the dispersion and nonlinear parameters as follows:

$$D(\xi) = r_0 \pm h\, sech^2(c(\xi - \xi_0))$$
$$R(\xi) = R_0$$
$$S(\xi) = S_0$$

In the above set of expressions, h and c represent the height and width of the barrier. ξ_0 represents the longitudinal co-ordinate indicating the location of the dispersion barrier/well. D_0, R_0 and S_0 are constant parameters. Here the positive or the negative sign of $\pm h$ denotes the barrier or the well. If $h = 0$, the soliton is said to propagate through a homogenous fiber.

To investigate the soliton propagation through the nonlinear barrier or well, we consider the dispersion and nonlinear parameters as follows:

$$D(\xi) = D_0$$
$$R(\xi) = R_0(r_0 \pm h\, sech^2(c(\xi - \xi_0))$$
$$S(\xi) = S_0(r_0 \pm h\, sech^2(c(\xi - \xi_0))$$

When the dark soliton is passing through the dispersion barrier, the amplitude of the soliton grows and forms a peak at $\xi = \xi_0$. After passing through the barrier, the pulse restored to its original shape as illustrated in Fig. 6.11(a). For the case of dispersion well, the amplitude of the soliton vanishes and a valley is formed at $\xi = \xi_0$; after the tunneling, solitons are retained their original shape

as shown in Fig. 6.11(b). On the other hand for nonlinear barrier/well, a valley is formed for nonlinear barrier and a peak is formed for well as evident from the Figs. 6.11(c) and 6.11(d), respectively. In similar lines with one-soliton case, the NL tunneling of two solitons is demonstrated in the Fig. 6.12.

Due to the existing region of dark soliton ($0 \leq A < a_0$), we can found that the height of the barrier (h) and amplitude of pulse (A) have a mutual relation in given soliton solutions. Thus we have studied the tunneling effect with suitable parametric choice of h. To investigate the dark soliton propagation through the dispersion barrier or well, we obtained a condition, where $h > 0$ indicates the dispersion barrier, and $-1 < h < 0$ represents the dispersion well. Similarly, in the case of nonlinear barrier or well, we also obtained a condition, where $h > 0$ indicates the nonlinear barrier, and $-1 < h < 0$ represents the nonlinear well.

6.6.1 Nonlinear tunneling with exponential background

Now, we consider the tunneling effect with exponential background. This case is of particular importance, because, pulse tunneling through the exponential background generally results in the compression of the pulse. To investigate this special case, we consider the dispersion and nonlinear parameter as follows:

$$D(\xi) = D_0 exp(-r\xi) \pm h\, sech^2(c(\xi - \xi_0))$$
$$R(\xi) = R_0 exp(-r\xi)$$
$$S(\xi) = S_0 exp(-r\xi)$$

Here, r in the above expression represents the decaying parameter, which accounts for the exponential decay. Figs. 6.13(a) and 6.13(b), represents the dark one and two solitons tunneling through dispersion barrier with exponential decay. It is observed that the amplitude of the soliton increases at $\xi = \xi_0$, and after tunneling through the barriers, the width of the soliton decreases gradually during propagation. Similarly, Figs. 6.13(c) and 6.13(d) illustrates the dark soliton tunneling through dispersion well with exponential background for the case of one and two solitons. As it is evident that the amplitude of the soliton

vanishes at $\xi = \xi_0$ and after emerging from the well, the soliton width compresses. From this result, one can infer that the input pulse can be compressed to a desired extent in a controllable manner by the proper choice of barrier or well parameters.

6.7 Conclusion

In this chapter, we have investigated Vc-MNLS model with distributed dispersion, SPM, SS and linear gain/loss, which describe the dynamics of ultrashort pulse propagation in the inhomogeneous fiber systems. Using Hirota's bilinear method, we have analytically derived the exact one and two dark soliton solutions. We illustrated the effect of self-steepening such as shock wave formation during the propagation, which has been confirmed through direct numerical simulation. In order to validate the stability of the soliton solution, we numerically perform the stability analysis in the presence of photon noise, and our simulation illustrates the stable propagation of the dark soliton pulse. The elastic interaction behaviors of the dark soliton pulses in inhomogeneous fibers have also been discussed through asymptotic analysis. For better insight about the effect of inhomogeneity, we have exclusively studied the dynamical behavior of dark soliton with different physical effects up to the level of two-dark soliton interactions. In particular, we focused on the nonlinear tunneling of dark soliton through barrier/well. It has been found that the intensity of the tunneling soliton either forms a peak or valley and retains its shape after tunneling through barrier/well. We also observed the pulse compression of dark soliton via NL tunneling with exponential background. We believe, the given detailed study on dark solitons in the Vc-MNLSE, incorporating most of the physical effects, may serve as a good reference for many future studies related to ultrashort dark soliton.

Bibliography

[1] F. De Martini, C. H. Townes, T. K. Gustafsson, and P. L. Kelley, Phys. Rev. 164(1967)312-323 .

[2] D. Anderson and M. Lisak, Phys. Rev. A 27(1983)1393-1398 .

[3] J. R. de Oliveira and M. A. Moura, Phys. Rev. E 57(1998) 4751-4756 .

[4] Jeffrey Moses, Boris A. Malomed, and Frank W. Wise, Phys. Rev. A 76 021802(R)(2007)1-4 .

[5] Seung-Ho Han and Q-Han Park, Phys. Rev. E 83 066601(2011)1-6 .

[6] Yu Yu , Jia Wei-Guo, Yan Qing, Menke Neimule, and Zhang Jun-Ping, Chin. Phys. 24(8) 084210(2015) 1-7.

[7] Hai-Qiang Zhang, Bo Tian, Xing Lu, He Li, and Xiang-Hua Meng, Physics Letters A 373 (2009) 43154321.

[8] M. Li, B. Tian, W.J. Liu, H.Q. Zhang, and P. Wang, Phys. Rev. E 81 046606(2010) 1-8.

[9] Zhang H Q, Tian B, Liu W J, and Xue Y S, Eur. Phys. J. D 59 (2010)443-449

[10] Hai-Qiang Zhang, Bao-Guo Zhai and Xiao-LiWang, Phys. Scr. 85 015006(2012)1-9.

[11] R. Hirota, The Direct Method in Soliton Theory, Cambridge University Press, Cambridge, 2004.

[12] R.Radhakrishnan and M.Lakshmanan,J.Phys.A:Math.Gen.28 (1995)2683-2692.

[13] K. Porsezian and K. Nakkeeran, Phys. Rev. Lett. 76 (1996)3955 .

[14] Liu W J, B Tian, H Q Zhang, T Xu and H Li, Phys. Rev. A 79(2009) 063810

[15] N. M. Musammil, K. Porsezian, P. A. Subha, and K. Nithyanandan, Chaos 27, 023113 (2017)1-12

[16] M J Ablowitz, S D Nixon, T P Horikis and D J Frantzeskakis, J. Phys. A: Math. Theor. 46(2013)095201 1-18

[17] Malomed B A, Soliton Management in Periodic Systems, Berlin, Springer,2006

[18] A. Mahalingam, A. Uthayakumar and P. Anandhi, J Opt.42(3)(2013)182

[19] . M.S. Mani Rajan, A. Mahalingam, A. Uthayakumar, J. Opt.14 (2012)105204 1-8

[20] K.Porsezian, A.Hasegawa, V.N.Serkin, T.L. Belyaeva and R.Ganapathy, Phys. Lett. A 361(2007) 504-508

[21] M N Vinoj and V C Kuriakose, J. Opt. A: Pure Appl. Opt. 6 (2004)63-70.

[22] K. Nithyanandan, R. Vasantha Jayakantha Raja, and K. Porsezian, J. Opt. Soc. Am. B 30(2013) 178-187 .

[23] Yu-Jie Feng, Yi-Tian Gao, Zhi-Yuan Sun, Da-Wei Zuo, Yu-Jia Shen, Yu-Hao Sun, Long Xue and Xin Yu, Phys. Scr. 90 (2015)045201 1-8

[24] A.C. Newell, J. Math. Phys. 19(1978) 1126-1133

[25] V.N. Serkin, T.L. Belyaeva, J. Exp. Theor. Phys. Lett. 74,(2001) 573-577

Chapter 7

Results and conclusions

The propagations and interactions bright and dark solitons in realistic fiber systems have been investigated in this thesis. Many intriguing results are reported, and its mathematical implications are successfully achieved. Different forms of nonlinear Schrödinger equations have been considered and the obtained results are summarized as follows

7.1 Summary of Results

- We have investigated the dark soliton dynamics in the Vc-NLSE with distributed dispersion, SPM and linear gain/loss. The one and two dark soliton solutions have been derived by using Hirota's bilinear method. Through the derived soliton expressions and graphical illustration, the dispersion managed pulse with amplification/absorption and the influence of gain/loss coefficient on the shape of the background have been discussed. Numerically, we have studied the dark soliton propagation in the continuous wave background, and our simulations confirm that the obtained soliton solution is very stable and robust against perturbations. We derived exact solution for the phase of dark solitons and reported the effect of blackness parameter and gain/loss coefficient on soliton phase profiles. Black and gray soliton interactions and elastic collision between dark solitons are exclusively studied via the asymptotic analysis. We have also studied the

nonlinear tunneling of dark soliton through barrier/well, it has been found that the intensity of the tunneling soliton either forms a peak or valley and retains its shape after tunneling through barrier/well. We also identified the tunneling of dark soliton with exponential background tends to compress the pulse. Moreover, a cascaded compression of dark soliton have been investigated by soliton passing through multiple nonlinear tunneling barrier. Unlike, the most conventional studies on HB method for constructing soliton solution, where the focus was primarily on the intensity part and the stability of the solution. Here, we have added new insight and extended the capability of HB method in understanding the phase profile of the obtained solutions. As it is known, the phase profile plays a vital role in multi-soliton solutions, especially in the bound state solution, where relative phase plays a very deterministic role in explaining the nature of interaction, such as attractive or repulsive.

- We have also investigated the bright solitons dynamics in the variable coefficient nonlinear Schrödinger (Vc-NLS)equation. Many fascinating results underlying spatial dependent bright soliton phase, which gives more insights for well-known inhomogeneous phenomenons, such as dispersion managed system, pulse compression and especially nonlinear tunneling effect, has been reported. By connecting an ansatz method with Hirota bilinear technique, we have introduced an explicit form of bright soliton phase. Exact bright two-soliton solution has also been derived by using the Hirota bilinear method. The elastic collision behavior of the bright solitons are observed by means of asymptotic analysis. Two-soliton phase are studied by the asymptotic expression which gives the description of individual solitons that existing before and after collision. Moreover, with a particular interest, we has been investigated the tunneling effect through the dispersion barrier or well. Soliton intensity either forms a peak or valley and regain its shape after the tunneling through the barrier/well. For the case of exponential background, the soliton tends to compress after

tunneling. Corresponding phase evolutions are illustrated in detail. For better insight, we reported the cascade compression of solitons with multiple successive dispersion barriers. Overall, a comprehensive study of bright soliton dynamics and its phase evolution in Vc-NLS equation is studied.

- We have investigated the dynamics of dark soliton pulse propagation in inhomogeneous fibers by employing Vc-CNLS model. The dark soliton solutions have been derived by Hirota's bilinear method. Through the analytical soliton solutions and detailed graphical illustration, the propagation dynamics and collision behaviors of the dark soliton pulses in inhomogeneous fibers have been discussed. Especially, we have studied the almost all dynamical related physical quantities up to the level of three-dark solitons interactions. The inhomogeneous effects on the evolution and interaction between dark solitons have also been considered. The shapes and velocities of the dark solitons can be controlled by modulating dispersion and gain/loss terms. The gain or loss term affects the amplitude and energy. The results obtained in this paper will be of good scientific value to the studies related to the propagation of dark solitons in the dispersion and nonlinear managed fiber system. Finally, we investigated the nonlinear tunneling effect of optical dark solitons with and without exponential background. It has been reported that tunneling of the soliton depends on a condition related to the height of the barrier and the soliton amplitude. The intensity of the tunneling soliton either forms a peak or valley and retains its shape after tunneling through barrier/well. We also identified the tunneling of dark soliton with exponential background tends to compress the pulse.

- We have investigated the phase dynamics of Manakov bright and dark vector soliton in inhomogeneous fibers by employing two component Vc-CNLS model. The exact one and two soliton solutions have been derived by Hirota's bilinear method. To study the phase dynamics of the system, we

have applied a general ansatz method which enabled an explicit analytical expressions for intensity as well as phase of the soliton. By equating the unknown parameters of this ansatz with the exact solutions of well-known HB method, we have obtained exact phase of Manakov soliton. By using the asymptotic analysis of two-soliton solutions, the phase of the individual solitons have been explored. Unlike the bright vector soliton which has constant phase in homogeneous medium, the time dependent phase of dark soliton exhibit a gradual phase change. The influence of varying coefficients such as periodically varying GVD, medium gain/loss and background oscillations on the dynamics of phase evolution have also been discussed in detail, up to the two-solitons level. Moreover, we have studied nonlinear tunneling effect of Manakov soliton in the context of dispersion barrier/well. When soliton pass through the dispersion barrier(well), the maximum(minimum) phase change takes place at the region of barrier(well) and the phase retains its original form after crossing the given barrier(well). In contrast to conventional way of intensity based soliton description, we have presented a comprehensive analysis on the phase dynamics of the soliton in a self-explanatory way. Unlike the common usage of HB method for soliton intensity, we have extended the capability of HB method in understanding the phase profile of the obtained multi-soliton solutions.

- We have further explored Vc-MNLS model with distributed dispersion, SPM, SS and linear gain/loss, which describes the dynamics of ultrashort pulse propagation in the inhomogeneous fiber systems. Using Hirota's bilinear method, we analytically derived the exact one and two dark soliton solutions. We illustrated the effect of self-steepening such as shock wave formation during the propagation, which has been confirmed through direct numerical simulation. In order to validate the stability of the soliton solution, we numerically perform the stability analysis in the presence of photon noise, and our simulation illustrates the stable propagation of the dark soliton pulse. The elastic interaction behaviors of the dark soliton

pulses in inhomogeneous fibers have also been discussed through asymptotic analysis. For better insight about the effect of inhomogeneity, we exclusively studied the dynamical behavior of dark soliton with different physical effects up to the level of two-dark soliton interactions. In particular, we have focused on the nonlinear tunneling of dark soliton through barrier/well. It has been found that the intensity of the tunneling soliton either forms a peak or valley and retains its shape after tunneling through barrier/well. We also observed the pulse compression of dark soliton via NL tunneling with exponential background.

7.2 Future prospective

Soliton driven communication system through fiber medium via the variable coefficient model gives more idea of soliton dynamics in realistic systems. We would like extend this study to coupled model with self-steepening effect and more higher order effect such as SRS, SBS, etc. Further more, similar studies can be extended to PT symmetric systems.

Appendix

In chapter 4 and 5, we have investigated the soliton dynamics in inhomogeneous Manakov model by the HB method. The scope of the our studies can be extended to understand the matter wave dynamics in the Bose-Einstein condensates (BEC). From an experimental BEC point of view, bright solitons are created themselves as condensates, while dark solitons exist as notches or holes within the condensates. The dynamics of BEC at absolute zero temperature is usually described by the mean-field Gross-Pitaevskii(GP) equation. It can be mapped onto the standard NLS equation under suitable transformation[1–4]. The interaction of bright-bright or dark-bright solitons in two component Bose-Einstein condensates by suitably tailoring the trap potential, atomic scattering length and atom gain or loss have been studied by Rajendran et al.[2–4]. Based on their studies, the coupled GP equation can be mapped onto the Manakov model. Multi-component generalization of the soliton dynamics is natural in the context of atomic BECs. The dimensionless form of two coupled GP equations can be written as[2, 3]

$$i\psi_{jt} = -\frac{1}{2}\psi_{jxx} + [R(t)\sum_{k=1}^{2} g_{jk}|\psi_k|^2 + V(x,t) - \mu_j + i\frac{\gamma(t)}{2}]\psi_j, \quad j = 1,2 \quad (1).$$

Here $V(x,t) = \frac{1}{2}\Omega^2(t)x^2$ is the external potential, μ is the chemical potential, $R(t)$ is the s-wave scattering length and $\gamma(t)$ is the gain/loss term . Using the

following transformation

$$\psi_j(x,t) = \Lambda_j(x,t) q_j(X,T), \quad j = 1,2 \quad (2)$$

equation (1) can be reduced to the set of two coupled nonlinear Schrödinger equations (2CNLS) of the form

$$iq_{jT} = -\frac{1}{2} q_{jXX} + q_j \sum_{k=1}^{2} g_{jk} |q_k|^2, \quad j = 1,2 \quad (3)$$

Where $\Lambda_j(x,t) = r_0 \sqrt{2R'(t)} exp[i(\theta(x,t) + \mu_j t) + \int \gamma(t) dt]$, $R'(t) = R(t) exp[\int \gamma(t) dt]$, $\theta = -\frac{R'_t}{2R} x^2 + 2c_1 r_0^2 R' x - 2c_1^2 r_0^4 \int R'^2 dt$, $X = \sqrt{2} r_0 R' x - 2\sqrt{2} c_1 r_0^3 \int R'^2 dt$, $T = 2r_0^2 \int R'^2 dt$. Now using the transformation (2) with suitable solution for q_j as

$$\begin{aligned} q_1(X,T) &= \tau \frac{1 - \frac{\rho}{\rho^*} \chi e^{\eta + \eta^*}}{1 + \chi e^{\eta + \eta^*}} \\ q_2(X,T) &= \frac{e^{\eta}}{1 + \chi e^{\eta + \eta^*}} \end{aligned}$$

where $\eta = \kappa X + i(\frac{1}{2}\kappa^2 - \tau^2)T$, $\kappa = a + ib$, $\rho = \kappa - ic$, the dark-bright one-soliton solution of the two coupled GP equation can be written as [2]

$$\psi_j(x,t) = \sqrt{2R'(t)} q_j(X,T)) \; exp[i(\theta(x,t) + \mu_j t) + \int \gamma(t) dt], \quad j = 1,2 \quad (4)$$

Here, authors investigated the exact dark-bright one and two soliton solutions of the two-component BECs with time varying parameters such as s-wave scattering length and gain/loss term. The snake-like effect of the one soliton solution for periodically modulated trap potential with $R(t) = [1 + \omega Cos(\omega t + \delta)]$ has been studied. Similar to the 2CNLS Eq.(3), the Manakov model and snaking soliton effect for the optical systems, with suitable choice of parameters, has been demonstrated in chapter 4 (see Fig 4.4). Also, the effect of gain/loss term in matter wave soliton has been discussed in Ref.[2]. Similar to our studies presented in chapter 4 and 5, the amplitude of BEC soliton shows oscillatory behavior when

we choose a periodic gain term.

The bright-bright soliton solutions of the two coupled GP equation have been studied in Ref.[3]. With help of two soliton solutions, that derived by the HB method, the shape changing interactions of bright-bright two soliton with suitable choice of parameter have been investigated in Ref. [3]. In this thesis (chapter 5), we have investigated the energy sharing collision of the optical bright vector soliton in the 2CNLS model (see Fig. 5.4). The BEC solitons are also exhibits similar energy sharing interactions. These studies provides an understanding of the possible mechanism for soliton excitations in multi-component BECs.

The exact bright and dark soliton solution with the periodic oscillating nature, gain/loss effect and pulse compression ($R(t) = exp(-\Omega_0 t)$) in the 1D BEC system have been investigated in Ref.[4]. Similar effects on NLS soliton have been presented in chapter 2 and 3 of this thesis (see Figs. 2.10, 3.2 and 3.3). These comparison studies with the work of Rajendran et. al, provides more insights about the scope of this thesis, ie, the mathematical techniques used in this thesis are widely applicable in many different physical systems.

Bibliography

[1] A. Kundu, Phys. Rev. E **79**, 015601, (2009)

[2] S Rajendran, P Muruganandam and M Lakshmanan, J. Phys. B: At.Mol. Phys **42**(14), 145307, (2009)

[3] S Rajendran, P Muruganandam and M Lakshmanan, Journal of Mathematical Physics **52**(2), 023515,(2011)

[4] S Rajendran, P Muruganandam and M Lakshmanan, Physica D: Nonlinear Phenomena **239**(7), 366,(2010)